UNIVERSITY OF TURKU

RECOGNITION OF SINGLE- AND DOUBLE-STRANDED NUCLEIC ACIDS BY COVALENTLY MERCURATED OLIGONUCLEOTIDES

Dattatraya Uttam Ukale

TURUN YLIOPISTON JULKAISUJA – ANNALES UNIVERSITATIS TURKUENSIS
SARJA – SER. AI OSA – TOM. 643 | ASTRONOMICA – CHEMICA – PHYSICA – MATHEMATICA | TURKU 2021

UNIVERSITY OF TURKU

RECOGNITION OF SINGLE- AND DOUBLE-STRANDED NUCLEIC ACIDS BY COVALENTLY MERCURATED OLIGONUCLEOTIDES

Dattatraya Uttam Ukale

TURUN YLIOPISTON JULKAISUJA – ANNALES UNIVERSITATIS TURKUENSIS
SARJA – SER. AI OSA – TOM. 643 | ASTRONOMICA – CHEMICA – PHYSICA-MATHEMATICA | TURKU 2021

University of Turku

Faculty of Science
Department of Chemistry
Laboratory of Organic Chemistry and Chemical Biology
Doctoral Programme in Physical and Chemical Sciences

Supervised by

Asst. Professor Dr Tuomas Lönnberg
Department of Chemistry
University of Turku
Turku, Finland

Reviewed by

Professor Dr Yoshiyuki Tanaka
Laboratory of Analytical Chemistry
Department of Pharmaceutical Sciences
Tokushima Bunri University, Japan

Assoc. Professor Dr Miguel A. Galindo
Departamento de Química Inorgánica
Universidad de Granada
Av. Fuentenueva S/N
Garanda, Spain

Opponent

Professor Dr Jens Müller
Westfälische Wilhelms-Universität Münster
Institut für Anorganische und Analytische Chemie, Germany

The originality of this thesis has been checked in accordance with the University of Turku quality assurance system using the Turnitin OriginalityCheck service.

ISBN 978-951-29-8365-0 (PRINT)
ISBN 978-951-29-8366-7 (PDF)
ISSN 0082-7002 (Print)
ISSN 2343-3175 (Online)
Painosalama Oy, Turku, Finland 2021

Dedicated to my beloved family

UNIVERSITY OF TURKU
Faculty of Science
Department of Chemistry
Chemistry
DATTATRAYA UKALE: Recognition of Single- and Double-Stranded Nucleic Acids by Covalently Mercurated Oligonucleotides
Doctoral Dissertation, 117 pp.
Doctoral Programme in Physical and Chemical Sciences (PCS)
January 2021

ABSTRACT

Metal-mediated base pairs have attracted considerable attention during the past decades for their potential in bio- and nanotechnological applications. The introduction of metal ions into DNA or RNA not only stabilizes various secondary structures but also confers new, metal-based functionalities. In this context, interactions of Hg(II) with nucleic acids containing artificial as well as natural nucleobases have been studied extensively. These studies have yielded promising results but also revealed notable shortcomings, such as off-target metalation and low stability in metal-deficient media. The covalently mercurated oligonucleotides presented in this thesis provide a new alternatives approach for Hg(II)-metal mediated base pairing, aiming to overcome these limitations.

In the present study, covalently mercurated natural and artificial nucleosides and corresponding oligonucleotides were synthesized. The binding affinity of mono- and dimercurated nucleosides with natural nucleotides was investigated at the monomer level by NMR studies. At oligomer level, the base-pairing properties of covalently mercurated nucleobases were investigated by measuring UV-melting temperatures of various duplexes and triplexes. Furthermore, the binding mode of a monofacial dimercurated nucleobase was also predicted theoretically by DFT calculations. The results obtained on monomers and oligomers generally agreed well, with the duplexes and triplexes containing the most stable base Hg(II)-mediated base pairs also exhibiting the highest melting temperatures. In some cases, the mercurated duplexes and triplexes were considerably more stable than their counterparts comprising only canonical base pairs.

KEYWORDS: mercury nucleobases, organometallic, base pair, duplex, base triple, Hg(II)-mediated base pair

TURUN YLIOPISTO
Matemaattis-luonnontieteellinen tiedekunta
Kemian laitos
Kemia
DATTATRAYA UKALE: Yksi- ja kaksijuosteisten nukleiinihappojen tunnistus käyttäen kovalenttisesti merkuroituja oligonukleotideja
Väitöskirja, 117 s.
Fysikaalisten ja kemiallisten tieteiden tohtoriohjelma
tammikuu 2021

TIIVISTELMÄ

Metallivälitteiset emäsparit ovat herättäneet huomattavaa mielenkiintoa viime vuosikymmeninä mahdollisten bio- ja nanoteknologisten sovellusten takia. Metalli-ionien liittäminen DNA:han tai RNA:han voi stabiloida erilaisia sekundaari-rakenteita ja lisäksi saada aikaan kokonaan uusia toiminnallisuuksia. Hg(II)-ionien vuorovaikutuksia sekä luonnollisten että muokattujen nukleiinihappojen kanssa on tutkittu laajasti tässä yhteydessä. Nämä tutkimukset ovat tuottaneet lupaavia tuloksia mutta myös paljastaneet huomattavia puutteita, kuten metalloitumisen muualla kuin halutussa kohdassa sekä heikon pysyvyyden alhaisissa metalli-ionikonsentraatioissa. Tässä väitöskirjassa esitetyt kovalenttisesti merkuroidut oligonukleotidit tarjoavat uuden vaihtoehtoisen tavan muodostaa Hg(II)-välitteisiä emäspareja, tavoitteena edellä mainittujen rajoitusten kiertäminen.

Väitöskirjatyössä syntetisoitiin kovalenttisesti merkuroituja luonnollisia ja keinotekoisia nukleosideja sekä vastaavia oligonukleotideja. Mono- ja dimerkuroitujen nukleosidien sitoutumista luonnollisten nukleotidien kanssa tutkittiin NMR-spektrometrisesti. Kovalenttisesti merkuroitujen nukleiinihappoemästen pariutumista kaksois- ja kolmoiskierteisissä oligonukleotideissa tutkittiin mittaamalla oligonukleotidien UV-sulamislämpötilat. Yksipuolisen kahdesti merkuroidun nukleiinihappoemäksen muodostaman Hg(II)-välitteisen emäsparin rakenne ennustettiin myös laskennallisesti käyttäen DFT-menetelmää. Nukleosideilla ja oligonukleotideilla saadut tulokset olivat pääpiirteittäin sopusoinnussa keskenään siten, että korkeimmat sulamislämpötilat mitattiin duplekseille ja triplekseille, jotka sisälsivät pysyvimmät Hg(II)-välitteiset emäsparit. Jotkin merkuroiduista duplekseista ja triplekseista olivat huomattavasti pysyvämpiä kuin niiden ainoastaan luonnollisia emäspareja sisältävät vastineet.

ASIASANAT: merkuroidut nukleiinihappoemäkset, organometallinen, emäspari, dupleksi, emäskolmikko, Hg(II)-välitteinen emäspari

Table of Contents

Abbreviations

A	adenosine
AMP	adenosine 5′-monophosphate
C	cytidine
CD	circular dichroism
CMP	cytidine 5′-monophosphate
CPG	controlled pore glass
dA	2′-deoxyadenosine
dC	2′-deoxycytidine
dG	2′-deoxyguanosine
DCA	dichloroacetic acid
DCM	dichloromethane
DMTr	4,4′-dimethoxytrityl (4,4′-dimethoxytriphenylmethyl)
DMTrCl	4,4′-dimethoxytrityl chloride
DMSO	dimethyl sulfoxide
DNA	deoxyribonucleic acid
ds	double-stranded
dT	2′-deoxythymidine
dU	2′-deoxyuridine
ESI-MS	electrospray ionization mass spectrometry
G	guanosine
GMP	guanosine 5′-monophosphate
GMS	guanine modified substrate
GNA	glycol nucleic acid
HG	Hoogsteen
HMBC	heteronuclear multiple bond correlation
HPLC	high performance liquid chromatography
HRMS	high resolution mass spectrometry
HSQC	heteronuclear single quantum coherence
IMP	inosine 5′-monophosphate
ITC	isothermal titration calorimetry
^{Me}C	5-methylcytosine

MES	2-ethanesulfonic acid
MOPS	(3-(N-morpholino)propanesulfonic acid)
MS	mass spectrometry
NMR	nuclear magnetic resonance
NMP	nucleoside 5′-monophosphate
ON	oligonucelotide
Py	pyridine
RNA	ribonucleic acid
RP-HPLC	reversed-phase high performance liquid chromatography
rt	room temperature
T_m	melting temperature
TBDMS	*tert*-butyldimethylsilyl
TEA	triethylamine
TEAA	triethylammonium acetate
TFO	triplex forming oligonucelotide
THF	tetrahydrofuran
Th	Therminator DNA polymerase
Tr	trityl
U	uridine
UMP	uridine 5′-monophosphate
UV	ultraviolet
WC	Watson-Crick

List of Original Publications

The thesis is based on the following publications:

I Ukale, D., Shinde, V. S., and Lönnberg, T.: 5-Mercuricytosine: An Organometallic Janus Nucleobase. *Chem. Eur. J*. **2016**, 22, 7917–7923.

II Ukale, D. U., and Lönnberg, T.: Triplex Formation by Oligonucleotides Containing Organomercurated Base Moieties. *ChemBioChem*. **2018**, 19, 1096–1101.

III Ukale, D. U., and Lönnberg, T.: 2,6-Dimercuriphenol as a Bifacial Dinuclear Organometallic Nucleobase. *Angew. Chem. Int. Ed*. **2018**, 57, 16171–16175; *Angew. Chem*. **2018**, 130, 16403–16407.

IV Ukale, D. U., Tähtinen, P., and Lönnberg, T.: 1, 8-Dimercuri-6-Phenyl-1H-Carbazole as a Monofacial Dinuclear Organometallic Nucleobase. *Chem. Eur. J*. **2020**, 26, 2164–2168.

List of Related Publications

I Ukale, D., Maity, S., Hande, M., and Lönnberg, T.: Synthesis and Hybridization Properties of Covalently Mercurated and Palladated Oligoncuelotides. *Synlett.* **2019**, 30, 1733–1737.

II Ukale, D. U., and Lönnberg, T.: Organomercury Nucleic Acids – Past, Present and Future. *ChemBioChem*. **2021**, doi.org/10.1002/cbic.202000821.

1 Introduction

1.1 Structure and biological significance of nucleic acids

Nucleic acids are fundamental macromolecules for the continuity of life. The two main types of nucleic acids are deoxyribonucleic acid (DNA) and ribonucleic acid (RNA). Inside the cells, DNA serves as the storehouse of genetic information and transfers that information from one generation to the next, providing a molecular basis for heredity, whereas RNA plays various important biological roles in coding, decoding, regulation, and expression of genes.

Nucleic acids are biopolymers composed of monomeric units termed as nucleotides.[1–9] Each repeating nucleotide unit in a nucleic acid biopolymer comprises three subunits linked together: a phosphate group, a 5-carbon (pentose) sugar, and one of the four nitrogenous bases (Figure 1). The nitrogenous bases are planar aromatic heterocyclic molecules and are divided into two groups: the pyrimidine bases cytosine (C), thymine (T, present in DNA only) and uracil (U, present in RNA only) and the purine bases adenine (A) and guanine (G). The bases form *N*-glycosidic bonds between N1 of pyrimidines and N9 of purines and the C1′ of the pentose sugar. The main structural difference between DNA and RNA is present in the sugar (2′-deoxyribose and ribose, respectively) and in one of the nucleobase units (thymine and uracil, respectively). In both purine and pyrimidine nucleotides, the phosphate group forms a bond between two sugar moieties. A monomer lacking the phosphate group is called a nucleoside. Individual nucleotide units are joined together in a nucleic acid in a linear manner through a 5′,3′-phosphodiester bond between the sugar moieties. A short chain of nucleotides (approximately 8-50) is termed as an oligonucleotide. In molecular biology, for the notation of nucleic acid or oligonucleotide sequences, single-letter codes (A, C, G, T and U) are conventionally used for the five canonical nucleotides and the two classes of nitrogenous bases can be abbreviated as Y (pyrimidine) and R (purine). The phosphate group, in turn, is often abbreviated simply as P.

Deoxyribonucleic acid (DNA) chains are typically found in a double-helical form, a structure in which two complementary (matching) chains are bound together by hydrogen bonding.[1–7,9] The sugar and phosphate moieties lie on the outside of the

helix, forming the backbone of the DNA. The nitrogenous bases extend into the interior, like the steps of a staircase, in pairs and the bases of a pair are bound to each other by hydrogen bonds.

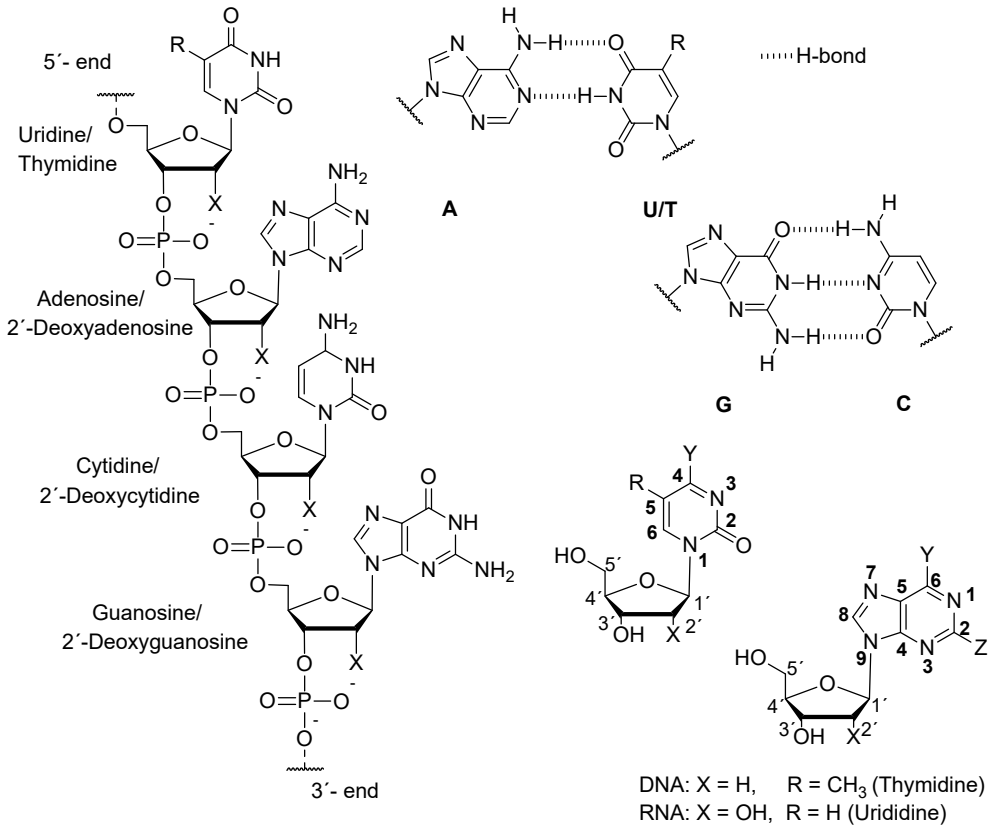

Figure 1. Primary molecular structure of DNA or RNA and Watson-Crick base pairing. DNA: X = H, N = T (R = CH_3); RNA: X = OH, N = U (R = H); Y or Z = NH_2 or O.

The other type of nucleic acid, RNA (Ribonucleic acid), unlike DNA, is usually a single-stranded polyribonucleotide chain. However, given a complementary sequence, RNA can also form a double helix. Even though RNA carries out a wide range of biological functions, the main function is to serve as the intermediary between DNA and proteins, carrying amino acid sequence information from genes to cytoplasm where proteins are assembled on ribosomes.[10–17]

1.2 Watson-Crick base pairing

The ability of DNA to encode information and control the synthesis of RNA arises from the pairing of the four nucleobases (A, T, G, and C) to form a double helix.[9,18–20] In Watson-Crick (WC) base pairing, a purine base always pairs with a pyrimidine base: adenine with thymine or uracil through two hydrogen bonds and guanine with cytosine through three hydrogen bonds (Figure 2). Hydrogen bonds are electrostatic in character; their strength depends on the partial charges located on the component atom in the bond. The most favorable bond angle for hydrogen bonding is 180° but sometimes in nucleic acid structures the bond angles are distorted. In the Watson-Crick base pairs, the two C1 atoms are equidistant at about 10.5 Å, whereas in other type base pairing the distance is varied. Generally, the two Watson-Crick base pairs (A•T/U and G•C) are by far the most abundant and energetically preferred base pairs in DNA. However, sometimes formation of non-complementary base pairs results in mutation.[2,3,6,9,17,21] The association of two nucleic acid strands through pairing of bases to form a double helix is called hybridization. The thermal stability of a double helix can be characterized by its UV-melting temperature. Melting temperature (T_m) is the temperature at which half of the DNA strands are in single-stranded (ssDNA) state.

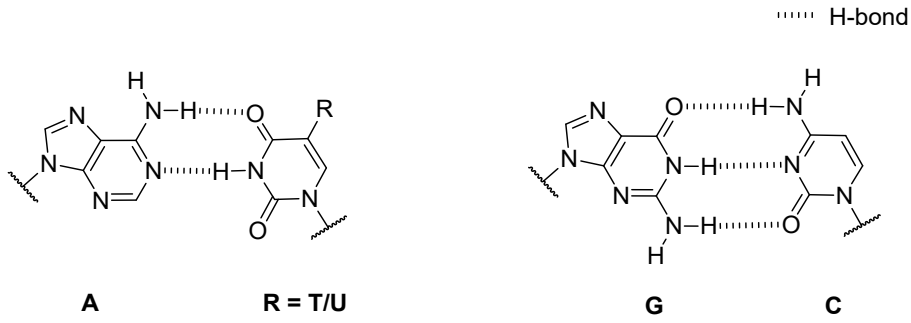

Figure 2. Watson-Crick base pairing of adenine with thymine or uracil (in RNA) and guanine with cytosine.

1.3 Hoogsteen base pairing

Many alternate helical forms and higher order nucleic acid secondary structures are stabilized by base pairs that exhibit a different mode of hydrogen bonding from Watson-Crick base pairs. One such hydrogen-bonding pattern was first reported by Hoogsteen in the 1960s based on X-ray crystallographic analysis of co-crystals of monomeric adenine and thymine (or uracil) derivatives.[22] Within nucleic acids, Hoogsteen (HG) base pairing involves flipping of the purine base around the

glycosidic bond, changing the nucleoside from *anti* to *syn* conformation. In Hoogsteen base pairs, the angle between the two glycosidic bonds is larger and the C1'-C1' distance smaller than in Watson-Crick base pairs. In reversed Hoogsteen base pairs one base is rotated 180° with respect to the other.[23] Hoogsteen base pairing is more common with AT than with GC base pairs as the latter requires protonation of the cytosine[24] (Figure 3). The change from a WC to a HG base pair substantially modifies the chemical environment around the base pair, which can have major implications for DNA-protein recognition, damage repair, and replication. In triple helical structures two purine-pyrimidine strands bind by the classical Watson-Crick hydrogen bonding, while the third strand binds in the major groove of the duplex via Hoogsteen hydrogen bonds. Hoogsteen base pairs are mainly encountered in higher order nucleic acid secondary structures like triplexes and quadruplexes and only rarely in double helical context.[25–27]

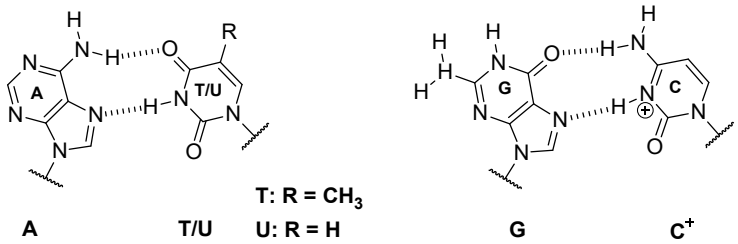

Figure 3. Hoogsteen base pairing in adenine with thymine and guanine with cytosine.

1.4 Artificial base pairing

Since nucleobases provide the prime recognition site for Watson-Crick base pairing via specific hydrogen bonding interactions, the scope of modification of the nucleobase is confined with the natural nucleobases. Both purine and pyrimidine bases have been modified focusing on a certain factor of stabilization, such as H-bonding, hydrophobic interactions, metal bridges and stacking effects. These modifications were carried out with native nucleobases by different ways like introduction of extra functional groups[28–34], insertion of extra rings[35–37] or attaching a linker[28,34] in between the sugar and the base (Figure 4). Moreover, in addition to the canonical bases, non-canonical or artificial bases have been frequently exploited in molecular biology research.[33] For the non-canonical base pairs, the boundaries of modification are less strict than with native base pairing.

Introduction of an extra amino function at position 2 of adenine, for example, allows formation of three hydrogen bonds with uracil and thus improves the miRNA performance of respective modified oligonucleotides.[31] 5′-formyluracil has the distinct ability to stabilize the G-quadruplex motif in telomere structures through

hydrogen bonding. In cases where the *N*-glycosidic bond proves too labile, it can be replaced with a *C*-glycosidic bond, giving rise to a *C*-nucleoside.[34] 6-ethynylpyridone combines the hydrogen bonding capabilities of T at the 3- and 4-positions with the ability of an ethynyl substituent to engage in stacking and van der Waals interactions with H2 of adenine.[30] As a result, the base pair formed between 6-ethynylpyridone and adenine stabilizes an oligonucleotide duplex more than the canonical T•A base pair.

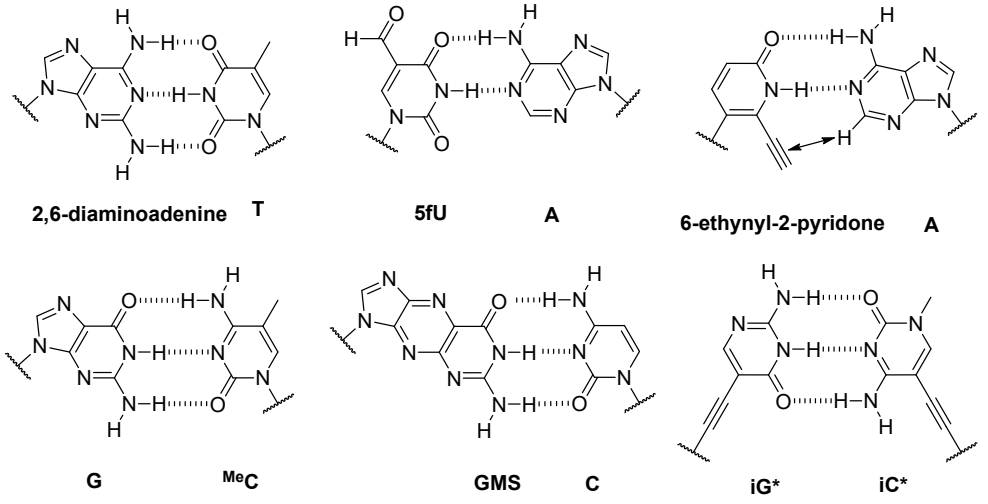

Figure 4. Examples of nucleobase modifications used in recognitions of nucleic acid sequences.

5-methylated cytosine (^{Me}C) stabilizes duplexes more than cytosine by hydrophobic interaction of the extra methyl group. Benzo-fused expanded guanine, in turn, stabilizes duplexes by increased stacking, while maintaining selective pairing with the natural Watson-Crick partner[35–37] (cytosine). The iG* and iC* artificial *C*-nucleosides with an acetylene bridge between the sugar and the base offer almost the same duplex stability as their natural counterparts.[34]

1.5 Base stacking

The structural features of nucleic acid double helices are governed by base-base interactions.[38–42] There are two main types of interactions: a) in the plane of the bases (horizontal) hydrogen bonds; b) perpendicular to the base planes or base stacking effect. Base stacking depends on several noncovalent interactions such as van der Waals dispersive forces, electrostatic attracton between dipoles and solvation.[38,40] The strength of base stacking interactions decreases in the order purine-purine >

purine-pyrimidine > pyrimidine-pyrimidine. These differences may be understood in terms of the larger surface area and greater polarizability of the purine bases.

Stacking of DNA (and RNA) bases strongly contributes to the stability of the double helix – even more than base pairing.[41] Measuring the stabilizing effect of unpaired bases allows direct quantification of stacking with no contribution from base pairing. With DNA, the stacking of overhung bases at the 5′-terminus is energetically more favorable than those at the 3′-terminus whereas the opposite is true with RNA. Stacking in the middle of a DNA or RNA double helix has a greater influence than at either terminus but the overall effect is complicated by rigidity and cooperativity.[40]

1.6 Metal-Nucleic acid interactions

While metals have been associated with biological systems from the origin of life, scientists began to truly appreciate the scale of their influence only after the breakthrough determination of nucleic acid structure. Metals can associate with all different segments of nucleic acids, *i.e.* base, phosphate, and sugar moieties (Figure 5).[43–51] The preferred metal binding sites in polynucleotides depend on various factors such as the size, charge, pK_a and geometry of the metal ion. The binding sites in polynucleotides at neutral pH include terminal phosphate oxygen (pK_a 6.6), endocyclic atoms in adenosine (N7 or N1, pK_a 3.8), guanosine (N7, pK_a 2.0) and cytidine (N3, pK_a 4.2). At basic pH, the deprotonation of some endocyclic nitrogens introduces additional binding sites, notably in guanosine (N1, pK_a 9.3), uridine (N3, pK_a 9.5) and thymidine (N3, pK_a 9.9). The binding of metals to nucleic acids also depends on the hardness/softness match between the metal ion (a Lewis acid) and the donor atom (a Lewis base). The hard metals bind to the hard donors, such as oxygen, while the soft metals bind to the soft donors such as sulfur and nitrogen.

Under physiological conditions, the phosphate backbone of nucleic acids is deprotonated and the resulting negative charge is stabilized by the binding of metal ions.[44,51] Alkali and alkaline earth metals (Li(I), Na(II), K(I), Rb(II), Cs(II), Mg(II), Al(III)) mainly bind to the phosphate, and the transition metal ions (Sc(II), Ti(II), V(II), Cr(II), Mn(II), Fe(II), Co(II), Ni(II), Cu(II), and Zn(II)) with decreasing softness are also capable of coordinating to the phosphate oxygen atoms.[45,51] Ionic versus covalent character of these complexes depends on the metal ion involved. Based on the dependence of duplex melting temperatures on the concentration of different metal ions, Eichhorn and coworkers found the binding preference of metals to phosphate over base to decrease in the order Mg(II) > Co(II) > Ni(II) > Mn(II) > Zn(II) > Cd(II) > Cu(II).[45]

The ribose sugar of nucleosides interacts with various metal ions in a neutral environment. A large number of metal ions, such as La(III), Ce(III), Pr(III), Sm(III),

Gd(III), Tb(III), Ca(II), Sr(II), Ba(II), Cu(II), and Mn(II) have been found to coordinate to the sugar by calorimetric methods and NMR spectroscopy.[52–57]

The metal coordination sites to the purine nucleobases are N1, N3 and N7 in adenine and N1, N3, O6 and N7 in guanine.[43–45,47,48,50,51,58,59] In case of pyrimidine nucleobases the coordination sites are cytosine O2, N3 and N4, thymine O2, N3, and O4 and uracil O2, N3 and O4.[50,51] In the purine nucleobases metal binding dichotomy is observed between the N7 and N1 positions whereas in pyrimidine bases binding at the N3 site usually dominates. Metal-carbon covalent bond formation can take place at C5 atoms of pyrimidine bases (C and U) and C8 atoms of purine bases.[51]

In addition to their important role in neutralizing the negative charge of the phosphate backbone, the alkali and alkaline earth metal ions bind to the O6 of guanine and exclusively stabilize G-quadruplex (GQ) structures. The magnitude of stabilization decreases in the order Sr(II) > Ba(II) > Ca(II) > Mg(II) > K(I) > Rb(I) > Na(I) > Li(I) = Cs(I).[60]

The binding interactions of transition metals have been studied more extensively with nucleobases than with the sugar phosphate backbone. Transition metals bind to N7 and N1 atoms of purine and N3 and O6 atoms of pyrimidine bases. Binding affinity of transition metal ions to the nucleobases decreases in the order Hg(II) > Cu(II) > Cd(II) > Zn(II) > Mn(II) > Ni(II) > Co(II) > Fe(II).[47,51,56,61–63]

At lower concentration, Fe(II) binds to guanine N7 and the phosphate backbone and at higher concentration also to adenine N7 and thymine O2.[64] Fe(III), in turn, binds strongly to the phosphate backbone at lower concentration and at higher concentration also to the N7 of guanine. Zn(II) metal complexes interact with thymine N3 and guanine N1.[61] The crystal structure of Zn(II) adenine complex offers direct evidence of Zn(II) binding to the N1 of adenine.[65] Cd(II) tightly coordinates to N3 of pyrimidine and N7 of purine bases.

Among the transition metals mercury is a frequently studied element for metal nucleic acid interactions. Hg(II) interacts with purine bases through the N7, N1 and O6 atoms and with pyrimidine bases through N3 and N4 (the exocyclic NH_2 group of cytosine).[47] Hg(II) also forms covalent bonds with cytosine and uracil bases at the C5 position. In oligonucleotides Hg(II) selectively stabilizes TT mismatches. Hg(II)—nucleic acid interactions are described in detail in section 1.6.2.

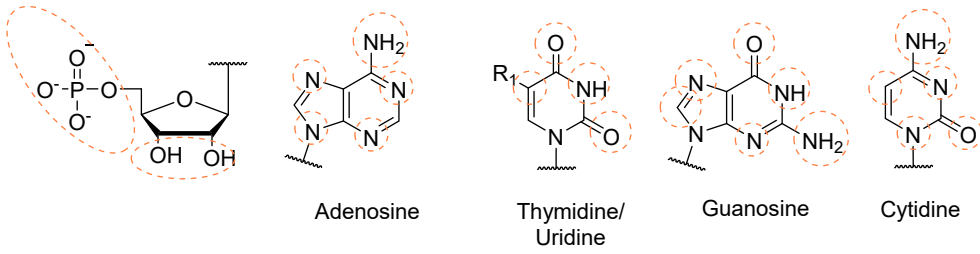

Figure 5. DNA-metal interactions. Metal-binding sites of sugar, phosphate and base are denoted by dotted circles.

Among the post-transition metal ions Ga(III), In(III), Tl(I), Sn(II), Pb(II), and Bi(I), only Sn(II), Pb(II), and Tl(I) frequently engage in DNA interactions.[51] At neutral pH, crystallographic data showed that Pb(II) coordinates to the phosphate backbone and to N7 and O6 of guanine, N3 and O2 of cytidine, and N1 and N7 of adenine. Pb(II) and Tl(I) interact with N7 of guanine and support formation of stable G-quadruplexes.[66]

Lanthanides (Ln(III)) bind mainly to the phosphate backbone of DNA via electrostatic interactions although secondary coordination to the endocyclic nitrogens of nucleobases is also possible. At acidic pH, Ln(III) ions selectively bind to the phosphate backbone via inner-sphere coordination and to N7 indirectly via outer-sphere coordination.[67,68] At basic pH, Ln(III) ions chelate directly to phosphate and N7 sites of purine bases. In the actinide series only thorium and uranium are non-radioactive metals accessible in laboratories. U(III)O_2 cations bind to the phosphate backbone, making DNA susceptible to cleavage in the presence of light.

After the breakthrough discovery of cisplatin as a potential anticancer drug, the noble metals (Ru, Rd, Pd, Ag, Os, Ir, Pt, and Au) have been extensively studied for their therapeutic potential. These soft metals interact strongly with DNA bases but weakly with the phosphate backbone. Ru, Os, Pd and Au bind to the N7 and can also form organometallic complexes at the C8 site of guanine.[69,70] Ir and Ru undergo C8 metalation of guanine by N-donor tethered strategy. Ag(I) is one of the most studied metals in the context of nucleic acid interactions.[47,71] Ag(I) strongly binds to cytosine N3, guanine N7 and O6 and adenine N7 and stabilizes CC, TC and CA mismatches. Au(III) forms coordination polymers with nucleobases, nucleosides and nucleotides. Au(I) binds to guanine N7, leading to dimerization through photo-cross-linking. Pd(II) and Pt(II) have quite similar binding properties although ligand-exchange kinetics of the latter are much slower, allowing formation of metastable cross-links. Pt(II) binds to the N7 and N1 of guanine, N3 of cytosine atoms, making it useful for detecting G-G and C-C mismatches. The anticancer activity of cisplatin is based on the formation of a

Pt(II) bridge between the N7 atoms of two guanine residues.[72] Pd(II) binds to the N1 and N3 of guanosine and thymidine monophosphates, respectively, at monomer level as well as in a double helical structure.[59,73–76]

1.6.1 Metal-mediated base pairing: state of the art

In metal-mediated base pairing, hydrogen bonds of canonical base pairs are formally replaced by coordinative covalent bonds. In these pairs, the donor atoms in the nucleobases donate their electron pair to the metal ion and a metal bridge is formed (Figure 6). Certain metal ions can be coordinated by a pair of either natural or artificial nucleobases, which are placed opposite to each other in the double helix. The bond energy of a typical metal-coordinative bond (10–30 kcal mol^{-1}) is significantly higher than that of a hydrogen bond (0.7–1.6 kcal mol^{-1}), resulting in superior stability of metal-mediated base pairs. In terms of bond energy, one coordinate bond can replace two or three hydrogen bonds.

The first metal-mediated base pair was reported in 1952 by Katz, who found that the interaction of Hg(II) with the sodium salt of calf thymus nucleic acid resulted in aggregation of DNA.[77] After this discovery a variety of metal ions have been studied in the context of metal-mediated base pairing with natural nucleobases. As described in section 1.6, various factors affecting the metal-nucleobase interaction will also affect the stability of secondary structures. The metal binding properties of nucleic acids can be altered by either modifying the natural or introducing completely new artificial nucleobases. For example, the metal binding affinity may be improved or expanded to different metal ions.

Incorporation of metal ions into artificial chelator-like nucleobases can enhance the stability of the modified oligonucleotide duplex. Predesigned artificial base pairs of a distinctive shape, size and function are promising candidates for creating molecular metal arrays inside DNA in a programmable manner. Over the last few decades numerous metal arrays have been incorporated in duplexes with natural as well as with the artificial nucleobase.[46,78–89] Additionally, metal mediated base pairing provides a new structural motif in higher-order DNA structures with superior thermal stability.

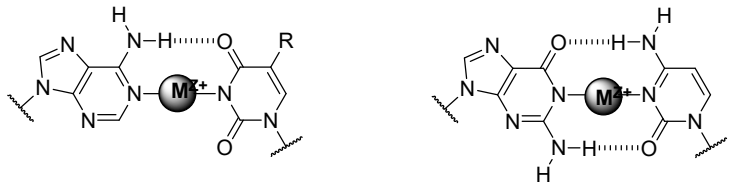

Figure 6. Schematic representation of metal mediated base pairing in the natural nucleobases.

1.6.2 Early studies on intraction of Hg(II) with nucleic acids

Katz's discovery of decrease in viscosity and increase in molecular weight of DNA upon reversible binding of Hg(II)[77,90] began a new era in the study of DNA-metal interactions and Hg(II) still remains the most studied metal ion in this context. The various detection techniques used to detect Hg(II)—DNA interactions included UV-spectrophotometric titration[91–93], vibrational (IR/Raman) spectrometric titration[94–102] and Cu_2SO_4 density gradient centrifugation.[103] The aggregation of DNA with decrease in viscosity was initially thought to be the result of Hg(II) forming cross-links through binding to the phosphate groups and NH_2 groups of adenine, guanine or cytosine. Subsequently UV-spectrophotometric investigations proved coordination of Hg(II) ions to the base moieties and not to the phosphate groups.[90] However, these early studies did not allow the exact position or nature of attachment of mercury to the various nucleosides to be established.[77,90,104–108]

The preliminary results showed that metal-DNA stoichiometry plays an important role in the DNA metal interactions. Subsequently, Katz reconsidered the concept of stoichiometry of Hg(II) binding to the DNA molecules[105,106] and proposed a chemical structure of T-Hg(II)-T mismatch base pairs, with a possible mechanism of DNA strand displacement[104] (Figure 7). Slippage in DNA double helices brings thymine bases of opposite strands together and this allows bridging of two deprotonated thymine bases by a mercury ion.[104] The binding of Hg(II) to DNA could be reversed by the addition of complexing ligands such as Cl-, CN, Br, SCN^- and cysteine, albeit with loss of the biological activity of native DNA.[109,110] The first ^1H NMR data on Hg(II)-DNA complexes in poly d(AT) was recorded by Young and coworkers in 1982 by varying the concentration of Hg(II).[111] The authors noticed that by increasing the concentration of Hg(II) the imino proton resonance decreased and disappeared at a molar ratio of 0.25, supporting the idea of the Katz strand-slippage model for the formation of T-Hg(II)-T base pairs.

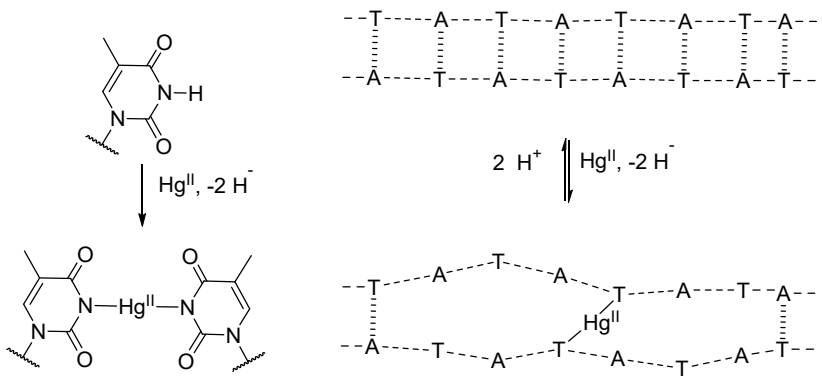

Figure 7. The structure of the T-Hg(II)-T base pair suggested by Katz and his proposed model for chain slippage process formation T-Hg(II)-T base pairs by bringing two-thymine base together.

The effect of Hg(II) interactions in polynucleotides was studied with varying the nucleobase content in the polynucleotides. Yamane *et.al.* proposed based on mercurimetric pH-stat titrations that in a polynucleotide sequence, Hg(II) specifically binds to A•T rather than G•C base pairs.[107] The number of protons released from the natural bases correlates with the number of mercury ions bound to the DNA. This interpretation has received further support from thermal melting and optical rotary dispersion.[112]

Unwinding and rewinding of the DNA double helix upon introduction of different metal ions has been studied CD spectropolarimetrically. Such "breathing reactions" are required in the biological role of DNA for recognition of base pairing characteristics. The conformational effect of MeHg(II) or Hg(II) on DNA was for the first time observed by Gruenwedel and coworkers.[92,113–120] The authors noted that Hg(II) induces topological changes in native calf thymus DNA with an increasing amount of $Hg(ClO_4)_2$ with $0.01 < r < 1.0$ (r is defined here and in all cases as the ratio [metal ion] / [ligands] in the polynucleotides). Exposing calf thymus DNA to increasing concentrations of $Hg(ClO_4)_2$ not only produced a more pronounced conformational change in the CD spectra from B- to A-type double helix but also decreases and ultimately prevents endonucleolytic DNA cleavage by staphylococcal nuclease.[118]

Interactions with MeHg(II) or Hg(II) can also change the chirality of the DNA helix. In poly[d(AT)•d(AT)] and poly[d(GC)•d(GC)], Hg(II) induced a transition from right-handed DNA to a putative left-handed form.[117] Addition of 0.05 and 0.12 equiv. of Hg(II) turned the right-handed poly[d(AT)•d(AT)] and poly[d(GC)•d(GC)] to left-handed structures. At pH 10, Hg(II) binding to poly[(dA)•poly(dT)] results in a more dramatic change in absorption than with poly[d(AT)•d(AT)] with an intense positive CD band at 296 nm.[117,121] Adding

complexing agents such as CN^- or Br^- regenerated the original sequences without disrupting Watson-Crick base pairing.[116,117,122]

The addition of Hg(II) to poly(A)•poly(U) at pH 7.0 results in an increase of UV absorbance, consistent with denaturation of the double helix.[123] In the poly(A)•poly(U) double helix, this hyperchromicity was exploited to study the kinetics of Hg(II) binding. Three steps could be distinguished: pre-equilibrium local unwinding of the double helix, followed by fast incorporation of Hg(II) and, finally a much slower strand dissociation.[114]

1.6.3 Merccury—nucleobase interactions at monomer level

Mercury exhibits oxidation states I, II, III, and IV, but I and II are the most common. The dicoordinate Hg(II) complexes exhibit considerable covalent character, the most stable complexes being formed with halogen, carbon, nitrogen, phosphorous, and especially sulfur ligands. In organomercuric compounds mercury is always divalent and usually dicoordinate with linear geometry. Consequently, compared to other metals commonly used in metal-mediated base pairing, such as Pd(II), Pt(II), Ni(II) and Cu(II), with octahedral or square planar configuration, Hg(II) has a lower tendency to form chelates. The binding sites of mercury in nucleic acids follow the Lewis soft-hard acid base theory. The distinct "soft acid" character of Hg(II) correspond to a strong binding affinity for ligands with "soft base" donor atoms such as sulfur, selenium, nitrogen, and phosphorus. In contrast, Hg(II) has little affinity to the sugar phosphate backbone.

Gunther et.al masked the exocyclic amino groups in nucleosides by formaldehyde and titrated with Hg(II) at different pH.[108] The masking of amino groups of adenosine and cytidine, but not guanine, inhibited interaction with Hg(II). In the case of uridine, addition of formaldehyde did not affect Hg(II) binding. These results suggested N3 (or O2/O4) of thymine, N1 (or O6) of guanine and the exocyclic amino groups of cytosine and adenine as the preferred binding sites of Hg(II). In the same period, Eichhorn-Clark and Simpson reported the thermodynamic association constants of methylmercuric hydroxide or mercuric hydroxide to nucleosides in water, obtained by potentiometric titration over a pH range of 1—11.[108,124,125] The relative binding affinity of Hg(II) to monomeric nucleosides decreases in the order of T > G >> A, C.[125]

Several NMR solution and X-ray crystal structures have been determined for adenine complexes of MeHg(II) and Hg(II) under neutral, acidic, and basic conditions. Beauchamp and co-workers reported binding of MeHg(II) to adenine or 9-methyladenine at any of the nitrogen donors (N1, N3, N6, N7 and N9) (Figure 8 a-e).[126–133] The binding of MeHg(II) to adenine depends on the metal ion to ligand ratio r (r is defined here and in all cases as the ratio [metal ion] / [ligands]). At pH 9,

MeHg(II) formed a complex with adenine at N9 (Figure 8 a). Increasing the r value to 2 under neutral conditions or in the presence of 1 equiv. of NaOH relative to adenine resulted in coordination of another Hg(II) ion at N7[130] (Figure 8 b). With r = 3 and 1 equiv. of NaOH, or r = 4 without added NaOH, a 3:1 MeHg(II)-adenine complex **c** was observed (Figure 8 c). X-ray crystallography with 9-methyladenine also proved the deprotonation of the exocyclic amino group, with 2 equiv. of MeHg(II) binding to N3, N6 and N9 (Figure 8 e). When r = 4 under neutral conditions in H_2O, MeHg(II) binds to N6 and N9 whereas in H_2O-EtOH mixture two MeHg(II) ions bind to the amino group[129] (Figure 8 d). The preferred binding site of Hg(II) on adenosine is N7 (Figure 8 f), binding at N1 and N3 positions being observed occasionally, especially when N7 is protonated. The apparently conflicting results for the various complexes probably stem from differences in the crystallization conditions and do not reflect differences in the solution structures.

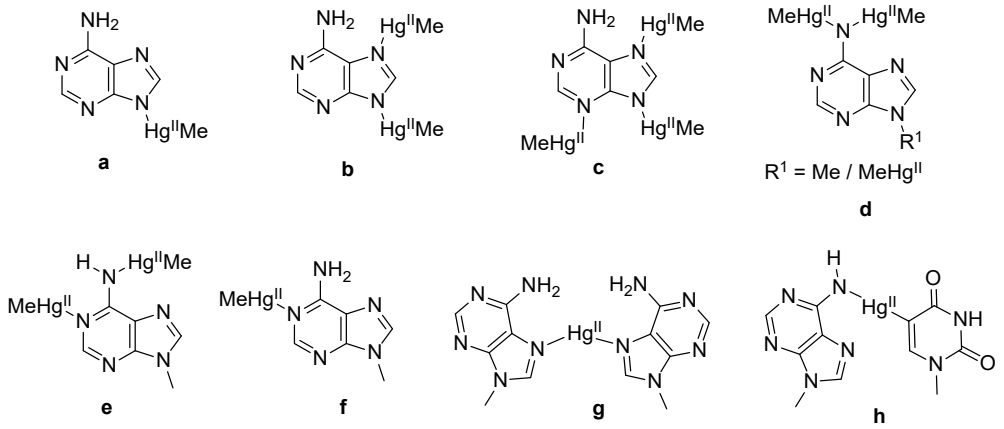

Figure 8. Crystal structures of adenine-MeHg(II) / Hg(II) interactions.

Hg(II) can also act as a bridge between two 9-methyladenines by forming the N7—N7 cross-linked complex g.[134] Finally, covalently C5-mercurated 1-methyluracil coordinates to the N6 of 9-methyladenine at pH ~ 1.2 complex h.[135]

Simpson for the first time postulated a number of complexes of guanosine with MeHg(II) and Hg(II) in solution on the basis of UV studies, later confirmed through Raman spectroscopy by Tobias and co-workers.[94,98–102,125,136] Methylmercury complexes of 7-methylguanine isolated as crystals show binding to N1, N3 and N9 (Figure 9 a). With 9-alkylated guanines (such as guanosine), on the other hand, MeHg(II) binds to N7 under acidic conditions (pH 2 - 3) (Figure 9 b) and to N1 (Figure 9 c) at higher pH (7-8).[137] Further addition of CH_3HgNO_3 to N7-mercurated guanosine leads to formation of complex d (Figure 9 d) and, in the presence of a

base, the organometallic complex e (Figure 9 e). The deprotonation of C8 under basic conditions MeHg(II) forms organometallic bond at C-8 carbon of guanine or guanosine (Figure 9 f).[138]

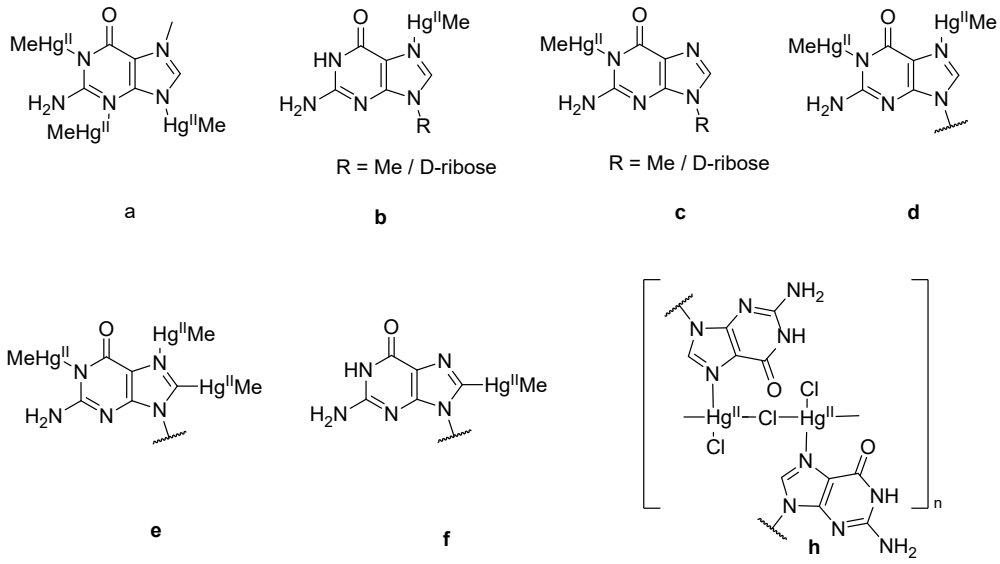

Figure 9. MeHg(II) / Hg(II)-guanine binding interaction.

Lippert and coworkers synthesized a 1D polymeric crystal structure of Hg(II)-guanine complexes.[72] The Hg(II) ions coordinated to N7 of one guanine nucleobase (1,9-dimethylguanine) with three Cl ligands, two of which acted as bridging ligands (Figure 9 h).

The most favorable coordination site for MeHg(II) and Hg(II) in the pyrimidine bases is N3 (Figure 10 a). Among the four canonical nucleobases the N3 of cytosine is the most basic site. Under alkaline conditions cytosine ligands of MeHg(II) or Hg(II) have additional possibilities of N3, N4 coordination [132] (Figure 10 b and c). Hg(II) may change the orientation of cytosine (*syn* or *anti*) by binding of Hg(II) ions at both N3 and N4. Under neutral conditions Hg(II) ions bind simultaneously through N3 and O2 either in a chelating (or semi-chelating) or a bridging fashion. Coordination of another metal ion, such as Pt(II), in addition to Hg(II), between two cytosines is also possible, giving heterodinuclear complexes (Figure 10 e).[139,140] Covalent mercuration readily takes place at C5 position of cytosine by electrophilic proton displacement reaction[141] (Figure 10 d).

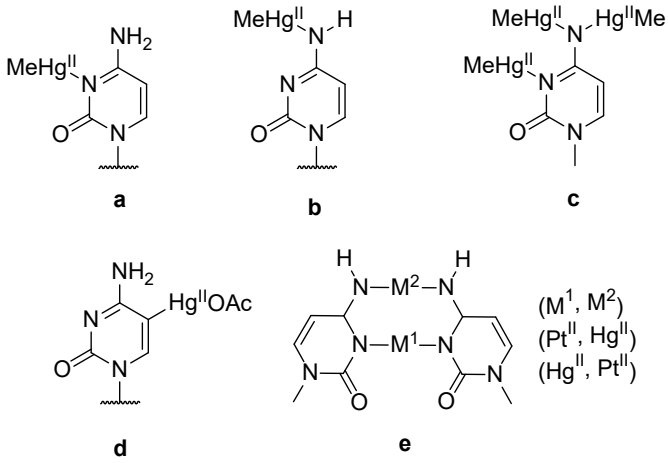

Figure 10. MeHg(II) / Hg(II)-interactions with cytosine and its analogue.

In thymine, as well as thymidine nucleoside and nucleotides, the preferred binding site of MeHg(II) and Hg(II) is N3. The first crystal structure of 1-methylthymine-Hg(II) (2:1) complex was solved by Kosturko, Folzer and Stewart in 1974.[142] The crystal structure had two thymine moieties linked by a N3-Hg(II)-N3 bridge, the N-Hg bond length being 2.04 Å, consistent with Katz's proposal of Hg(II) binding to DNA (Figure 11 a).[142] The change in Raman shift further confirmed coordination of N3 of 1-methylthymine by MeHg(II) (Figure 11 b).[94] Phenylmercuric hydroxide reacts with thymine in aqueous solution forming N3 bonded phenylmercuric thymidine derivatives (Figure 11 c).[137]

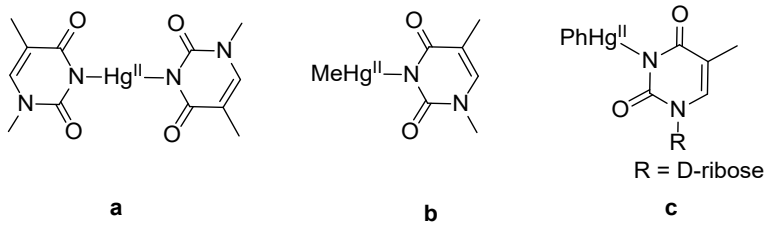

Figure 11. MeHg(II) / Hg(II)-interactions with thymine and thymidine.

In uracil the most favorable binding site of MeHg(II) and Hg(II) is N3. Coordination of Hg(II) to the N3 donors of two uridines, forming a U-Hg(II)-U base pair has been detected by UV-visible, FT-IR, and Raman spectroscopy.[102] The first crystal structures of the U-Hg(II)-U base pair, on the other hand, showed the two uracil

moieties bound to one Hg(II) through their O4 atoms (Figure 12 e), in contrast to the binding mode proposed by Katz.[143]

Covalent mercuration of uridine at C5 position was first reported by Dale *et.al.* with unprotected nucleosides as well as with various polynucleotides (Figure 12 b).[141,144,145] When both N1 and N3 are blocked by a methyl group, mercuration takes place at C5 instead (Figure 12 c).[145] Analogues with an unmasked N3, on the other hand, may form N3-Hg(II)-C5-bridged polymeric compounds.[146] In the presence of a strong ligand for Hg(II), such as Cl^-, Br^-, I^-, NO_3^-, SCN^-, CN^-, disproportionation giving rise to a C5-Hg(II)-C5 bridged dimer has been observed NMR spectrometrically and X-ray crystallographically (Figure 12 d)[147]. Nucleobase-Hg(II) interactions have also been studied by monitoring the change in the chemical shift of ^{199}Hg, for first time by Norris and Kumar.[146,148] The authors determined ^{199}Hg chemical shifts and signal widths of seven different types of MeHg(II)-nucleobase complexes in DMSO solution. Coordination of MeHg(II) to N3 of thymine and uridine (Figure 12 a) and N1 of guanosine was confirmed also by this technique. Additionally, they reported a U-Hg(II)-U base pair with a C5-Hg(II)-N3 linkage and a U-Hg(II)-6-thioguanosine base pair with a C5-Hg(II)-S6 linkage.[148] Subsequently, Lippert and coworkers reported the ^{199}Hg NMR data of (1,3-dimethyluracil-5-yl)mercury complexes.[147]

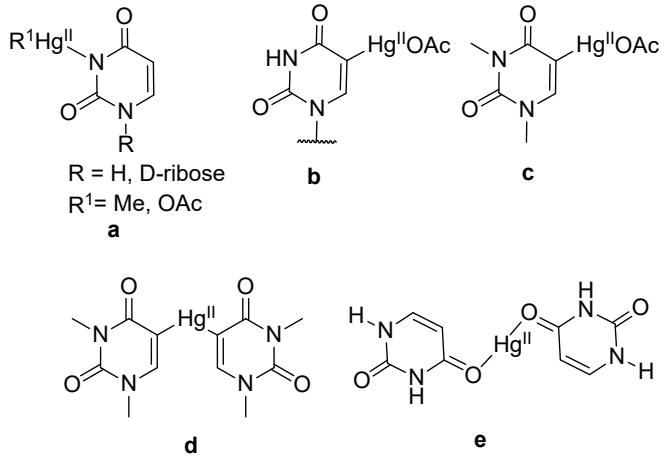

Figure 12. MeHg(II) / Hg(II)-interactions with uracil and its analogue.

1.6.4 Merccury—nucleobase interactions at oligomer level

Hg(II)-mediated base pairing within an oligonucleotide can be studied by UV melting temperature experiments.[47,82–84,87,149–154] The formation of T-Hg(II)-T base pairs in oligonucleotides has mostly been studied by UV, IR/Raman and NMR

spectrometry. In addition to these studies, theoretical calculations of thermodynamic parameters (ΔG, ΔH, ΔS, and K_d) have provided valuable insight on the formation of T-Hg(II)-T base pairs.

The binding constant of Hg(II) to duplexes with either one or two consecutive TT mispairs has been determined by various techniques including isothermal calorimetric, UV or IR/Raman titrations. The binding constant of Hg(II) to a single TT mispair at 1:1 molar ratio is 10^6 M^{-1}, significantly larger than those of nonspecific metal ion-DNA interactions.[155] The formation of T-Hg(II)-T base pairs within oligonucleotides is governed by positive enthalpy (ΔH) and positive entropy (ΔS).[153,156–160]

Based on X-ray crystal structures as well as computational studies, the positive entropy (ΔS) change arises mainly from the release of the aqua ligands of Hg(II) into bulk solution upon binding to the TT mismatch.[153,157–159] The dehydrated Hg(II) ion can bind to the two deprotonated thymine bases with significant contribution from negative binding enthalpy. In the case of consecutive TT mispairs, binding affinity of Hg(II) to the second one was larger than to the first one.[160] The decrease of covalency of N3-Hg(II) bond (bond order 0.22) compared to N3-H bond of thymine (0.50) suggested that the highly cationic nature of Hg(II) helps in the formation of T-Hg(II)-T base pairs. This positive cooperativity may be explained by the metallophilic attraction of heavy metal ions and facilitates construction of arrays of metal ions in nucleic acid sequences, as exemplified by the recent incorporation of 10 consecutive T-Hg(II)-T base pairs.[158,161]

The stability of U-Hg(II)-U and U-Ag(I)-U base pairs depends not only on the functional groups on the Watson-Crick face but also on the acidity of the uracil moiety and thus on substitution at the 5-position (Figure 14).[162] To elucidate this point, melting temperatures of duplexes formed by oligonucleotides **ON1t**, **ON1b**, **ON1f**, and **ON1cn** with the complementary strand **ON2t**, **ON2b**, **ON2f**, and **ON2cn** (Table 1) were determined at various pH in the absence and presence of Hg(II) or Ag(I). Under acidic conditions (pH 5.5), Hg(II) binds to all duplexes more readily than Ag(I). At pH 7.1, Hg(II) selectively binds to the **ON1t•ON2**t, ON1b•**ON2**b, and **ON1f•ON2f** duplexes, whereas Ag(I) selectively binds to the **ON1cn•ON2cn** duplex. Under basic conditions (pH 9.0), Ag(I) selectively binds to the **ON1b•ON2b**, **ON1f•ON2f** and **ON1cn•ON2cn** duplexes and Hg(II) to duplex **ON1t•ON2t**. In solutions containing both Hg(II) and Ag(I) ions, duplex **ON1f•ON2f** prefers Hg(II) at pH 7 and Ag(I) at pH 9. Besides affecting the acidity of the N3 donor, C5 substituents may also engage in direct interaction with Hg(II) or sterically block U-Hg(II)-U base pairing.[163]

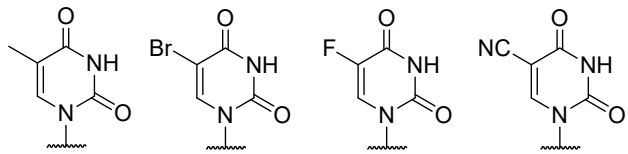

N	ON1t	ON1b	ON1f	ON1cn
pKa	9.8	8.4	7.7	6.5

Figure 14. Structures of the 5-substituted uracil bases used in oligonucleotides **ON1t**, **ON1b**, **ON1f**, **ON1cn** and **ON2t**, **ON2b**, **ON2f** and **ON2cn**.

Strand orientation plays an important role in metal-mediated base pairing. In metal-mediated duplexes, depending on the properties of the metallo-base pairs, the orientation of strands could be either antiparallel or parallel (Figure 15). In parallel duplexes, the base pairs have reverse Watson-Crick geometry. In comparison to the AT base pair, the GC base pair is unstable in parallel duplexes. As a result, most of the studies of metal mediated base pairing in parallel duplexes have been carried out on AT-rich sequences. Increased thermal stability has been observed with several parallel duplexes involving metal-mediated pairing of modified nucleobases.[149,164–171] T-Hg(II)-T base pairs can adopt both Watson-Crick and reverse Watson-Crick orientation. The first parallel duplex incorporating a T-Hg(II)-T base pair was prepared by covalently cross-linking the 5′-termini of a homothymidine and a homoadenine strand.[166] The covalently linked parallel duplex **ON3t●ON4a** was thermally stabilized by 6 °C on addition of 1 equivalent of Hg(II) (Table 1).

Table 1. Sequences used in the parallel and antiparallel duplex studies.

	Sequence	pH	T_m (no metal ions) [°C]	T_m (number of equiv. metal ions) [°C]
ON1b	5′-d(GTGACCA**U^{B}**TGCAGTG)-3′	5.5	47[a]	55[a] (1 Hg(II))
ON2b	5′-d(CACTGGT**U^{B}**ACGTCAC)-3′	7.1	48[a]	56[a] (1 Hg(II))
		9.0	41[a]	55[a] (1 Ag(I))
ON1cn	5′-d(GTGACCA**U^{CN}**TGCAGTG)-3′	5.5	42[a]	48[a] (1 Hg(II))
ON2cn	5′-d(CACTGGT**U^{CN}**ACGTCAC)-3′	7.1	44[a]	57[a] (1 Ag(I))
		9.0	39[a]	53[a] (1 Ag(I))
ON1f	5′-d(GTGACCA**U^{F}**TGCAGTG)-3′	5.5	44[a]	51[a] (1 Hg(II))
ON2f	5′-d(CACTGGT**U^{F}**ACGTCAC)-3′	7.1	47[a]	54[a] (1 Hg(II))
		9.0	41[a]	55[a] (1 Ag(I))
ON1t	5′-d(GTGACCA**T**TGCAGTG)-3′	5.5	47[a]	53[a] (1 Hg(II))
ON2t	5′-d(CACTGGT**T**ACGTCAC)-3′	7.1	49[a]	57[a] (1 Hg(II))
		9.0	48[a]	50[a] (1 Hg(II))
ON3t	5′-d(TTTTTTT**T**TTTTT)-3′	7.1	41[b]	47[b] (1 Hg(II))
ON4a	5′-d(TAAAAA**T**AAAAA)-3′			
ON5a	5′-d(AAA AAA AAA **I**TA ATT TT**I** AAT ATT T)-3′	5.5	28[c]	42[c] (2 Hg(II))
ON6t	5′-d(TTT TTT TTT **I**AT TAA AA**T** TTA TAA A)-3′	6.8	27[c]	38[c] (2 Hg(II))
ON7a	5′-(AAA AAA AAA **I**TA ATT TT**I** AAT ATT T)-3′	5.5	28[c]	42[c] (2 Hg(II))
ON8t	5′-d(TTT TTT TTT **C**AT TAA AA**T** TTA TAA A)-3′	6.8	27[c]	38[c] (2 Hg(II))
ON9i	5′-d(GAGGGA**I**AGAAG)-3′	6.8	36.7[d]	41.0[d] (1 Hg(II))
ON10i	5′-d(CTCCCT**I**TCTTTC)-3′			
ON11a	5′-d(^{i}GA^{i}G^{i}G^{i}GA**T**A^{i}GAAA^{i}G)-3′	6.8	46.9[b]	54.9[b] (2Hg(II))
ON12c	5′-(dCTCCC T **ε**A TC TTT C)-3′	9.0	43.9[b]	45.9[b] (2Hg(II))
ON13t	5′-d(CTT TCT **T$_{NPP}$**TC CCT C)-3′	6.8	29.4[e]	29.3[e], 46.2[e] (1 Hg(II))
ON14t	5′-d(GAGGGA**T$_{NPP}$**AG AGAG)-3′	9.0	29.5[e]	28.8[e], 43.4[e] (1 Hg(II))
ON15t	5′-d(CGCG**TT**GTCC)-3′	6.0	25[g]	54[g] (2 Hg(II))
ON16t	5′-d(GCGC**TT**CAGG)-3′			
ON17a	5′-d(GCGC**TTTT**CCGC)-3′			(1 Hg(II))
ON17b	5′-d(ATGGG**TT**CCAT)-3′			(1 Hg(II))
ON18c	5′-d(GCGC**TTT**GCGC)-3′			(1.5 Hg(II))

Experimental conditions. a) 2 μM duplex, 4 μM metal ion, 100 mM $NaNO_3$, 10 mM appropriate buffer (sodium cacodylate HCl buffer for pH 5.5 and 7.0, and boric acid NaOH for pH 9.0); b) 2 μM duplex, 2.4 μM $Hg(NO_3)_2$, 100 mM NaCl, 10 mM MOPS buffer for pH 7.1; c) 2 μM duplex, 2 μM $Hg(ClO_4)_2$, 500 mM $NaClO_4$, 2.5 mM $Mg(ClO_4)_2$, 5 mM buffer (MES, pH 5.5 and MOPS, pH 6.8); d) 1 μM duplex, 1 μM $Hg(ClO_4)_2$, 150 mM $NaClO_4$, 2.5 mM $Mg(ClO_4)_2$, 5 mM MOPS (pH 6.8); e) 1 μM duplex, 2.5 mM $Mg(ClO_4)_2$, 150 mM NaCl, 5 mM buffer (pH 6.8: MOPS, pH 9.0: borate); g) 5 μM duplex, 10.5 μM $Hg(ClO_4)_2$, 100 mM $NaClO_4$, 10 mM Na-cacodylate buffer.

A glycol nucleic acid (GNA) based nucleoside analogue bearing a bidentate 1*H*-imidazo[4,5-*f*][1,10]phenanthroline (**I**) ligand as the base moiety form a stable Hg(II)-mediated **I**-Hg(II)-T base pair in both parallel and antiparallel duplexes (Figure 15e,f).[168,169] The duplex **ON5a●ON6t** having two GNA (**I**) nucleosides forms Hg(II) mediated base pairs with thymine as the preferred partner (Figure 15f).

At pH 5.5 and pH 6.8 duplex **ON5a●ON6t**, holding two Hg(II) ions, is thermally stabilized by 14 and 11 °C, respectively. Heterometallic assemblies of Ag(I) and Hg(II) were also created in duplex **ON7a●ON8t** by changing one **I**T pair to an **I**C pair.[168] The same heterometallic assembly was obtained regardless of the order of introduction of the two metal ions. In the context of antiparallel **ON9i●ON10i** duplexes,[169] formation of stable **I**-Hg(II)-**I** base pair was stabilizing by 4.3 °C. The respective duplex incorporating the hetero base pair **I**-Hg(II)-**T** in place of the **I**-Hg(II)-**I** base pair, in turn, was stabilized by the 14.5 °C with respect to the unmercurated counterpart.

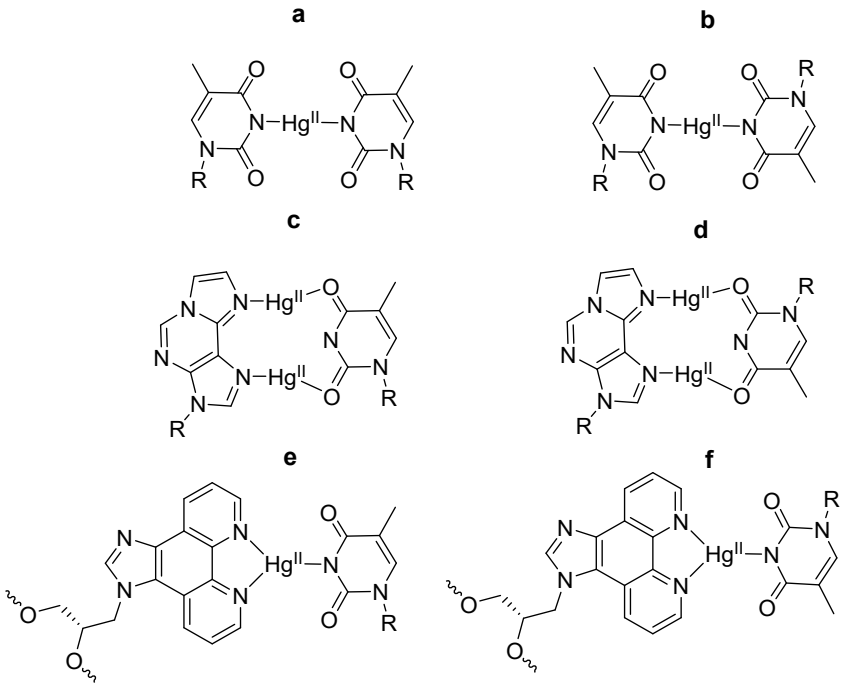

Figure 15. Hg(II)-mediated base pairs between natural and artificial nucleobases with Watson-Crick (antiparallel duplex orientation) and reverse Watson-Crick (parallel duplex orientation) geometry.

In addition to mononuclear metal-mediated base pairs, a variety of dinuclear or trinuclear metal-mediated base pairs have been incorporated in oligonucleotide duplexes.[149] Müller and coworkers reported metal mediated base pair formation in parallel duplexes using the modified purine nucleobase 1,N^6-ethenoadenine (**εA**).[149,168,170,172] 1, N^6-ethenoadenine has an additional fused imidazole ring than can also serve as a transition metal binding site, making it capable of simultaneously binding two metal ions with the N-M bonds oriented in a parallel alignment to form

a dinuclear metal mediated base pair.[170] When a thymine residue is introduced opposite to the **ε**A in the parallel duplex **ON11a●ON12c**, the resulting reversed base pair can bind two Hg(II) ions (Figure 15d). In the **ε**A-Hg(II)$_2$-T base pair, both Hg(II) ions are coordinated by an endocyclic nitrogen atom of **ε**A and an exocyclic oxygen atom of thymine. The thermal stability of the corresponding dimetallated duplex was increased by 8 °C relative to its unmercurated counterpart (Figure 15d).

Recently, light-triggered metal-mediated base pairing was reported by Müller and coworkers.[173] Instead of thymine residue in the double helical structures, the authors used caged 2′-deoxythymidine derivatives having a photolabile ortho-nitrophenylpropyl protecting group at the exocyclic O4 position. The 1*H*-imidazo[4,5-*f*][1,10]phenanthroline bidentate ligand was employed as the complementary nucleobase. Initially, duplex **ON13t●ON14t** (Table 1) was destabilized due to the bulky protecting group and addition of Hg(II) did not affect duplex stability. After irradiation of duplex **ON13t●ON14t** at 260 nm in the presence of Hg(II) ions, the duplex stabilized by 16.9 °C.

Binding of Hg(II) to thymine N3 can be detected through the loss of the respective imino proton signal in the ^{1}H NMR spectrum in H_2O. For example, Ono *et. al.* monitored the disappearance of the imino proton resonance after the addition of 1 equivalent of Hg(II) to oligonucleotide duplex **ON15t●ON16t**, incorporating two consecutive TT mispairs.[151] In NMR time scale the bridging Hg(II) does not readily transfer between neighboring TT pairs but two distinct sets of NMR signals were observed.

^{15}N labeled nucleobases have been used primarily to detect hydrogen bonding within oligonucleotides through the scalar coupling by 1D and 2D NMR experiments.[174–179180] Buchanan and coworkers introduced ^{15}N NMR spectroscopy for probing Hg(II)-DNA interactions.[179,181,182] Hg(II) interaction was monitored with labelled guanosine, cytosine, adenosine and inosine. The very large change in the chemical shift of ^{15}N labelled guanosine N7, but not N1, indicated that Hg(II) binds to the N7 of guanosine. Subsequently, Froystein *et. al.* used ^{15}N NMR to show that within the [d(CGCGAATTCGCG)]$_2$ homoduplex, Hg(II) binds to the AT base pairs. The changes in chemical shift of the imino protons of thymine and cross peak splitting pattern of the ^{1}H-^{15}N HMBC spectra confirmed that Hg(II) interacts solely with the AT base pairs, through bridging of adenine N6 and thymine O4.[174]

Ono and coworkers studied a thymidine-labeled version of the same DNA duplex as used in the Hg(II) titration experiments above to determine the structure of the T-Hg(II)-T base pair by ^{15}N 1D NMR spectroscopy[176] (Figure 16). Splitting of the thymidine ^{15}N resonance ($^2J_{NN}$) in duplex **ON15t●ON16t** with one or two Hg(II) ions provided compelling evidence for the formation of T5-Hg(II)-T16 and T6-Hg(II)-T15 base pairs. To evaluate the magnitude of chemical shift perturbation of N3 of thymidine upon Hg(II) binding, chemical shift of thymidine N3 was measured

with and without Hg(II) ions by ^{1}H-^{15}N HSQC. A large downfield shift of approximately 30 ppm was observed upon Hg(II) binding, underlining the promise of ^{15}N NMR for detection of Hg(II)-mediated base pairing.[176]

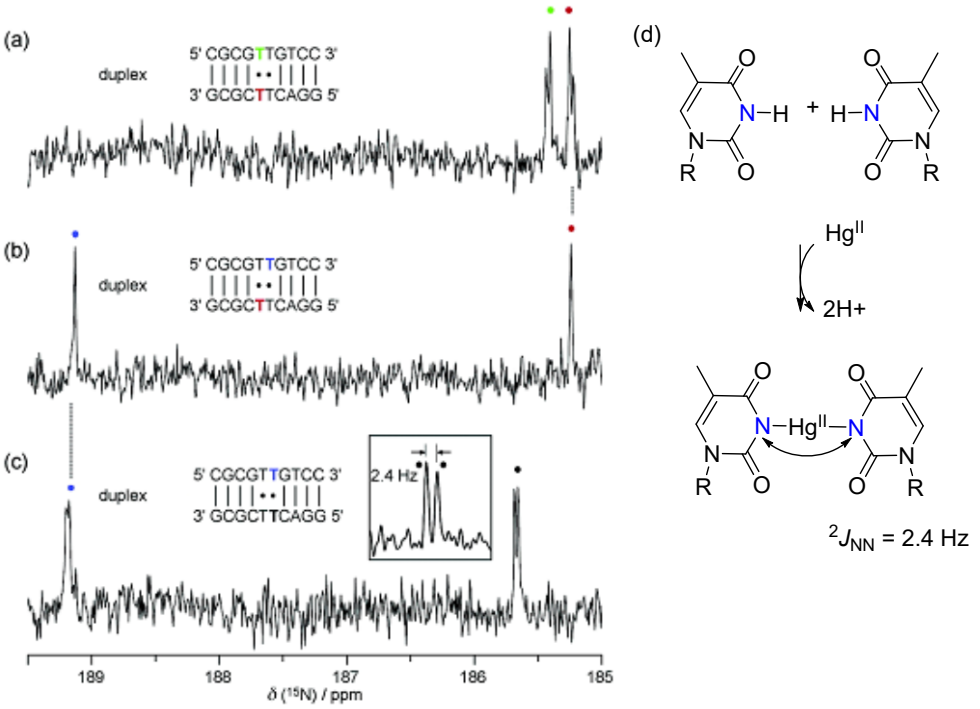

Figure 16. ^{15}N NMR spectra of Hg(II)-duplex (2:1) complexes and the base pairing mode: (a) duplex (1•3)-Hg(II) complex; (b) duplex (2•3)-Hg(II) complex; (c) duplex (2•4)-Hg(II) complex. The inset of panel (c) shows the resolution-enhanced spectrum of the N-3 resonance of T 16 [N3(T 16)]. The coupling constant of T5-Hg(II)-T16 ($^{2}J_{NN}$) is shown in Hz as an absolute value. N3 resonances of the thymidines are labeled with colored circles. Each color represents the position of the residue. ^{15}N- frequency (0 ppm) is 81.07646745 MHz. Reprinted with permission from *J. Am. Chem. Soc.*, **2007**, 129, 244-245. Copyright 2007 American Chemical Society[176]; (d) base pairing mode in the ^{15}N labeled thymidine (^{15}N with a blue color).

NMR spectrometric data revealed dynamic interconversion of a DNA duplex containing C-Hg(II)-T base pairs between A and B conformations, connected to different binding modes of the metal-mediated base pair. Different coupling constants between ^{1}H and ^{15}N indicated equilibrium between a major C(N3)-Hg(II)-T(N3) base paired and a minor C(N4)-Hg(II)-T(N3) base paired species, exhibiting B and A form helical conformation, respectively.[183] Ono and coworkers used also ^{199}Hg spectroscopy to detect Hg(II)-mediated base pairing in oligonucleotide duplexes. They measured 1-bond coupling constants between directly bonded ^{199}Hg

and ^{15}N in T-Hg(II)-T base pairs.[146,178,184–186]. Comparison of observed and predicted ^{199}Hg chemical shifts (1784 and 1848, respectively) and coupling constants (1050 and 931 Hz, respectively) also supported T-Hg(II)-T base pairing.

Uracil derivatives bearing a fluorophore at C5 allow fluorometric detection of Hg(II)-mediated base pairing. A recent study using 5-methoxybenzofuran-funcitonalized U, for example, revealed that Hg(II) binds better to a TT mispair within a DNA/RNA heteroduplex than to a UU mispair within an RNA/RNA homoduplex.[187]

Crystal structures of oligonucleotides can provide valuable information on metal-mediated base pairing.[188–195] The first crystal structure of a DNA duplex containing T-Hg(II)-T base pairs was reported by Kondo and coworkers at a resolution of 2.7Å.[192] Crystal structure of the dodecamer DNA homoduplex [5′-d(CGCGATTTCGCG)-3′]$_2$ was solved both in the presence and absence of Hg(II). Formation of T-Hg(II)-T base pairs was found to stabilize the B conformation of DNA. In contrast, the TT mismatch containing double helical structure was largely distorted. The relatively short mercury-mercury distance (2.0 Å) inside the DNA suggests stabilizing metallophilic attraction between the Hg(II) ions of consecutive T-Hg(II)-T base pairs (Figure 17).

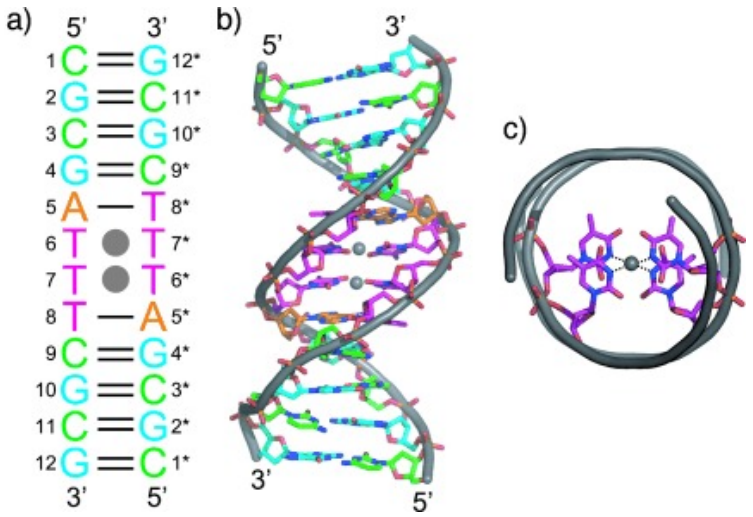

Figure 17. a) Secondary structure of a double helix containing two consecutive T-Hg(II)-T base pairs and b), c) crystal structures (side vive and top view, respectively) of the same B-form double helix. In these figures, Hg(II) ions are shown as gray spheres. In (c), only the two T-Hg(II)-T base pairs are shown, and dashed lines represent covalent bond between N3 of T and Hg(II). Reprinted with permission from Kondo, J.; Yamada, T.; Hirose, C.; Okamoto, I.; Tanaka, Y.; Ono, A. *Angew. Chemie - Int. Ed.* **2014**, *53*, 2385–2388. Copyright (2014) WILEY-VCH Verlag GmBH & Co. KGaA, Weinheim.[192]

Theoretical calculations not only support the existence of an N3-Hg(II)-N3 linkage in the T-Hg(II)-T base pair but also suggest a probable two-step mechanism for the binding of Hg(II) (Scheme 1). [47,153,155–160,192,196–199] The first step involves abstraction of the thymine imino protons by a Hg(II) hydroxo ligand and concomitant coordination of Hg(II) to the newly deprotonated N3. The water molecule formed by the combination of the released imino proton and hydoxo ligand is no longer coordinated to Hg(II) but assists in imino proton transfer to thymine O2. Coordination of Hg(II) to N3 of the other thymine appears to be the rate-limiting step, involving either tautomerization of the remaining Hg(II)-nonbonded thymine base or deprotonation by the hydroxo ligand of the Hg(II) ion already bound to the first thymine base.

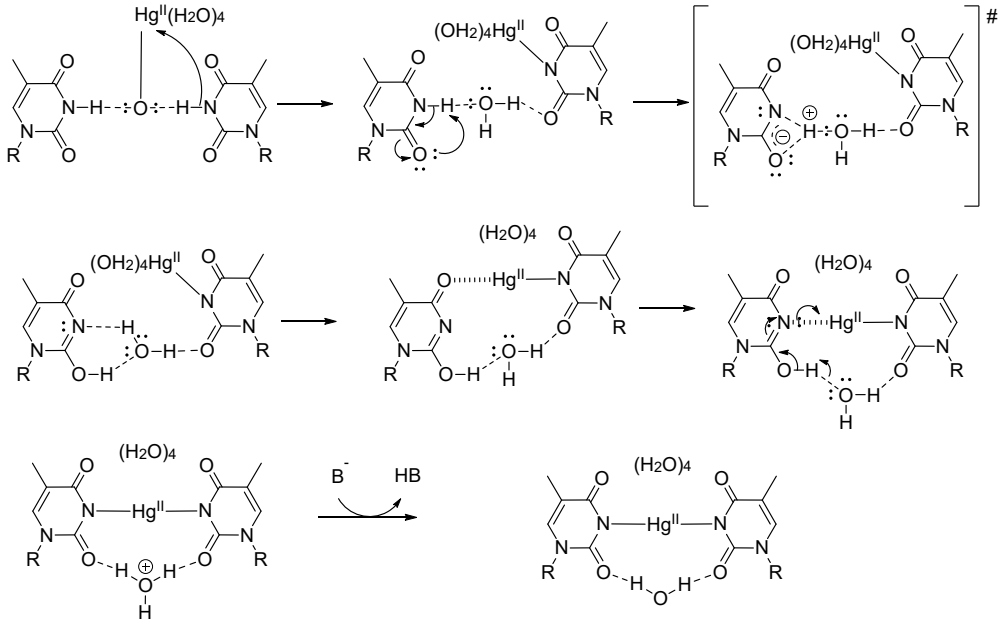

Scheme 1. Proposed mechanism of the formation of a T-Hg(II)-T base pair.

1.6.5 Applications of mercury-mediated base pairing

The bottom-up approach of self-assembly properties of DNA molecules provides a diverse approach to develop DNA nanotechnology. The precise base-pairing system, dynamic nature of hybridization, chemical stability and inertness of DNA molecules allows generating the predicted nanostructures in a programmable manner. The DNA nanostructures can be achived with natural as well as synthetic DNA with different entities including metals excesivley expedient in the biomedical applications.[200–205]

The affinity of Hg(II) to T has been used to induce nucleic acid sequences to adopt various types of secondary structures such as duplexes[116,119,183], triplexes[206], G-quadruplexes[207] and hairpins.[208–210] Hg(II) binding to TT mispairs can lead to formation of stable inter- and intrastrand cross-linked secondary structures. The first example of Hg(II)-induced transformation of a duplex to a hairpin was reported by Kuklenyik and Marzili using oligonucleotides containing stretches of several thymines between two mutually complementary strands.[208] The sequences were designed to allow the oligonucleotides to from either a duplex or a hairpin (Figure 18). These oligonucleotides were designed to adopt the hairpin structures in the absence of Hg(II). ^{1}H and ^{13}CNMR spectrometric titration with $Hg(NO_3)_2$ has been used to confirm the secondary structures. The appearance of a new set of ^{1}H and ^{13}C signals with concomitant decay of the free oligonucleotide's signals indicates that $Hg(NO_3)_2$ formed an adduct with the oligonucleotide. **ON17a** forms a stable hairpin with a T-Hg(II)-T cross-link between the first and the fourth T residue of the loop (Figure 18 a). Oligonucleotides **ON17b** and **ON18c**, with two or three consecutive T bases in the loop, also formed hairpin structures in the absence of Hg(II). In contrast to **ON17a**, however, addition of Hg(II) lead to homoduplex formation with interstrand cross-linking of the T-rich stretches (Figure 18 b and c). Apparently an intraloop Hg(II)-mediated base pairing would cause too much strain within the shorter loops.

Metal induced conformational changes have also been followed by isothermal calorimetric titrations, proving that Hg(II) induces random coil single stranded thymine rich oligonucleotides to adopt hairpin structures.[210] Another example utilized T-Hg(II)-T base pairing in the loop of chair-type G4 structures to reduce the polymorphism of G4 structures and stabilize the G4 conformation.[207]

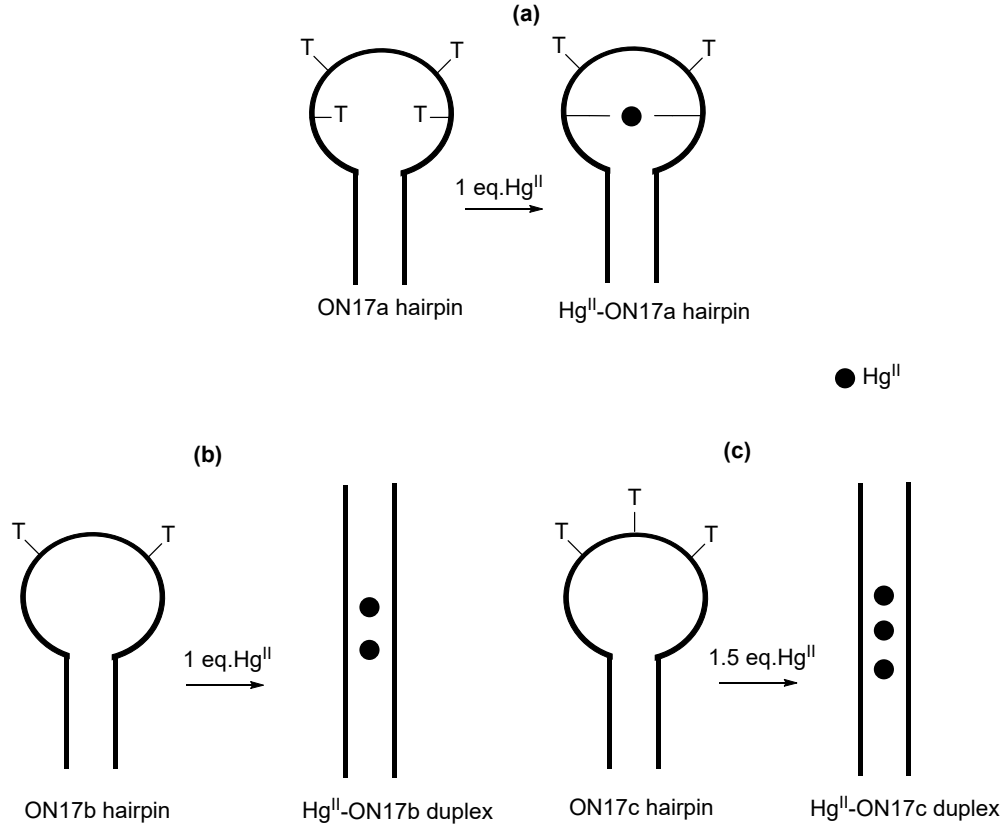

Figure 18. Hg(II)-mediated duplex-hairpin equilibrium of partly self-complementary oligonucleotide; a) equilibrium between duplex and hairpin; b) intramolecular Hg(II)-mediated hairpin formation, c and d) Hg(II)-mediated duplex formation.

The incorporation of one or multiple metal ions into nucleic acids through coordination to natural or artificial nucleobases is currently of great interest for the development of DNA therapeutics and nanotechnology. After Shionoya´s first report of artificial nucleosides for alternative DNA base pairing, diverse metal ions have been incorporated into nucleic acid sequences.[78,79,82,87,150,154,189,192,211–214] Oligonucleotides incorporating modified nucleobases exploit the programmable self-assembling properties of nucleic acids but can also expand them through recognition of different metal ions.

Kondo and coworkers reported the crystal structure of a metallated nanowire consisting of an array of Hg(II)-mediated base pairs.[198] Pentanucleotides d(TTTGC) were mixed with Hg(II) in an appropriate solution, yielding right-handed antiparallel double helices with Hg(II) ions embedded along the axis. The crystal structure revealed formation of T-Hg(II)-T and G-Hg(II)-T pairs as well as a water-mediated CC base pair (Figure 19).

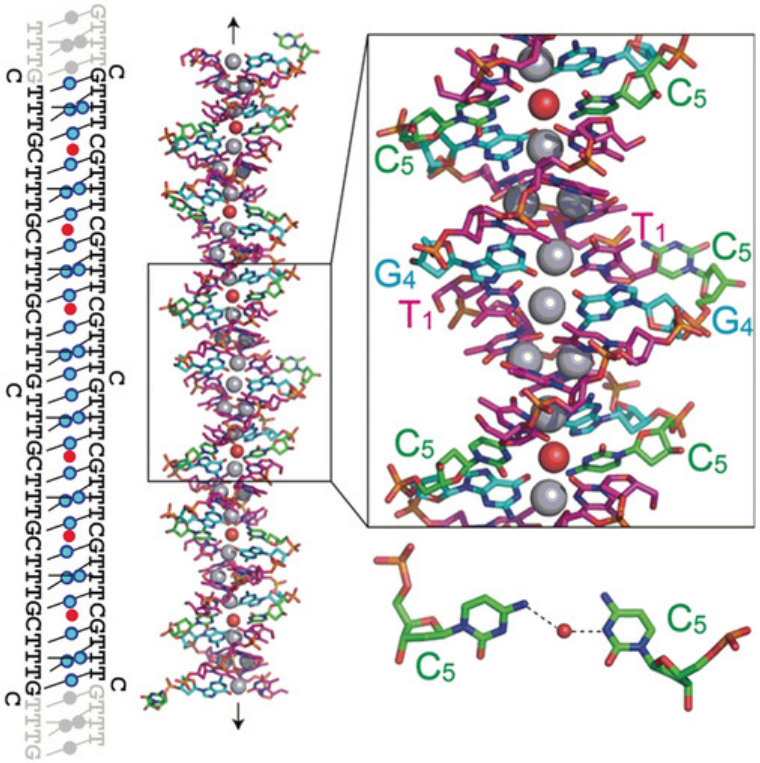

Figure 19. A wire-like structure composed of dsDNA units. Mercury ions and water oxygen atoms are illustrated as gray and red spheres, respectively. Hydrogen bonds are shown as dashed lines in the water-mediated CC base pair. Reprinted with permission from Ono, A.; Kanazawa, H.; Ito, H.; Goto, M.; Nakamura, K.; Saneyoshi, H.; Kondo, J. *Angew. Chemie - Int. Ed.* **2019**, *58*, 16835–16838. Copyright (2019) WILEY-VCH Verlag GmbH & Co. KGaA, Weinheim.[198]

An appropriate combination of ligands allows more than one kind of metal ion to be incorporated into a nucleic acid sequence.[82,83,87,215,216] Tanaka *et.al.* reported the programmable assembly of Cu(II) and Hg(II) within double helical structures through metal-mediated base pairing.[215] Two hydroxypyridone nucleobases (**H**) and one intervening pyridine nucleobase (**P**) were incorporated in the short [5′-d(G**HPH**C)-3′]$_2$ DNA homoduplex in addition to canonical nucleobases at each terminus. Cu(II) binds between the hydroxypyridone nucleobases (**H**) and Hg(II) between the pyridine nucleobases in a programmable manner (Figure 20). Addition of Cu(II) and Hg(II) was monitored by UV spectrophotometric and CD spectropolarimetric titration. Similar studies have been carried out on longer duplexes incorporating Cu(II)-salen and T-Hg(II)-T base pairs.[215]

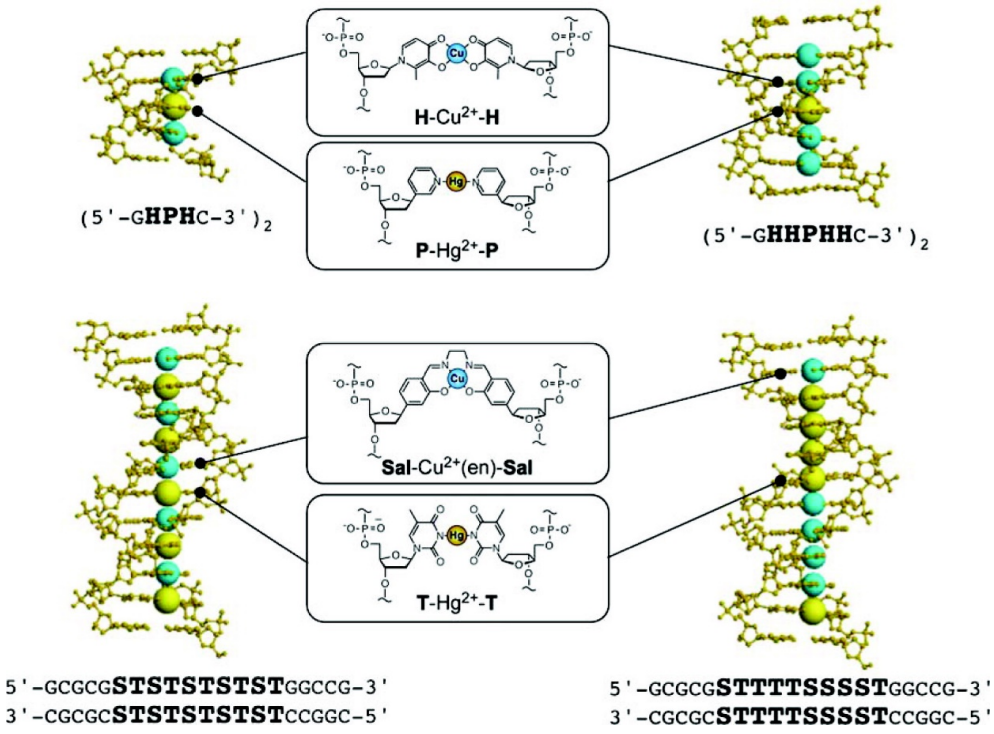

Figure 20. Incorporation of Cu(II)- and Hg(II)-mediated base pairs in double helical structures by using hydroxypyridone (**H**), salicylic aldehyde (**S**) with ethylene diamine, pyridine (**P**) and thymine (**T**) nucleobases. Reprinted with permission from Tanaka, K.; Shionoya, M. *Coord. Chem. Rev.* **2007**, *251*, 2732–2742; Takezawa, Y.; Shionoya, M. *Acc. Chem. Res.* **2012**, *45*, 2066–2076. Copyright (2007) Elsevier and Copyright (2012) American Chemical Society.[82,87]

Another way to build metal-mediated base pairs is by enzymatic polymerization. The feasibility of this approach has been demonstrated with Hg(II)-, Ag(I)- and Cu(I)-mediated base pairs.[161,187,217–225] Taq DNA polymerase can recognize thymine in the presence of Hg(II) and incorporate thymidine 5'-triphosphate (dTTP) opposite to it by formation of a T-Hg(II)-T base pair.[220] Up to ten consecutive Hg(II) ions were embedded as T-Hg(II)-T base pairs by Therminator DNA polymerase (Th) catalyzed primer extension reaction in the presence of Mn(II) ions.[161] Six consecutive Hg(II) ions were introduced in RNA double helices through *in vitro* transcription by T7 RNA polymerase. Various experimental techniques such as NMR spectroscopy, dynamic light scattering (DLS), UV, and CD spectroscopy confirmed the formation of U-Hg(II)-U pairs in the middle of an RNA double helix.[219]

1.6.6 Organometallic approach of Hg(II)-mediated base paring

Coordinative interaction between DNA and Hg(II) has been extensively studied, the T-Hg(II)-T base pair being a well-documented example of such interactions. Coordinative DNA-metal interactions, however, suffer from limitations in both DNA therapeutics as well as DNA nanotechnology, notably stability in metal-deficient media. Integration of organometallic bases into oligonucleotides can overcome some of these issues. Organometallic compounds comprise at least one bond between a metal and a carbon atom of the organic moiety. Even though the first organometallic nucleobases were synthesized by Dale and coworkers[141,144,218] already in the early 1970s, this type of compounds remains unexplored in oligonucleotides despite their promise for introducing various functionalities. One reason is undoubtedly the well-known toxicity of mercury and small molecular organomercury compounds, such as methylmercury. On the other hand, the high aqueous solubility of oligonucleotides, even covalently mercurated ones, should make them considerably less toxic than typical organomercury compounds.

To be useful in oligonucleotide therapeutics, metal-mediated base pairs have to persist in the metal-deficient intracellular medium. In principle, sufficiently stable complexes can be achieved either by kinetically inert metal ions, such as Pt(II) or Ru(II), or by using labile metal ions such as Hg(II) or Pd(II) in organometallic complexes. Natural nucleobases offer limited sites for covalent metalation and therefore artificial nucleobases are being studied as an alternative. Metals can incorporated covalently into oligonucleotides by various methods such as electrophilic aromatic substitution[226–233], ligand directed metalation[234–237], oxidative addition[238], and post synthetic conjugation with an organometallic moiety.[237,239] Mercury is particularly attractive in this regard owing to the easy accessibility of arylmercury compounds through electrophilic aromatic substitution with Hg(II) salts.

2 Aims of the thesis

Metal-mediated base pairs have attracted considerable attention during the past decades because of their potential in therapeutic applications as well as in DNA nanotechnology. The potential of metal-mediated base pairing to stabilize DNA and RNA secondary structures has been studied with a wide variety of metal ions using natural and artificial nucleobases. One of the most extensively studied metal ions in this context is Hg(II). Although Hg(II)-mediated base pairs have been successfully introduced to diverse nucleic acid sequences, several shortcomings, such as off-target metalation and stability in metal-deficient media have been identified. Covalently mercurated nucleobases presented in this thesis were developed to overcome these weaknesses and thus provide a new alternative approach for Hg(II)-metal mediated base pairing. The primary goals of this thesis include:

I. Development of synthetic methods for natural and non-natural covalently mercurated nucleoside analogues.
II. Development of synthetic and purification methods for oligonucleotides incorporating covalently mercurated nucleoside analogues.
III. Elucidation of the base pairing properties of covalently mercurated nucleoside analogues at monomer level as well as within oligonucleotides of various secondary structures.

3 Result and Discussion

3.1 Synthesis of 5-chloromercuri-2'-deoxycytidine

Preparation of 5-chloromercuri-2′-deoxycytidine was carried out using the previously described procedure[141,144] (Scheme 1).

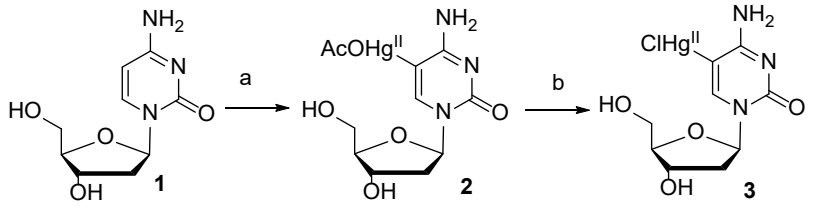

Scheme 2. Preparation of 5-chloromercuri-2′-deoxycytidine. Reagents and conditions: a) $Hg(OAc)_2$, H_2O; b) NaCl, H_2O.

3.2 Synthesis of 6-phenyl-1*H*-carbazole *C*-nucleoside and its phosphoramidite building block

For the synthesis of the 6-phenyl-1*H*-carbazole *C*-nucleoside (Scheme 3), 6-bromo-1*H* carbazole **4** was iodinated by using previously described procedure,[240] giving compound **5**. Heck coupling between {(*2R, 3S*)-3-[(*tert*-butyldimethylsily)oxy]-2,3-dihydrofuran-2-yl}methanol and 3-iodo-6-bromo-1*H*-carbazole (**5**) furnished the desilylated ketone **7** exclusively as the β anomer. Reduction of compound **7** gave 6-bromo-1*H*-carbazole C-nucleoside (**8**). Subsequently, Suzuki-Miyaura coupling of compound **8** with phenylboronic acid afforded the 6-phenyl-1*H*-carbazole *C*-nucleoside **9** and treatment of compound **9** with dimethoxytrityl chloride the 5′-tritylated *C*-nucleoside **10**. Finally, phosphitylation of the 3′-OH of compound **10** gave the phosphoramidite building block **11**.

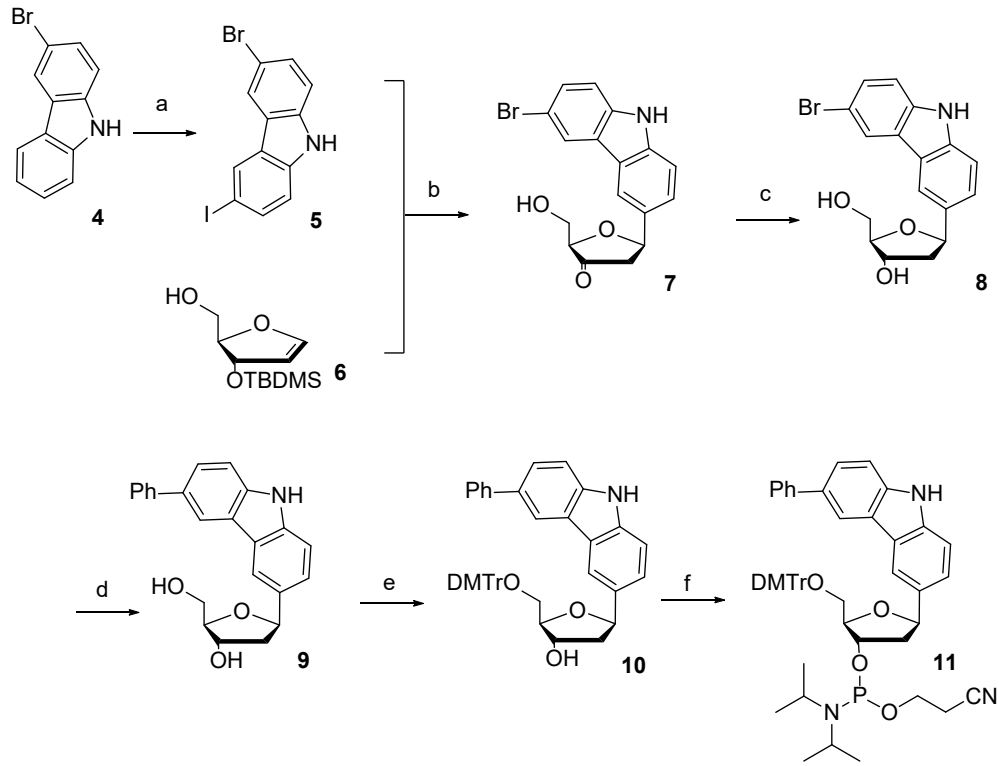

Scheme 3. Synthesis of the 6-phenyl-1*H*-carbazole *C*-nucleoside and its phosphoramidite building block. Reagents and conditions: a) $NaIO_4$, I_2, H_2SO_4, EtOH, 25 ºC, 16 h; b) $Pd(OAc)_2$, Ph_3As, Et_3N, MeCN, Ar atmosphere, 70 ºC, 15 h; c) $NaBH(OAc)_3$, AcOH, MeCN, Ar atmosphere, 0 ºC, 15 min; d) $Pd(PPh_3)_4$, $PhB(OH)_2$, K_2CO_3, MeOH: H_2O, Ar atmosphere, reflux, 15 h; e) DMtrCl, pyridine, 25 ºC, 48 h; f) 2-cyanoethyl-*N*,*N*-diisopropylchlorophosphoramidite, Et_3N, CH_2Cl_2, N_2 atmosphere, 25 ºC, 2.5 h.

3.3 Synthesis of phenol *C*-nucleoside and its phosphoramidite building block and 2,6-dimercuriphenol *C*-nucleoside

Synthesis of the Phenol *C*-nucleoside and its phosphoramidite building block (Scheme 4) was started by Heck coupling between compound **6** and 4-iodophenyl benzoate to yield compound **12**. Desilylation of compound **12** furnished the benzoyl protected ketone intermediate **13**. Reduction of compound **13** gave the benzoyl protected phenol *C*-nucleoside **14** and removal of the benzoyl group its unprotected analogue **15.** Treatment of compound **15** with $Hg(OAc)_2$ gave the 2,6-dimercurated phenol *C*-nucleoside **16**. 5′-dimethoxytritylation of the base protected nucleoside **14** afforded compound **17** and 3′-phosphitylation of this intermediate, finally, the phosphoramidite building block **18**.

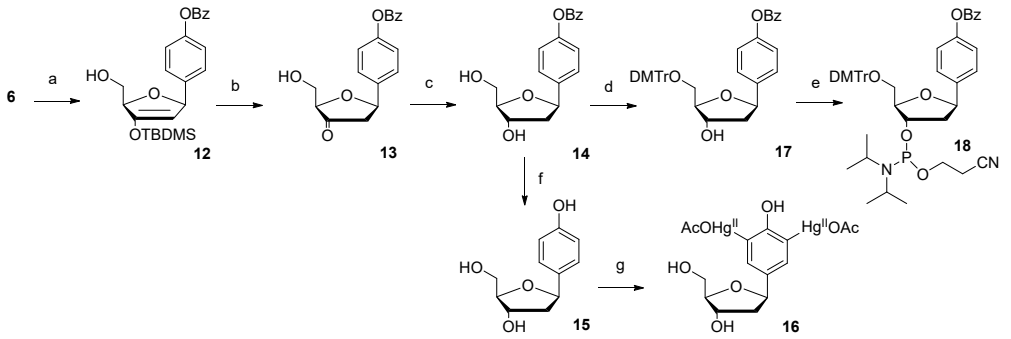

Scheme 4. Synthesis of Phenol *C*-nucleoside and its dimercurated derivative and phosphoramidite building block. Reagent and conditions: a) $Pd(OAc)_2$, $P(C_6F_5)_3$, 4-iodo-phenyl benzoate, Ag_2CO_3, $CHCl_3$, Ar atmosphere, 70 °C, 12 h; b) Et_3N•HF, THF, Ar atmosphere, 25 °C, 15 Min; c) $NaBH(OAc)_3$, MeCN, ACOH, Ar atmosphere 0 °C; d) DMTrCl, pyridine 25 °C, 16 h; e) 2-cynoethyl-*N,N*- diisopropylchlorophosphoramidite, Et_3N, CH_2Cl_2, N_2 atmosphere, 25 °C, 3 h; f) NH_3, MeOH, H_2O, 25 °C, 16 h; g) $Hg(OAc)_2$, MeOH, 25 °C, 16 h.

3.4 NMR spectrometric affinity measurements

The binding affinity and selectivity of mercurated nucleosides **3** and **16** towards natural nucleotides were studied NMR spectrometrically. Because of solubility problems with compounds **3** and **16**, the measurements were carried out with nucleoside 5′-monophosphates (AMP, CMP, GMP, TMP, and IMP) instead of nucleosides and in a mixture of deuterated 120 mM phosphate buffer (pH 7.2) and DMSO-d_6 (50:50, *v*/*v*). Control experiments were performed under the same conditions otherwise, but in the absence of a base pairing partner.

The starting concentration was 10 mM for 5-chloromercuri-2′-deoxycytidine (**3**), 4.0 mM for the 2,6-bis(acetoxymercuri)phenol *C*-nucleoside **16** and either 10 mM (in the case of **3**) or 8 mM (in the case of **16**) for the nucleoside monophosphates. The samples were diluted stepwise while keeping the solvent composition, pH, ionic strength and the molar ratio of the mercurated nucleoside analogue and the nucleoside monophosphate constant. At each dilution, a ^{1}H-NMR spectrum was acquired at 25 °C and the chemical shift of the H6 proton of **3** or the H3 and H5 protons of **16** recorded. Due to the rapid ligand exchange of Hg(II) the signals represent the average of all species in equilibrium with one another.

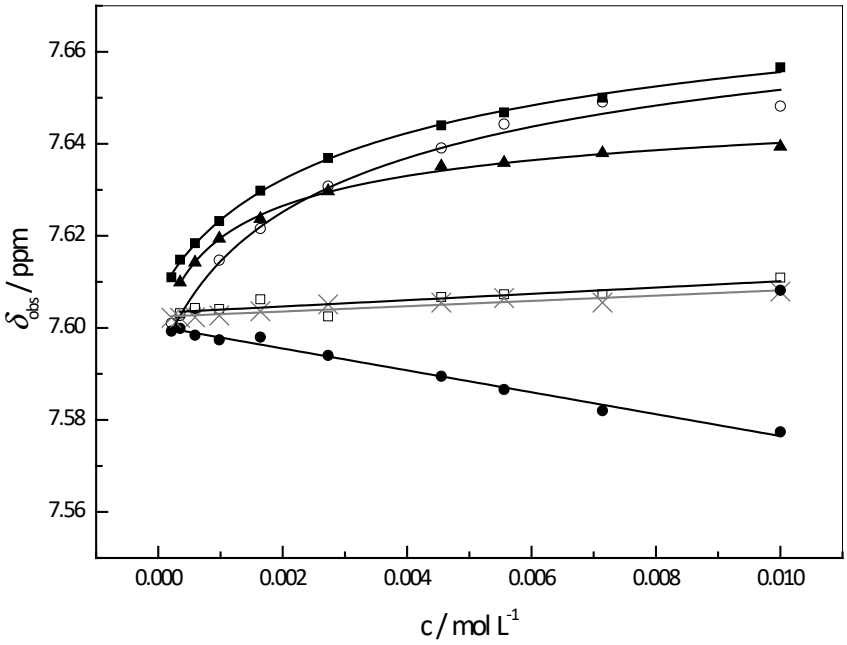

Figure 21. Chemical shift of the H6 proton of the (**3**) as a function of concentration in an equimolar mixture with 5'- AMP (●), 5'- CMP (□), 5'- GMP (▲), 5'- IMP (■) and 5'- UMP(○), as well as in the absence of any nucleoside triphosphate (×); *T* = 25 °C; pH 7.2 (120 mM phosphate buffer in D_2O / DMSO-d_6 (1:1, *v*/*v*)).

Complexes of **3** with nucleoside monophosphates fell into two distinct categories based on the dependence of the H6 chemical shift on concentration (Figure 21). Complexation with 5′-GMP, 5′-UMP and 5′-IMP induced a marked downfield shift with saturation at high concentration, while with 5′-AMP an upfield shift with no detectable deviation from linearity was observed. With 5′-CMP as well as in the absence of any nucleoside monophosphates, a very slight linear downfield shift of the H6 signal on increasing concentration was observed, suggesting little interaction between **3** and cytosine.

The stability of the binary complexes formed by **3** with nucleoside monophosphates was estimated by non-linear least-squares fitting of the data obtained with 5′-GMP, 5′-IMP and 5′-UMP to Equation (1).

$$\delta_{obs} = \delta_o + (\delta_\infty - \delta_o)\left(1 + \frac{1-\sqrt{4Kc+1}}{2Kc}\right) \quad (1)$$

where δ_0 and δ_∞ are the H6 chemical shifts at zero and infinite concentration, respectively. K is the stability constant of the binary complex and c is the concentration of 5-chloromercuri-2′-deoxycytidine and the relevant nucleoside monophosphate. Stability constants of 1000 ± 200, 290 ± 30 and 400 ± 100 M^{-1} were determined for 5′-GMP, 5′-IMP, and 5′-UMP, respectively, whereas the linear plots

obtained with 5′-AMP and 5′-CMP indicated complexes of much lower stability. This result is consistent with the fact that coordination of Hg(II) to N3 of guanine (and hypoxanthine) and N1 of thymine and uracil takes place with concomitant deprotonation of the donor atom, leading to more stable complexes than those formed by uncharged nitrogen ligands.[241] For comparison, the association constant for the GC Watson-Crick base pair has been estimated as 3.7 in DMSO at 32 °C[242] and 6.7 in a mixture of DMSO and methanol (2:1, *v*/*v*) at 30 °C.[243]

Ternary complexes of the 2,6-dimercuriphenol *C*-nucleoside **16** with nucleoside monophosphates fell into three categories based on the dependence of the chemical shift of the H3 and H5 protons on concentration (Figure 22). Increasing the concentration of **16** and 5′-UMP induced a marked downfield shift with saturation at high concentration. Saturation curves were also obtained with 5′-AMP and 5′-CMP but with an upfield shift and a somewhat lower affinity. In the case of 5′-GMP, unexpectedly, minor NMR signals were observed near the main signals of H3 and H5 which could suggest formation of higher-order secondary structures with coordination of Hg(II) to both N1 and N7 of guanine. In the absence of any nucleoside monophosphates, a very small downfield shift of the H3 and H5 signals was observed on increasing concentration of **16**, indicating negligible intermolecular interactions.

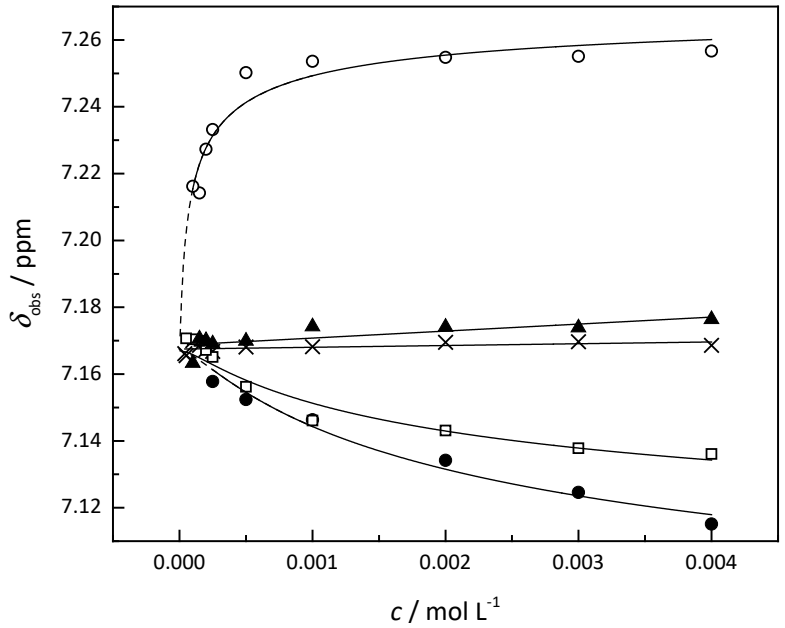

Figure 22. Chemical shift of the H3 and H5 protons of the (**16**) as a function of concentration in an equimolar mixture in a 1:2 mixture with 5'- AMP (●), 5'- CMP (□), 5'- GMP (▲) and 5'- UMP (○), as well as in the absence of any nucleoside triphosphate (×); *T* = 25 °C; pH 7.2 (120 mM phosphate buffer in D_2O / DMSO-d_6 (1:1, *v*/*v*)).

Formation of ternary 1:2 complexes between the 2,6-dimercuriphenol *C*-nucleoside **16** and the nucleoside monophosphates (AMP, CMP, GMP, UMP), assuming equal equilibrium constants for the two coordination steps, may be expressed by Equation (2).

$$\delta_{obs} = \delta_o + (\delta_\infty - \delta_o)\frac{\left(K_d + 2c - \sqrt{K_d^2 + 4K_d c}\right)^2}{4c^2} \quad (2)$$

where δ_0 and δ_∞ are the H3 and H5 chemical shifts at zero and infinite concentration, respectively. K_d is the dissociation constant for the binary complex between the 2,6-dimercuriphenol *C*-nucleoside **16** and the nucleoside monophosphate and *c* is the concentration of **16**. Dissociation of the ternary complex to its monomeric constituents was assumed to proceed in a stepwise manner and the dissociation constants for the two steps were assumed to be equal. The dissociation constants were obtained by nonlinear least-square fitting of the experimental data to equation (2) were 700 ± 200, 600 ± 300 and 15 ± 4 μM of 5′-AMP, 5′-CMP, and 5′-UMP respectively. In other words, complexation with 5′-UMP was strongly favored, consistent with deprotonation of N3 proton. The ternary complexes between 2,6-dimercuriphenol *C*-nucleoside **16** and cytosine or adenine were approximately 40-fold less stable.

3.5 Oligonucleotide synthesis

Synthesis of oligodeoxyribonucleotides was performed in a 1.0 μM scale using an Applied Biosystems incorporated 3400 automated DNA/RNA synthesizer and traditional phosphoramidite strategy. Sequences and structural modifications of the oligonucleotides studied are summarized in table 2. The detailed syntheses of mercurated oligonucleotides are schematically described in scheme 3. Oligonucleotides **ON18c-ON18t**, **ON19a-ON19s**, **ON20c-ON20u**, **ON21a-ON21t**, **ON22a-ON22t**, **ON23a**, and **ON24a-ON24s** were commercially purchased and used as received. The modified oligonucleotide sequences were constructed with 5-methylcytosine residues instead of cytosine residues to avoid off-target mercuration. For duplex studies, oligonucleotides **ON18c** and **ON18z** were synthesized incorporating a cytosine or a 6-phenyl-1*H*-carbazole residue in the middle of the chain. In the case of TFOs **ON20c and ON20u**, a 15-mer homothymine sequence was extended at the 3′-terminus with a cytosine or a uracil residue, respectively. Finally, oligonucleotide **ON23f**, designed for recognition of a non-canonical nucleic acid structure, incorporated a phenol *C*-nucleoside between two 7-mer homoadenine sequences. The natural phosphoramidite building blocks were incorporated into oligonucleotides following the standard oligonucleotide synthesis protocols. In the case of modified phosphoramidite building blocks (**11** and **16**), the coupling time

was increased to 300 s, with no other adjustments made to the standard coupling cycles. The coupling yields of all modified oligoncuelotide sequences were comparable to those of commercially available phosphoramidite building blocks (> 98%) according to the trityl assay. After oligonucleotide synthesis, cleavage of the solid support and deprotection of phosphate and base moieties was achieved by incubation in 33% aqueous ammonia at 55 °C for 16 h. The mercuration conditions were optimized separately for **ON18c**, **ON18z ON20c**, **ON20u** and **ON23f** and summarized in Scheme 5. The mercuration reactions were monitored by RP HPLC and HRMS.

Purification of the modified oligonucleotides **ON18c**, **ON18z** and **ON23f** was performed by RP HPLC using a mixture of aqueous triethylammonium acetate buffer and acetonitrile as eluent. With **ON18c-Hg**, the reaction mixture was first diluted with saturated aqueous NaCl to precipitate any remaining free Hg(II), after which the RP HPLC purification was carried out as described above. In the case of **ON20c-Hg** and **ON20u-Hg** repeated RP-HPLC purifications were carried out for complete removal of excess mercury salts.

Purification procedure for the dimercurated oligonucleotide **ON18z-Hg2** consisted of two RP HPLC runs, the first one including EtSH in the eluent to suppress nucleobase coordination of Hg(II) (either free or as part of the organomercuric oligonucleotide). With this solvent system, the dimercurated product was clearly separated from the unreacted starting material. The second RP HPLC run, affording the pure oligonucleotide without thiol contaminants, was carried out as described above. **ON23-Hg2**, in turn, was first fractioned by anion exchange HPLC eluting with a gradient of $NaClO_4$ in a TRIS•MsOH buffer (pH = 7), after which the fraction containing the desired material was purified by RP HPLC as described above.

Table 2. Oligonucleotides sequences used in the hybridization studies.

	Sequence[a]
ON18c	5´-d(C^{m}GA GC^{m}**C** C^{m}TG GC^{m}) -3´
ON18c-Hg	5´-d(C^{m}GA GC^{m}**C^{Hg}** C^{m}TG GC^{m}) -3´
ON18z	5´-d(C^{m}GA GC^{m}**Z** C^{m}TG GC^{m}) -3´
ON18z-Hg2	5´-d(C^{m}GA GC^{m}**Z^{Hg2}** C^{m}TG GC^{m}) -3´
ON18t	5´-d(C^{m}GA GC^{m}**T** C^{m}TG GC^{m}) -3´
ON19a	5´-d(GCC AG**A** GCT CG) -3´
ON19c	5´-d(GCC AG**C** GCT CG) -3´
ON19g	5´-d(GCC AG**G** GCT CG) -3´
ON19t	5´-d(GCC AGT GCT CG) -3´
ON19s	5´-d(GCC AG**S** GCT CG) -3´
ON20c	5´- d(TTT TTT TTT TTT TTT **C**) -3´
ON20c-Hg	5´- d(TTT TTT TTT TTT TTT **C^{Hg}**) -3´
ON20u	5´- d(TTT TTT TTT TTT TTT **U**) -3´
ON20u-Hg	5´- d(TTT TTT TTT TTT TTT **U^{Hg}**) -3´
ON21a	5´-d(G**A**T TTT TTT TTT TTT TTG C) -3´
ON21c	5´-d(G**C**T TTT TTT TTT TTT TTG)-3´
ON21g	5´-d(G**G**T TTT TTT TTT TTT TTG) -3´
ON21t	5´- d(G**T**T TTT TTT TTT TTT TTG) -3´
ON22a	5´- d(GCA AAA AAA AAA AAA AA**A** C) -3´
ON22c	5´- d(GCA AAA AAA AAA AAA AA**C** C) -3´
ON22g	5´- d(GCA AAA AAA AAA AAA AA**G** C) -3´
ON22t	5´- d(GCA AAA AAA AAA AAA AA**T** C) -3´
ON23f	5´-d(AAA AAA A**F**A AAA AAA) -3´
ON23f-Hg2	5´-d(AAA AAA A**F^{Hg2}** A AAA AAA) -3´
ON23a	5´-d(AAA AAA AA A AAA AAA) -3´
ON24a	5´-d(TTT TTT T**A**T TTT TTT)-3´
ON24c	5´-d(TTT TTT T**C**T TTT TTT)-3´
ON24g	5´-d(TTT TTT T**G**T TTT TTT)-3´
ON24t	5´-d(TTT TTT T**T**T TTT TTT)-3´
ON24s	5´-d(TTT TTT T**S**T TTT TTT)-3´

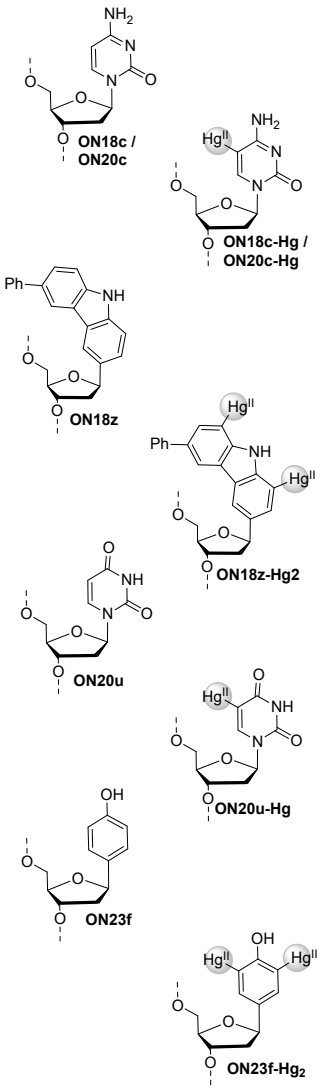

[a] C^{m} refers to 5-methylcytosine, C^{Hg} to 5-chloromercuricytosine, Z to 6-phenyl-1*H*-carbazole, Z^{Hg2} to 1,8-dimercuri-6-phenyl-1*H*-carbazole, C^{Hg} to 5-acetoxymercuricytosine, U^{Hg} 5-acetoxymercuriuracil, F to phenol, F^{Hg2} to 2,6-dimercuriphenol and S to an abasic site (2-(hydroxymethyl)tetrahydrofuran-3-ol-spacer). In each sequence, the residue varied in the hybridization studies has been underlined.

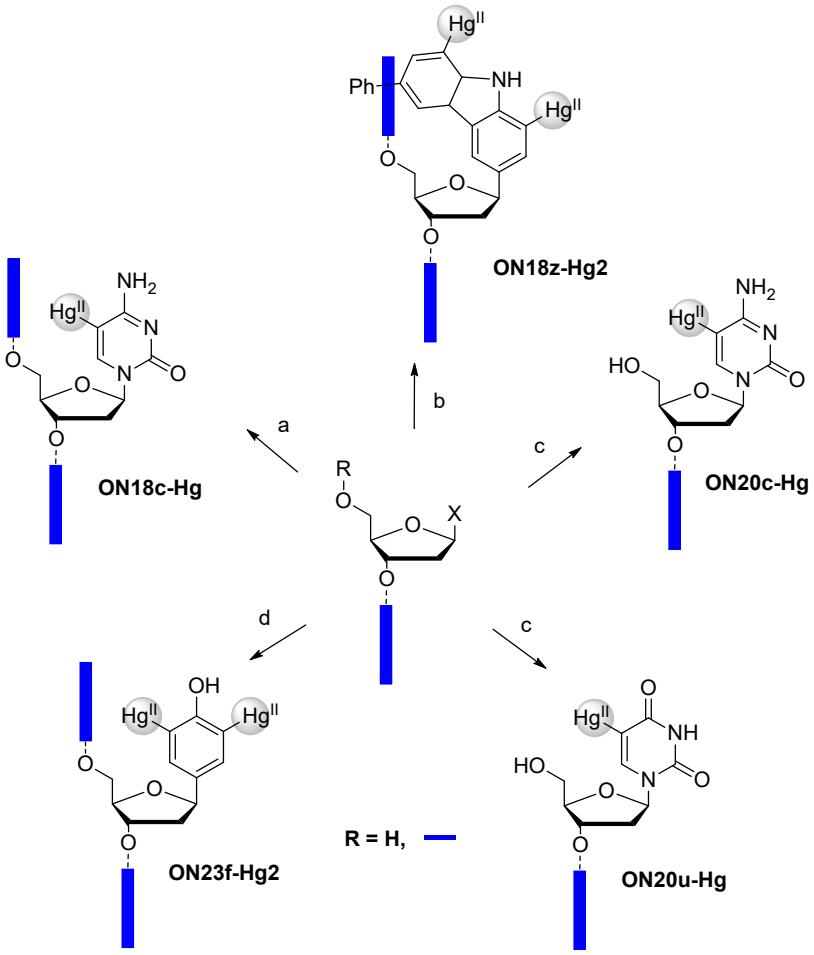

Scheme 5. Schematic representation of synthesis mono **ON18c-Hg**, **ON20c-Hg**, **ON20u-Hg**, dimercurated **ON18z-Hg2** and **ON23f-Hg2** oligonucleotides; X represents either cytosine, 6-Phenyl-1*H*-carbazole, uracil or phenol; Reagents and conditions: a) $Hg(OAc)_2$, H_2O, 60 °C, 16 h; b) $Hg(OAc)_2$, NaOAc, H_2O, 55 °C, 24 h; c) $Hg(OAc)_2$, H_2O, 55 °C, 24 h. d) $Hg(OAc)_2$, NaOAc, H_2O, 70 °C, 16 h.

The authenticity of the modified (including mono- and dimercurated) oligonucleotides was verified by electrospray ionization time of flight mass spectrometry (ESI-TOF MS). Quantification of oligonucleotides **ON18c**, **ON18c-Hg**, **ON18z**, **ON18z-Hg2**, **ON20c**, **ON20c-Hg**, **ON20u**, **ON20u-Hg**, **ON23f**, and **ON23f-Hg2** was done by UV spectroscopy using an implementation of the nearest-neighbors method.[228–230,232] Molar absorptivities of the phenol *C*-nucleoside **15** and the 2,6-dimercuriphenol *C*-nucleoside **16** were assumed to be negligible compared to the 14 adenine residues. For the 6-phenyl-1*H*-carbazole *C*-nucleoside **9**, in turn, a value of 124000 L mol^{-1} cm^{-1} was determined in MeOH solution.

The site of mercuration in **ON18z-Hg2** and **ON23f-Hg2** was confirmed by enzymatic digestion with P1 nuclease in a 25 mM triethylammonium acetate buffer (pH = 7) at 60 and 37 °C, respectively. Samples were withdrawn and analyzed by ESI-TOF-MS at appropriate time intervals. Samples withdrawn immediately after addition of the enzyme did not show any cleavage of either of the dimercurated oligonucleotides. With **ON18z-Hg2**, significant reaction was observed after 10 min, whereas **ON23f-Hg2** had to be incubated for several hours to achieve similar conversion. In all of the samples studied, the mercury-containing digestion products also contained the modified base moiety (6-phenyl-1*H*-carbazole or phenol), strongly suggesting that mercuration exclusively took place at the desired site.

3.6 UV-melting studies

Hybridization affinities of the mercurated oligonucleotides for three different types of nucleic acid targets, namely single- and double-stranded DNA as well as a PAN RNA model as an example of a non-canonical structure, were assessed by conventional UV-melting experiments. Sequences used in the UV melting studies are summarized in Table 2. The UV melting temperatures were determined at 3.0 or 1.0 μM oligonucleotide concentration in 20 mM cacodylate buffer (pH = 7.4), the ionic strength of which was adjusted to 0.10 M with $NaClO_4$. A detection wavelength of 260 nm was used. Watson-Crick and Hoogsteen base melting temperatures were obtained as inflection points on the UV melting curves.

3.7 Recongnition of single-stranded nucleic acids

Recognition of single-stranded nucleic acid sequences was studied with two different types of organomercurated oligonucleotides, *viz.* the monomercurated **ON18c-Hg** and the dimercurated **ON18z-Hg2**. The hybridization efficiency of each of these oligonucleotides, as well as their unmercurated counterparts **ON18c** and **ON18z**, with unmodified oligonucleotides **ON19a, ON19c, ON19g, ON19t** and **ON19s** was assessed by melting temperature experiments. In the duplexes studied, each of the canonical nucleobases or an abasic site was placed opposite to the modified nucleobase (Figure 23).

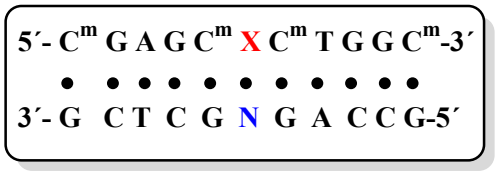

Figure 23. General outline of the hybridization assay used in the duplex study. X denotes cytosine, 5-mercuricytosine, thymine, 6-phenyl-1*H*-carbazole and 1,8-dimerucri- 6-phenyl-1*H*-carbazole or whereas N denotes the any of the natural nucleobases (A, T, G, and C) or an abasic site.

All of the duplexes formed by the unmercurated oligonucleotides **ON18c** and **ON18z** exhibited sigmoidal monophasic UV melting curves (Figure 24). Most of the duplexes formed by the mercurated counterparts **ON18c-Hg** and **ON18z-Hg2** also showed sigmoidal and monophasic melting curves but the thermal hyperchromicity was more gradual. A notable exception was observed with duplexes **ON18z-Hg2•ON19a** and **ON18z-Hg2•ON19c**, exhibiting biphasic sigmoidal curves with an additional low-temperature transition. In these cases, the higher-temperature inflection point was taken as the duplex melting temperature. In borderline cases, such as duplex **ON18c-Hg•ON19t**, the analysis was based on the simplest thermodynamic assumption, *i.e.* monophasic melting. Comparison of all the melting temperatures is presented in Figure 25.

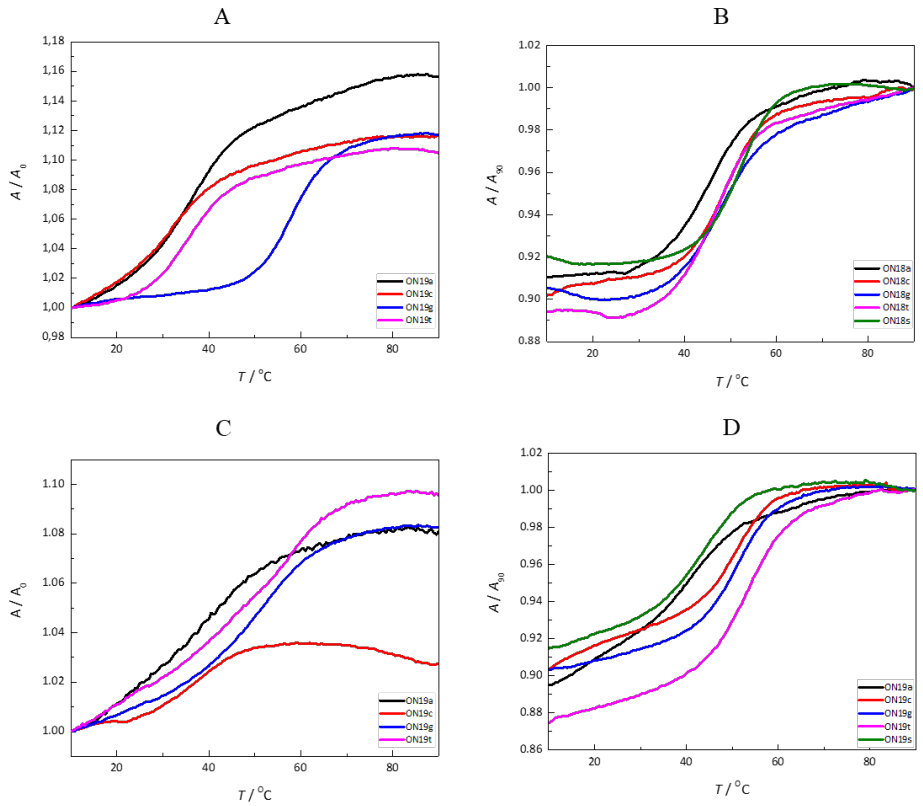

Figure 24. UV melting profiles of duplexes formed by **ON18c** (A), **ON18z** (B), **ON18c-Hg** (C) and **ON18z-Hg2** (D) with **ON19a** (black line), **ON19c** (red line), **ON19g** (blue line), **ON19t** (magenta line), and **ON19s** (green line); pH 7.4 (20 mM cacodylate buffer); I(NaClO$_4$) = 0.10 M; [oligonucleotides] = 3.0 μM with **ON18c-Hg** and 1.0 μM with **ON18z-Hg2**.

As expected, **ON18c** formed the most stable duplex with the fully complementary sequence **ON19g** (T_m = 59 °C) and the mismatched duplexes **ON18c•ON19a**, **ON18c•ON18c** and **ON18c•ON19t** melted at much lower temperatures (30—35 °C). Analogously, **ON18t** preferred hybridization with **ON19a** (T_m = 56.9 °C) but the mismatched duplexes were somewhat more stable than in the case of **ON18c**, the melting temperatures ranging from 38 to 45 °C.

In the case of **ON18z**, all duplexes exhibited similar melting temperatures (46—48 °C), significantly higher than those of the mismatched duplexes formed by **ON18c** and **ON18t**. Presumably, the large aromatic carbazole moiety increases the melting temperature by increased base stacking. The nearly identical stabilities of duplexes **ON18z•ON19a**, **ON18z•ON19c**, **ON18z•ON19g** and **ON18z•ON19t** could indicate that the base opposite to the carbazole residue is flipping out of the base stack. This hypothesis is further supported by the observation that replacing the opposite base with an abasic site has no impact on duplex stability.

The mercurated oligonucleotide **ON18c-Hg** formed the most stable duplex with **ON19t** (T_m = 56 °C). Stabilization relative to the respective unmercurated duplex **ON18c•ON19t** was 22 °C, in line with the known ability of thymine to form Hg(II)-mediated base pairs accompanied by deprotonation of N3. Although still more stable than the mismatched duplexes, the duplex formed by **ON18c-Hg** with **ON19g** was destabilized by 6.8 °C compared to the unmercurated duplex **ON18c•ON19g**. With the other duplexes (**ON18c-Hg•ON19a** and **ON18c-Hg•ON19c**) the effect of mercuration on the stability was minor.

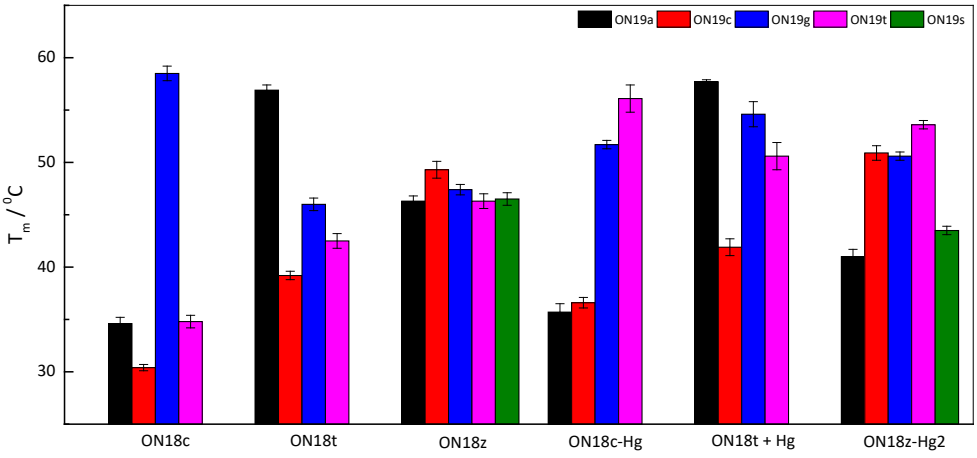

Figure 25. UV melting temperatures of duplexes formed by **ON18c**, **ON18c-Hg**, **ON18t** (in the presence and absence of Hg(II), **ON18c** and **ON18z-Hg2**; pH 7.4 (20 mM cacodylate buffer); [oligonucleotides] = 1.0 / 3.0 μM; $I(NaClO_4)$ = 0.10 M.

To compare duplex stabilization on covalent mercuration of the central cytosine residue of **ON18c** with stabilization by the well-known T-Hg(II)-T base pair, the hybridization efficiency of **ON18t** was measured in the absence and presence of Hg(II) ions. Two of the duplexes (**ON18t•ON19t** and **ON18t•ON19g**) exhibited considerable stabilization in the presence of free Hg(II) ions. Stabilization of **ON18t•ON19t** is in line with the well-known T-Hg(II)-T base pairing and the even higher stability of **ON18t•ON19g** is in all likelihood attributable to T-Hg(II)-G base pairing. As discussed above, thymine and guanine both coordinate Hg(II) as anionic ligands, through deprotonation of N3 and N1, respectively (Figure 26). Finally, the difference between the melting temperatures of **ON18t•ON19t** in the absence and presence of Hg(II) (8.1 °C) was comparable to the difference between the melting temperatures of **ON18c•ON19t** and **ON18c-Hg•ON19t** (14.1 °C), suggesting Hg(II)-mediated base pairing as the origin of stabilization also in the latter case. Within a double-helical oligonucleotide, the 5-mercuricytosine base has to adopt the unfavorable *syn* conformation but evidently this destabilization is overcome by favorable formation of the Hg(II)-mediated base pairs, especially with thymine and guanine.

The duplexes formed by the dimercurated oligonucleotide **ON18z-Hg2** with **ON19a**, **ON19c**, **ON19g**, **ON19t,** and **ON19s** exhibited a wider range of melting temperatures (41—54 °C) than their unmercurated counterparts. Among these duplexes, **ON18z-Hg2•ON19t** showed the highest stabilization (7.3 °C compared to **ON18z•ON19t**), suggesting Hg(II)-mediated base pairing between 1,8-dimercuri-6-phenyl-1*H*–carbazole and thymine. In the case of **ON18z-Hg2•ON19g** and **ON18z-Hg2•ON19c** minor stabilization was observed, whereas **ON18z-Hg2•ON19a** and **ON18z-Hg2•ON19s** were somewhat less stable than their unmercurated counterparts.

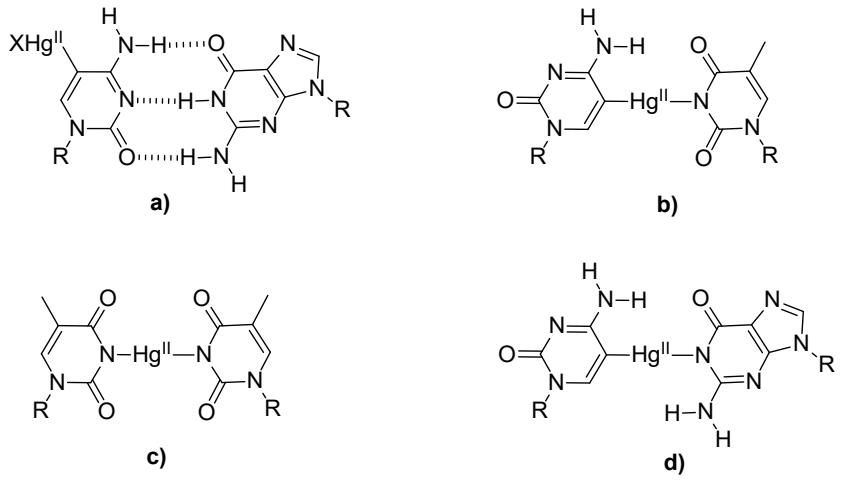

Figure 26. a) Watson-Crick base pairs between mercurated cytidine and guanosine and Hg(II)–mediated base pairs between b) mercurated cytidine and thymidine, c) two thymidine, and d) mercurated cytidine and guanosine. X denotes an exchangeable ligand, such as Cl or H_2O.

To confirm Hg(II)-mediated base pairing, UV melting measurements on duplexes formed by **ON18c-Hg** and **ON18t** in the presence of Hg(II) ion were also carried out in the presence of 30 μm 2-mercaptoethanol. As the sulfhydryl group has a strong affinity towards mercury, after the addition of mercaptoethanol coordination of Hg(II) with N3 of pyrimidine and N1 purine bases is no longer possible. As expected, destabilization upon addition of 2-mercaptoethanol was observed with **ON18c-Hg•ON19t** and **ON18c-Hg•ON19g**, as well as with **ON18t•ON19t** and **ON18t•ON19g** in the presence of Hg(II). In the case of unmercurated duplexes, on the other hand, no notable thermal melting effect was observed.

3.7.1 Thermodynamic analysis of the UV melting curves

Thermodynamic parameters for the hybridization of oligonucleotides can be determined from the renaturation and denaturation curves. The stability of DNA and RNA structures depends on Watson-Crick hydrogen bonding and base stacking effect, both of which are associated with a favorable (negative) enthalpic and an unfavorable (negative) entropic contribution.

The gradual thermal denaturation of the duplexes incorporating a putative Hg(II)-mediated base pair implies a decreased entropic penalty for hybridization, attributed to desolvation of the Hg(II) ion on being embedded within the base stack of a double helix.[82,151,156,198,244] With covalently mercurated bases, such as 5-mercuricytosine and 1,8-dimercuri-6-phenyl-1*H*-carbazole, the effect might be

somewhat less pronounced since the Hg(II) ion has already lost part of its solvation shell on formation of the organometallic bond. For a detailed thermodynamic analysis, equilibrium constants for hybridization were calculated at each temperature point and van't Hoff plots were constructed as described in the literature.[245]

Table 3. Enthalpies of hybridization for various duplexes formed by the modified oligonucleotides **ON18c**, **ON18c-Hg**, **ON18t** (in the absence and presence of Hg(II)), **ON18z** and **ON18z-Hg2** with the unmodified counterparts **ON19a**, **ON19c**, **ON19g**, **ON19t** and **ON19s**; pH 7.4 (20 mM cacodylate buffer); [oligonucleotides] = 1.0 / 3.0 μM; *I*($NaClO_4$) = 0.10 M.

	$\Delta H°$/ kJ mol^{-1}				
	ON19a	**ON19c**	**ON19g**	**ON19t**	**ON19s**
ON18c	-270 ± 10	-310 ± 30	-360 ± 20	-290 ± 20	-
ON18c-Hg	-160 ± 20	-310 ± 50	-220 ± 10	-180 ± 20	-
ON18t	-390 ± 10	-290 ± 10	-280 ± 20	-340 ± 30	-
ON18t + Hg	-360 ± 20	-223 ± 9	-240 ± 40	-180 ± 30	-
ON18z[b]	-315 ± 5	-335 ± 3	-286 ± 2	-355 ± 5	-298 ± 3
ON18z-Hg2[b]	-383 ± 8	-394 ± 3	-342 ± 2	-322 ± 3	-321 ± 5

[b] 1.0 μM oligonucleotide concentration.

Table 4. Entropies of hybridization for various duplexes formed by the modified oligonucleotides **ON18c**, **ON18c-Hg**, **ON18t** (in the absence and presence of Hg(II)), **ON18z** and **ON18z-Hg2** with the unmodified counterparts **ON19a**, **ON19c**, **ON19g**, **ON19t** and **ON19s**; pH 7.4 (20 mM cacodylate buffer); [oligonucleotides] = 1.0 / 3.0 μM; *I*($NaClO_4$) = 0.10 M.

	$\Delta S°$ / J mol^{-1} K^{-1}				
	ON19a	**ON19c**	**ON19g**	**ON19t**	**ON19s**
ON18c	-760 ± 50	-900 ± 100	-970 ± 60	-830 ± 60	-
ON18c-Hg	-410 ± 50	-900 ± 100	-560 ± 40	-430 ± 60	-
ON18t	-1080 ± 40	-830 ± 50	-760 ± 60	-980 ± 70	-
ON18t+Hg	-970 ± 70	-590 ± 30	-600 ± 100	-440 ± 80	-
ON18z[b]	-870 ± 20	-920 ± 10	-772 ± 6	-990 ± 20	-817 ± 9
ON18z-Hg2[b]	-1090 ± 30	-1090 ± 10	-934 ± 7	-869 ± 8	-890 ± 20

[b] 1.0 μM oligonucleotide concentration.

The enthalpies and entropies of hybridization of **ON18c**, **ON18c-Hg**, **ON18z, ON18z-Hg2** and **ON18t** in the absence and presence of free Hg(II) with **ON19a**, **ON19c**, **ON19g**, **ON19t** and **ON19s** are summarized in Tables 3 and 4, respectively. Two different types of enthalpy and entropy values were observed with **ON18c-Hg** and **ON18z-Hg2**. In most cases, the enthalpies and entropies of hybridization were considerably smaller (less negative) with **ON18c-Hg** than with **ON18c**, in line with previous reports on the T-Hg(II)-T base pair.[158,159] The sole exception was **ON18c-**

Hg•ON19c, arguing against Hg(II)-mediated base pairing in this duplex. Even greater differences were observed with **ON18t** in the absence and presence of Hg(II), consistent with a more thorough desolvation of Hg(II). In the case of Hg(II)-mediated base pairing one or two Hg-N bonds are formed but the enthalpic effect is partially offset by the cleavage of one or two Hg-Cl and H-N bonds. Release of Cl^- and H^+ ions and the solvation shell of the Hg(II) into solution, in turn, alleviates some of the entropic penalty.[157,159]

In contrast to the hybridization of **ON18c-Hg** and the previous reports on T-Hg(II)-T base pairing, the entropies and enthalpies of hybridization of the dimercurated oligonucleotide **ON18z-Hg2** were in most cases more negative than those of the respective unmercurated duplexes. Only **ON18z-Hg2•ON19t** exhibited the typical pattern of less negative enthalpy and entropy of hybridization for the mercurated duplex. The highly negative enthalpies and entropies of hybridization support the idea of increased stacking of the carbazole moiety in the oligonucleotide duplexes. Additionally, restricted rotation of the phenyl substituent may have contributed to the increase of the absolute value of entropy. The relatively high melting temperature of **ON18z-Hg2•ON19t** is correlated with a relatively low entropic penalty of hybridization and, hence, probably is due to Hg(II)-mediated base pairing. Thermodynamic parameters of hybridization of the other duplexes formed by **ON18z-Hg2** were not easy to interpret and whether the stabilization or destabilization of these duplexes is due to Hg(II)-mediated base pairing or changes in stacking interactions remains an open question.

3.7.2 DFT calculations

The binding mode of dimercurated 1,8-dimercuri-6-phenyl-1*H*-carabzole with thymine cannot be established unambiguously based on the hybridization experiments.[232] In principle, the putative metal-mediated base pair could be either mono- or dinuclear (Figure 27). To elucidate this point, geometry of the 1,8-dimercuri-6-phenyl-1*H*-carbazole—thymine base pair was optimized by DFT calculations performed with Gaussian 16 software[246] with PBE0DH double hybrid method.[247] Def-2VSP basis set and pseudopotential were used for Hg[248], 6-31+G(d,p) basis set for N and O atoms[249] and 6-31G(d,p) basis set for C and H atoms.[250,251] The sugar residues of the two nucleosides were replaced by methyl groups and the phenyl substituent by a hydrogen atom for a simplified system. Coordination of Hg(II) by thymine at neutral pH takes place with concomitant deprotonation of N3 so the monoanionic form of thymine was used in the calculations, resulting in an overall charge of the +1 for the Hg(II)-mediated base pair. Both mono- and dinuclar structures (Figure 27) were used as starting geometries for the calculations.

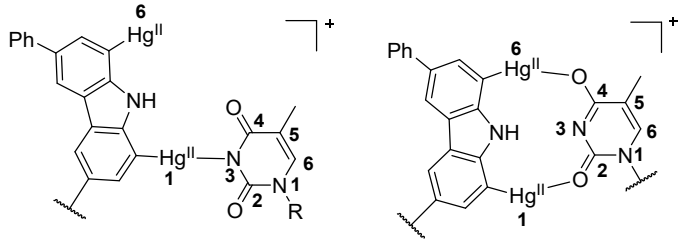

Figure 27. Binding modes of a) mono- and b) dinuclear Hg(II)-mediated base pairs between 1,8-dimercuri-6-phenyl-1*H*-carbazole and thymine.

The optimized mononuclear Hg(II)-mediated base pair has a planar structure with Hg1 coordinated to thymine N3 and the carbazole NH hydrogen-bonded to thymine O4. The angle between C1, Hg1 and N3 was reduced to 155.9 º and the Hg6-O4 distance to 2.35 Å, suggesting weak coordination of Hg6 also to thymine O4. The distance between the anomeric carbon atoms was 10.8 Å, very close to the canonical value of 10.7 Å.[192,193,198,212] On the other hand, optimization of the dinuclear Hg(II)-mediated base pair largely preserved the initial geometry having Hg1 and Hg6 coordinated to thymine O2 and O4, respectively. The dinuclear Hg(II)-mediated base pair was also planar but the distance between the anomeric carbon atoms (10.2 Å) was somewhat shorter than the canonical value. The dinuclear Hg(II)-mediated base pair was 96 kJ mol^{-1} more stable than the mononuclear one and thus represents the most likely binding mode between 1,8-dimercury-6-phenyl-1*H*-carbazole and thymine within the **ON18z-Hg•ON19t** duplex.

3.8 Recongnition of double-stranded nucleic acids

The potential of Hg(II)-mediated base pairing to enhance the hybridization affinity of triplex-forming oligonucleotides (TFOs) was assessed with 15-mer homothymine sequences having either 2′-deoxycytidine or 2′-deoxyuridine or their covalently mercurated analogs at their 3′-termini. The target duplexes, in turn, were designed to allow the triplex study to be performed at physiological pH and, accordingly, featured a 15-mer homoadenine•homothymine sequence sandwiched between CG base pairs to ensure antiparallel duplex formation. A variable target base pair was included at the 3′-end of the homoadenine sequence. The general outline of hybridization assay is outlined in Figure 28. Apart from Watson-Crick base pairs, homo base pairs (mismatched) were also tested, for a total of eight target duplexes.

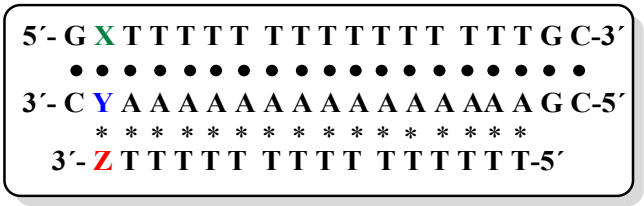

Figure 28. General outline of the hybridization assay used. Bases **X** and **Y** are any of the canonical nucleobases and **Z** is cytosine, uracil, 5-acetoxymercuricytosine, or 5-acetoxymercuriuracil. Watson-Crick base pairs are indicated by bullets and Hoogsteen base pairs by asterisks.

Melting profiles of most of the triplexes studied were sigmoidal and biphasic (the melting profiles of triplexes formed by **ON20c** and **ON20c-Hg** are shown in Figure 29 as representative examples). Hoogsteen and Watson-Crick melting temperatures (T_m) of all of the triplexes studied are summarized in Tables 5 and 6, respectively.

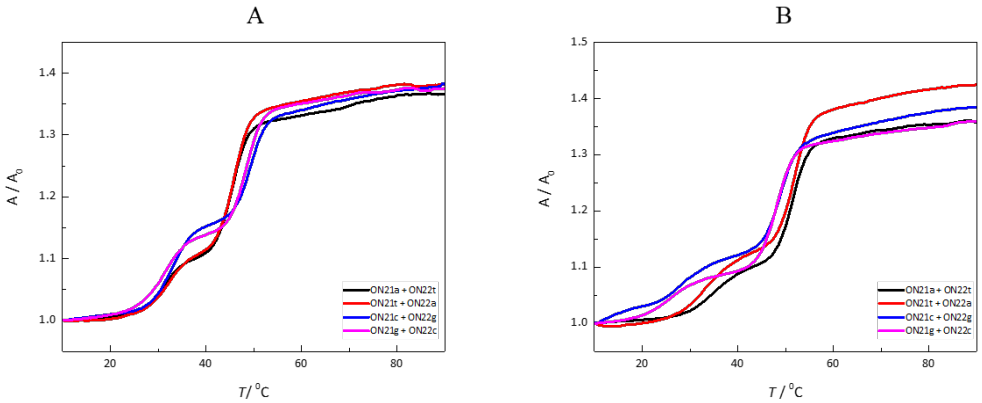

Figure 29. UV melting profile of **ON20c** (A) and **ON20c-Hg** (B) with target duplexes; pH 7.4 (20 mM cacodylate buffer); [oligonucleotides] = 1.0 μM; *I*($NaClO_4$) = 0.10 M; [**ON21a●ON22t** (black line) / **ON21t●ON22a** (red line) / **ON21c●ON2g** (blue line) /**ON21g●ON22c** (magenta line).

Table 5. Hoogsteen melting temperatures of triplexes formed by **ON20c**, **ON20c-Hg**, **ON20u**, **ON20u-Hg** with various target duplexes; pH 7.4 (20 mM cacodylate buffer); [oligonucleotides] = 1.0 μM; $I(NaClO_4)$ = 0.10 M; $[Hg(ClO_4)_2]$ = 0 / 1.0 μm.

	Hoogsteen T_m[°C]					
duplex	**ON20c**	**ON20c + Hg[a]**	**ON20c-Hg[a]**	**ON20u**	**ON20u + Hg[a]**	**ON20u-Hg[a]**
ON21t•ON22a	31.8 ± 0.5	31.8 ± 0.8 (±0.0)	33.7 ± 0.7 (+1.9)	34.7 ± 0.5	33.8 ± 0.4 (-0.9)	26.2 ± 0.9 (-8.5)
ON21a•ON22t	30.8 ± 0.6	34.1 ± 0.2 (+3.3)	34.6 ± 0.2 (+3.8)	n.a[b]	n.a[b]	30.0 ± 0.9
ON21g•ON22c	30.9 ± 0.7	30.5 ± 0.6 (-0.4)	27.5 ± 0.2 (-3.4)	33.3 ± 0.5	32.7 ± 0.6 (-0.6)	27.1 ± 0.4 (-6.2)
ON21c•ON22g	31.0 ± 0.8	32.1 ± 0.6 (+1.1)	26.1 ± 0.7 (-4.6)	33.8 ± 0.3	33.2 ± 0.2 (-0.6)	27.8 ± 0.6 (-6.0)
ON21a•ON22a	n.a[b]	n.a[b]	26.8 ± 0.9	35.0 ± 0.9	34.4 ± 0.5 (-0.6)	28.4 ± 0.8 (-6.6)
ON21c•ON22c	31.9 ± 0.2	31.3 ± 0.2 (-0.6)	25.8 ± 0.7 (-6.1)	n.a[b]	n.a[b]	n.a[b]
ON21g•ON22g	32.4 ± 0.2	31.9 ± 0.5 (-0.5)	29.0 ± 0.6 (-3.4)	34.5±0.4	33.5 ± 0.3 (-1.0)	27.4 ± 0.4 (-7.1)
ON21t•ON22t	32.2 ± 0.4	32.8 ± 0.5 (-0.6)	27.9 ± 1.2 (-4.3)	n.a[b]	n.a[b]	n.a[b]

[a] Values in parentheses refer to the change in T_m relative to the value obtained with unmercurated TFO (**ON20c** or **ON20u**) in the absence of Hg(II).

[b] Hoogsteen T_m could not be determined reliably from the UV melting profile; n.a: not available.

Table 6. Watson-Crick melting temperatures of triplexes formed by **ON20c**, **ON20c-Hg**, **ON20u**, **ON20u-Hg** with various target duplexes; pH 7.4 (20 mM cacodylate buffer); [oligonucleotides] = 1.0 μM; $I(NaClO_4)$ = 0.10 M; $[Hg(ClO_4)_2]$ = 0 / 1.0 μm.

	Watson-Crick T_m[°C]					
duplex	**ON20c**	**ON20c + Hg[a]**	**ON20c-Hg[a]**	**ON20u**	**ON20u + Hg[a]**	**ON20u-Hg[a]**
ON21t•ON22a	45.7 ± 0.3	46.2 ± 0.7 (+0.5)	51.8 ± 0.2 (+6.1)	47.3 ± 0.3	46.7 ± 0.4 (-0.6)	46.3 ± 0.4 (-1.0)
ON21a•ON22t	45.3 ± 0.3	46.5 ± 0.7 (+1.2)	51.5 ± 0.4 (+6.2)	46.8 ± 0.7	46.8 ± 0.3 (± 0.0)	45.4 ± 0.3 (-1.4)
ON21g•ON22c	47.1 ± 0.5	47.7 ± 0.7 (+0.6)	46.9 ± 0.6 (-0.2)	48.3 ± 0.2	47.7 ± 0.2 (-0.6)	47.5 ± 0.3 (-0.8)
ON21c•ON22g	48.1 ± 0.6	48.9 ± 0.4 (+0.8)	47.9 ± 0.5 (-0.2)	49.5 ± 0.2	49.2 ± 0.2 (-0.3)	48.4 ± 0.3 (-1.1)
ON21a•ON22a	40.9 ± 0.3	41.3 ± 0.8 (+0.4)	40.9 ± 0.4 (±0.0)	42.0 ± 0.4	41.3 ± 0.4 (-0.7)	41.3 ± 0.2 (-0.7)
ON21c•ON22c	41.8 ± 0.2	42.3 ± 0.5 (+0.5)	41.7 ± 0.6 (-0.1)	42.3 ± 0.3	41.5 ± 0.3 (-0.8)	41.6 ± 0.4 (-0.7)
ON21g•ON22g	43.2 ± 0.4	46.2 ± 0.6 (+1.0)	43.0 ± 0.6 (+0.2)	44.4 ± 0.3	43.4 ± 0.3 (-1.0)	43.1 ± 0.4 (-1.3)
ON21t•ON22t	41.8 ± 0.3	45.2 ± 0.2 (+3.4)	44.0 ± 0.3 (+2.2)	42.4 ± 0.4	44.3 ± 0.3 (+1.9)	43.0 ± 0.7 (+0.6)

[a] Values in parentheses refer to the change in T_m relative to the value obtained with unmercurated TFO (**ON20c** or **ON20u**) in the absence of Hg(II).

[b] Hoogsteen T_m could not be determined reliably from the UV melting profile; n.a: not available.

Watson—Crick melting temperatures of triplexes formed by either of the unmercurated TFOs (**ON20c** or **ON20u**) ranged from 45 to 50 °C with matched target duplexes and from 40 to 44 °C with mismatched target duplexes. The Hoogsteen melting temperatures, on the other hand, were largely independent on the target duplex but somewhat different for the two TFOs, ranging from 31 to 32 °C with **ON20c** and from 33 to 35 °C with **ON20u.** Addition of free Hg(II) ions had only a minor effect on the Watson—Crick melting temperatures, except for the **ON21t•ON22t** target duplex, in which case the expected stabilization by the well-documented T-Hg(II)-T base pairing was observed.[47,185] The Hoogsteen melting temperatures, in turn, slightly decreased on addition of Hg(II) with almost all triplexes. The sole exception was **ON21a•ON22t*ON20c**, exhibiting an increase of +3.4 °C with **ON20c** and +1.9 °C with **ON20u**.

In most cases, Watson—Crick melting temperatures of triplexes formed by the mercurated TFOs **ON20c-Hg** and **ON20u-Hg** were similar to the respective values obtained with their unmercurated counterparts. The Hoogsteen melting temperatures, on the other hand, were 3–9 °C lower. This destabilization was more pronounced with **ON20u-Hg** than with **ON20c-Hg** and possibly arises from competition between Hoogsteen base pairing and intrastrand Hg(II)-mediated base pairing of the mercurated residue with one of the 15 thymine bases. With **ON21t•ON22a*ON20c-Hg** and **ON21a•ON22t*ON20c-Hg**, however, both Hoogsteen (+1.9 °C) and especially Watson—Crick (+6.1 °C) melting temperatures were higher than those of respective unmercurated triplexes. Mutual dependence of Hoogsteen and Watson-Crick melting temperatures of a triplex has been reported previously with the number of related systems.[252,253]

In the case of **ON20c-Hg**, the increased triplex stability specifically with A•T or T•A as the target base pair might indicate Hg(II)-mediated Hoogsteen-type base pairing although this explanation fails to account for the lack of similar stabilization with **ON20u-Hg**. To test this hypothesis, the UV melting experiments were repeated in the presence of 2-mercaptoethanol. As discussed above in section 3.6, Hg(II)-mediated base pairing should be abolished in the presence of this very strong ligand for Hg(II), whereas hydrogen-bonded Watson-Crick and Hoogsteen base pairs are unaffected.

Hoogsteen and Watson-Crick melting temperatures (T_m) of all of the triplexes studied in the presence of 2-mercaptoethanol are summarized in Tables 7 and 8, respectively. Under these conditions, triplexes formed by the mercurated and unmercurated TFOs exhibited very similar melting temperatures with almost all target duplexes. The selective stabilization of triplexes **ON21t•ON22a*ON20c-Hg** and **ON21a•ON22t*ON20c-Hg** relative to their unmercurated counterparts, however, persisted and was even somewhat amplified (+7.3 and +7.6 °C for Hoogsteen and +6.5 and +6.3 °C for Watson-Crick T_m, respectively). Evidently, stabilization of these triplexes cannot be attributed to Hg(II)-mediated base pairing.

Table 7. Hoogsteen melting temperatures of triplexes formed by **ON20c**, **ON20c-Hg**, **ON20u**, **ON20u-Hg** with various target duplexes; pH 7.4 (20 mM cacodylate buffer); [oligonucleotides] = 1.0 μM; *I*($NaClO_4$) = 0.10 M; [$Hg(ClO_4)_2$] = 0 / 1.0 μm; [2-meraptoethanol] = 100 μM.

	Hoogsteen T_m[°C]					
duplex	**ON20c**	**ON20c + Hg[a]**	**ON20c-Hg[a]**	**ON20u**	**ON20u + Hg[a]**	**ON20u-Hg[a]**
ON21t•ON22a	31.7 ± 0.4	32.8 ± 0.8 (+1.1)	39.0 ± 0.6 (+7.3)	34.0 ± 0.6	34.9 ± 0.8 (-0.9)	n.a[b]
ON21a•ON22t	30.5 ± 0.3	32.5 ± 0.7 (+2.0)	38.1 ± 0.5 (+7.6)	n.a[b]	n.a[b]	32.5 ± 0.8
ON21g•ON22c	31.3 ± 0.1	31.1 ± 0.6 (+0.2)	30.4 ± 0.2 (-0.9)	n.a[b]	33.5 ± 0.4	31.3 ± 0.5
ON21c•ON22g	33.0 ± 0.2	32.8 ± 0.6 (-0.2)	32.3 ± 0.5 (-0.7)	32.6 ± 0.3	34.3 ± 0.6 (+1.7)	33.1 ± 0.4 (+0.5)
ON21a•ON22a	n.a[b]	n.a[b]	34.1 ± 0.4	n.a[b]	35.3 ± 0.7	n.a[b]
ON21c•ON22c	31.4 ± 0.4	32.5 ± 0.4 (+0.9)	30.6 ± 0.4 (-0.8)	n.a[b]	n.a[b]	n.a[b]
ON21g•ON22g	32.5 ± 0.5	32.8 ± 0.3 (+0.3)	32.0 ± 0.5 (-0.5)	32.8 ± 0.2	34.2 ± 0.5 (+1.4)	32.7 ± 0.7 (+0.1)
ON21t•ON22t	32.2 ± 0.4	33.0 ± 0.4 (-0.2)	31.8 ± 0.2 (-1.4)	n.a[b]	n.a[b]	n.a[b]

[a] Values in parentheses refer to the change in T_m relative to the value obtained with unmercurated TFO (**ON20c** or **ON20u**) in the absence of Hg(II).
[b] Hoogsteen T_m could not be determined reliably from the UV melting profile; n.a: not available.

Table 8. Watson-Crick melting temperatures of triplexes formed by **ON20c**, **ON20c-Hg**, **ON20u**, **ON20u-Hg** with various target duplexes; pH 7.4 (20 mM cacodylate buffer); [oligonucleotides] = 1.0 μM; *I*($NaClO_4$) = 0.10 M; [$Hg(ClO_4)_2$] = 0 / 1.0 μm; [2-meraptoethanol] = 100 μM.

	Watson-Crick T_m[°C]					
duplex	**ON20c**	**ON20c + Hg[a]**	**ON20c-Hg[a]**	**ON20u**	**ON20u + Hg[a]**	**ON20u-Hg[a]**
ON21t•ON22a	45.5 ± 0.3	47.0 ± 0.5 (+1.5)	52.0 ± 0.4 (+6.5)	46.3 ± 0.5	47.6 ± 0.7 (+1.4)	47.3 ± 0.4 (+0.8)
ON21a•ON22t	45.3 ± 0.3	47.2 ± 0.6 (+1.9)	51.6 ± 0.4 (+6.3)	45.7 ± 0.2	47.3 ± 0.7 (+1.6)	46.5 ± 0.6 (+0.8)
ON21g•ON22c	48.2 ± 0.2	48.3 ± 0.3 (+0.1)	47.8 ± 0.3 (-0.4)	47.7 ± 0.2	48.5 ± 0.4 (+0.8)	48.3 ± 0.6 (+0.6)
ON21c•ON22g	49.2 ± 0.2	49.7 ± 0.4 (+0.5)	48.8 ± 0.2 (-0.4)	48.8 ± 0.3	49.9 ± 0.7 (+1.1)	49.5 ± 0.6 (+0.7)
ON21a•ON22a	42.3 ± 0.2	42.4 ± 0.4 (+0.1)	42.0 ± 0.4 (-0.3)	41.8 ± 0.3	41.7 ± 0.4 (-0.1)	41.3 ± 0.3 (-0.5)
ON21c•ON22c	41.8 ± 0.2	42.6 ± 0.4 (+0.8)	41.6 ± 0.6 (-0.2)	41.8 ± 0.4	41.9 ± 0.4 (+0.1)	42.2 ± 0.4 (+0.4)
ON21g•ON22g	45.5 ± 0.6	44.2 ± 0.2 (-1.3)	43.0 ± 0.5 (-2.5)	42.6 ± 0.4	44.1 ± 0.5 (+1.5)	43.2 ± 0.2 (+0.6)
ON21t•ON22t	42.7 ± 0.2	43.1 ± 0.4 (+0.4)	41.3 ± 0.2 (-1.4)	41.6 ± 0.4	41.9 ± 0.6 (+0.3)	41.7 ± 0.4 (+0.1)

[a] Values in parentheses refer to the change in T_m relative to the value obtained with unmercurated TFO (**ON20c** or **ON20u**) in the absence of Hg(II).

The unexpected additional stabilization of the mercurated triplexes **ON21t•ON22a*ON20c-Hg** and **ON21a•ON22t*ON20c-Hg** in the presence of 2-mercaptoethanol lead us to investigate the role of the exchangeable ligand of Hg(II). Accordingly, the melting temperatures of **ON21t•ON22a*ON20c-Hg** were determined also in the presence of 100 μM of different types of thiols, specifically hexanethiol, thiophenol, and cysteine, allowing assessment of the importance of hydrophobic interactions, intercalation and hydrogen bonding. As hexanethiol has no functional groups apart from sulfhydryl donor, it would be expected to stabilize the triple helix through only a hydrophobic effect. Thiophenol, on the other hand, would increase the stacking surface of 5-mercuricytosine and could stabilize the triplex by intercalation. Finally, the amino and carboxylate functions of a cysteine ligand should allow more extensive hydrogen-bonding and/or electrostatic interactions than the hydroxyl function of 2-mercaptoethanol. Hoogsteen and Watson-Crick melting temperatures of triplex **ON21t•ON22a*ON20c-Hg** and its unmercurated counterpart **ON21t•ON22a*ON20c** in the presence of 2-mercaptoethanol, hexanethiol, thiophenol, and cysteine, as well in the absence of any thiols, are presented in Figure 30. Hoogsteen and Watson-Crick T_m values of **ON21t•ON22a*ON20c-Hg** decreased back to the level observed with the respective unmercurated triplex **ON21t•ON22a*ON20c** after treatment with hexanethiol, thiophenol and cysteine**.** In other words, the extra stabilization observed in the presence of 2-mercaptoethanol was not reproducible with any of these other thiols.

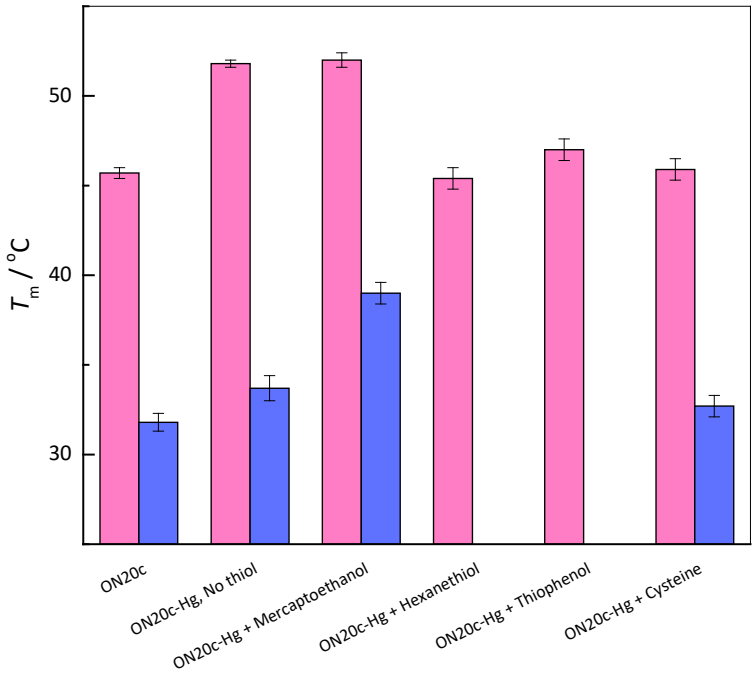

Figure 30. Watson-Crick (hashed bar) and Hoogsteen (solid black bar) melting temperatures of triplexes **ON21t•ON22t*ON20c** and **ON21t•ON22t*ON20c-Hg** in the presence of 2-mercaptoethanol, hexanethiol, thiophenol and cysteine, as well as in the absence of any thiol; pH 7.4 (20 mM cacodylate buffer); $I(NaClO_4)$ = 0.10 M; [oligonucleotides] = 1.0 μM; [thiols] = 0 / 100 μM.

3.9 Recongnition of non-canonical nucleic acids

The possibility of recognition of a non-canonical nucleic acid target by an oligonucleotide bearing a bifacial dimercurated nucleobase surrogate was explored on an assay (Figure 31) designed to mimic the binding of the polyadenylated tail of the polyadenylated nuclear (PAN) RNA between two U-rich sequences of the same strand.[254] Accordingly, the modified residue (or, for reference, adenine) was incorporated in the middle of a 15-mer homodenine sequence and the target consisted of two identical 15-mer homothymine sequences with a variable central nucleobase. The ability of the modified oligonucleotides **ON23a, ON23f**, and **ON23-Hg2** to form triple helices with the unmodified oligonucleotides **ON24a**, **ON24c**, **ON24g**, **ON24t**, and **ON24s** was studied by UV melting temperature measurements under the same conditions as described above in sections 3.7 Melting profiles of **ON23a** (A) **ON23f** (B), and **ON23-Hg2** (C) are presented in Figure 32.

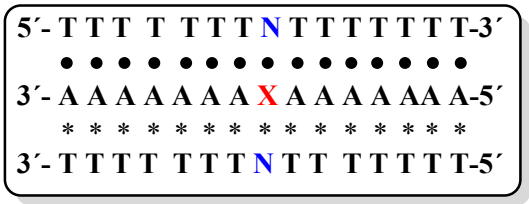

Figure 31. General outlines of the hybridization assay used. X denotes an adenine, a phenol or a 2,6-dimercuriphenol residue whereas N denotes any of the natural bases (A, T, G, C) or an abasic site (S). Watson-Crick base pairs are indicated by bullets and Hoogsteen base pairs by asterisks.

First, formation of a triple helix was studied between the oligonucleotide **ON23a** and the target oligonucleotides **ON24a**, **ON24c**, **ON24g**, **ON24t**, and **ON22s**. In these experiments, monophasic sigmoidal melting curves were observed with all combinations, suggesting that triplex formation does not take place over the temperature range used (10–90 °C). The highest Watson—Crick melting temperature (35 °C) was expectedly observed with **ON24t•ON23a*ON24t**, the other triplexes exhibiting much lower values (approximately 20 °C). Watson-Crick melting temperatures of all triplexes formed by **ON23a**, **ON23f** and **ON23-Hg2** are summarized in Figure 33.

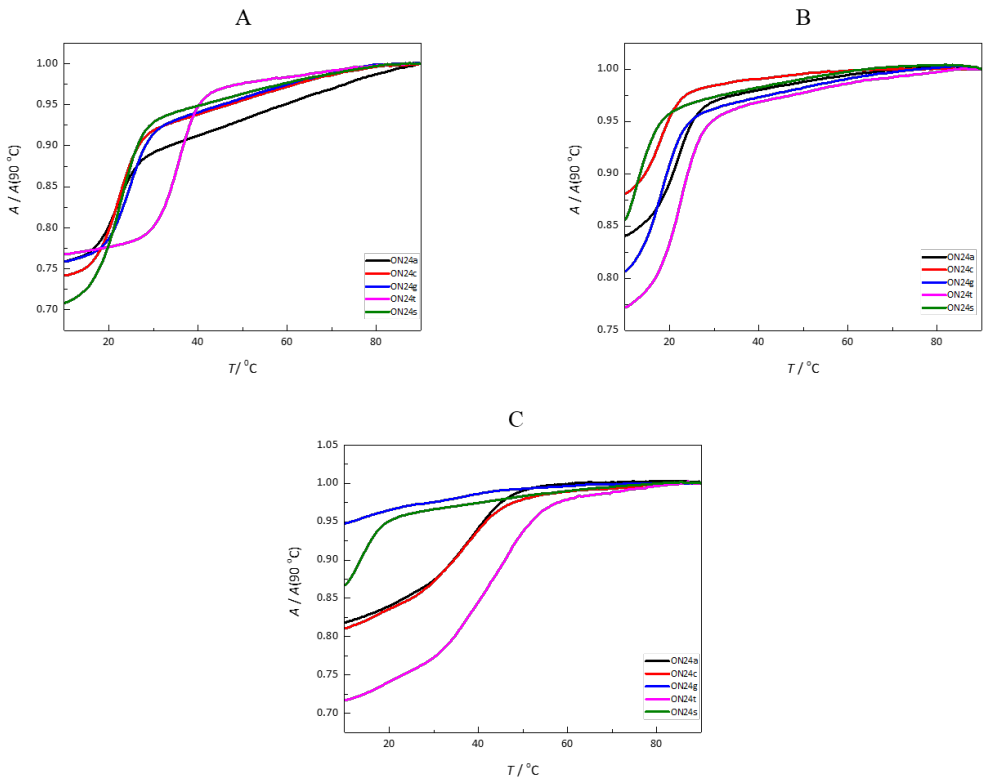

Figure 32. UV melting profile of unmercurated **ON23a** (A), **ON23f** (B) and dimercurated **ON23-Hg2** (C) with **ON24a**, **ON24c**, **ON24g**, **ON24t** and **ON24s**; pH 7.4 (20 mM cacodylate buffer); [**ON23f**] or [**ON23f-Hg2**] = 1.0 μM; [**ON24a** (black line) / **ON24c** (red line) / **ON24g** (blue line) /**ON24t** (magenta line) / **ON24s** (green line)] = 2.0 μM; *I* ($NaClO_4$) = 0.10 M.

All of the triplexes formed by the modified oligonucleotide **ON23f** were less stable than those formed by its unmodified counterpart **ON23a**, the Watson-Crick melting temperatures ranging from 17 to 21 °C and Hoogsteen melting temperatures being too low to be detected. In case of **ON24s•ON23f*ON24s**, having abasic sites opposite to the phenol residue, no sigmoidal melting profile was observed.

Three types of melting profiles were observed for triplexes formed by the dimercurated oligonucleotide **ON23f-Hg2**. The curves for **ON23a•ON22-Hg2*ON24a**, **ON24c•ON7f-Hg2*ON24c** and **ON24t•ON23f-Hg2*ON24t** were biphasic, consistent with successive Hoogsteen and Watson—Crick melting of a triple helix. **ON24s•ON23-Hg2*ON24s** exhibited a monophasic melting profile with a very low melting temperature, whereas no sigmoidal curve was obtained with **ON24g•ON23-Hg2*ON24g**. Consistent with the affinities of the various Hg(II)-mediated base triples determined by NMR, the highest Watson—Crick melting temperature was observed with **ON24t•ON23f-Hg2*ON24t** (45.7 °C), followed by

ON24a•ON23f-Hg2*ON24a (38.5 °C) and **ON24c•ON23f-Hg2*ON24c** (36.4 °C). Even the anomalous melting profile of **ON24g•ON23f-Hg2*ON24g** appears to reflect the similarly anomalous results of the NMR study on the 2,6-dimercuryphenol-*C*-nucleoside and guanosine-5′-monophosphate. The Hoogsteen melting temperatures were low (19.5, 16.2 and 22.3 °C for **ON24a•ON23-Hg2*ON24a**, **ON24c•ON23f-Hg2*ON24c** and **ON24t•ON23f-Hg2*ON24t**) but still clearly higher than those of the triplexes formed by the unmercurated oligonucleotides **ON23a** and **ON23f**.

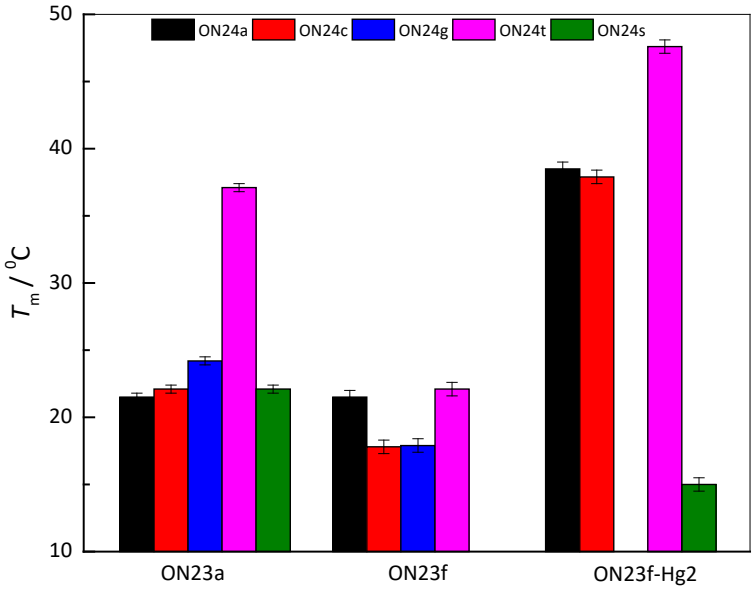

Figure 33. Watson—Crick melting temperatures of triplexes formed by **ON23a**, **ON23f** and **ON23f-Hg2** with **ON24a**, **ON24c**, **ON24g**, **ON24t** and **ON24s**; pH 7.4 (20 mM cacodylate buffer); [**ON23a** / **ON23f** / **ON23f-Hg2**] = 1.0 μM; [**ON24a** / **ON24c** / **ON24g** / **ON24t** / **ON24s**] = 2.0 μM; *I*($NaClO_4$) = 0.10 M.

The results of both the UV melting as well as the NMR studies suggest formation of dinuclear Hg(II)-mediated base triples as the reason behind the stability of triplexes formed by the dimercurated oligonucleotide **ON23f-Hg2**. In the case of thymine the Hg(II) coordination site is undoubtedly N3, with concomitant deprotonation. N3 also appears as the most likely donor atom in cytosine although coordination to the exocyclic amino group has also been reported.[80,164,189,255] With adenine N1- and N7-coordination are both feasible, the latter usually being favored for steric reasons.[27] Proposed structures of the Hg(II)-mediated base triples are presented in Figure 34.

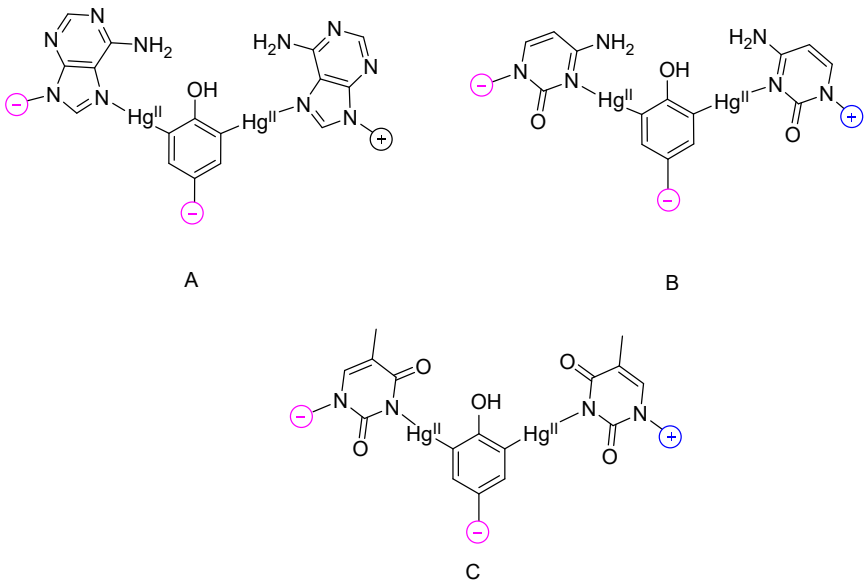

Figure 34. Proposed structures of base triples formed between 2,6-dimercuriphenol and (A) adenine, (B) cytosine, and (C) thymine. Relative polarities of the three strands are indicated by (+) and (-) signs.

3.10 CD spectropolarimetric studies

The secondary structure of the duplexes and triplexes formed by the modified oligonucleotides was studied CD spectropolarimetrically. CD spectra of oligonucleotides were measured over a wide temperature range (5–90 °C) under the conditions that were used for UV melting temperature experiments.[228,232]

In the case of duplexes, the spectra obtained at low temperature exhibited a positive band at 280 nm and a negative band at 240 nm, typical of right-handed B-type helical structures (spectra of **ON18c-Hg•ON19t** and **ON18z-Hg2•ON19t** are presented in Figure 35 as representative examples). An increase in the temperature resulted in a gradual decrease of CD signals with all duplexes. Thermal diminution of the positive cotton effect at 280 nm, however, was much less pronounced with the duplexes formed by **ON18z** than with other duplexes.

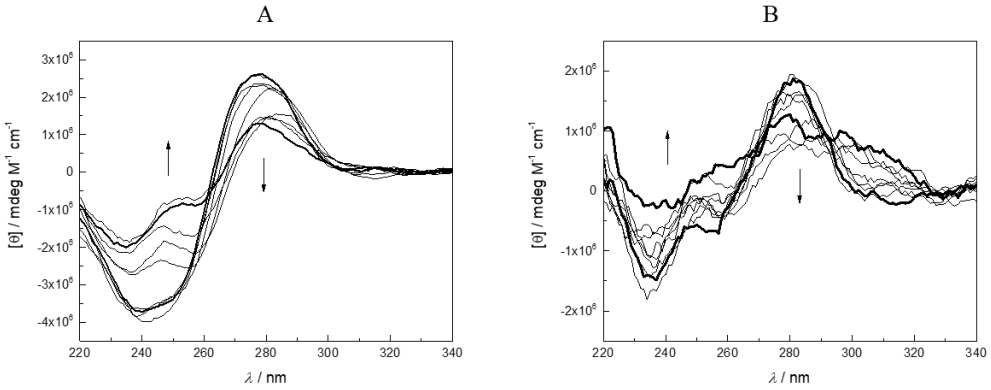

Figure 35. CD spectra of oligonucleotide duplexes (A) **ON18c-Hg•ON19t** and (B) **ON18z-Hg2•ON19t**, recorded at 10 °C intervals between 10 and 90 °C; [oligonucleotides] = 3.0 / 1.0 μM; pH = 7.4 (20 mM cacodylate buffer); *I*($NaClO_4$) = 0.10 M. Spectra acquired at the extreme temperatures are indicated by thicker lines and thermal shifts of the minima and maxima by arrows.

CD spectra of mercurated triplexes **ON21t•ON22a*ON20c-Hg** and **ON24t•ON23f-Hg2*ON24t** are presented in Figure 36. All spectra obtained at 10 °C were characteristic of pyrimine•purine*pyrimidine triple helices[256,257] with minima at λ =248 nm and maxima at λ = 260 and 284 nm. With increasing temperature, the minima at λ = 248 nm and maxima at λ = 260 nm diminished and the maxima at λ = 284 nm shifted towards shorter wavelengths. In the case of triplexes formed by **ON20c-Hg** and **ON20u-Hg** and their unmercurated counterparts, biphasicity of the CD melting profile was evident even when a Hoogsteen UV melting temperature could not be detected. With **ON24t•ON23f-Hg2*ON24t**, on the other hand, plotting the CD signal at 275 nm as a function of temperature (Figure 37) allowed a more reliable estimation of the Hoogsteen melting temperature (27 ± 1 °C).

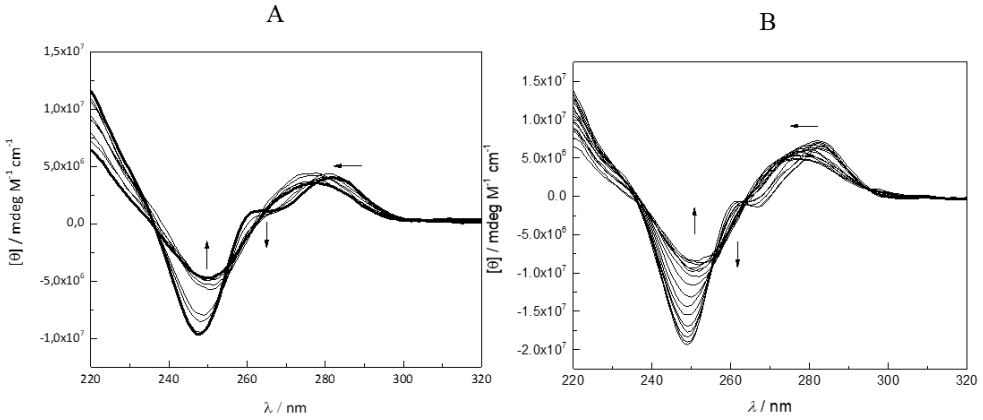

Figure 36. CD spectra of triplexes (A) **ON21t•ON22a*ON20c-Hg** and (B) **ON24t•ON23f-Hg2*ON24t**, recorded at 10 and 5 °C intervals between 10 and 90 °C resepectively; pH = 7.4 (20 mM cacodylate buffer); I(NaClO4) = 0.10 M; [oligonucleotides] = 1.0 μM. Spectra acquired at the extreme temperatures are indicated by thicker lines and thermal shifts of the minima and maxima by arrows.

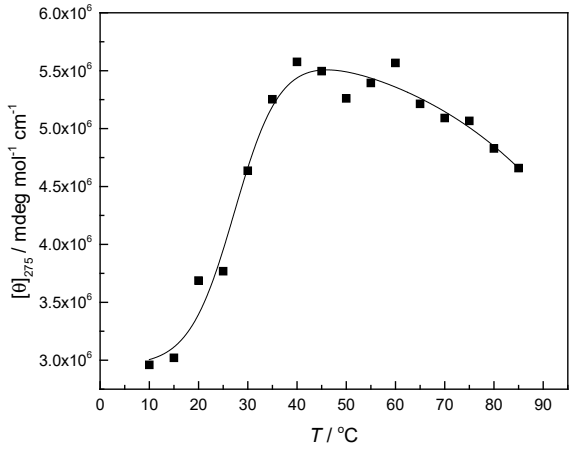

Figure 37. CD spectra of triplex **ON24t•ON23f-Hg2*ON24t**, recorded at 275 nm, 5 °C intervals between 10 and 90 °C; pH = 7.4 (20 mM cacodylate buffer); $I(NaClO_4)$ = 0.10 M; [oligonucleotides] = 1.0 μM.

4 Conclusions

Oligonucleotides covalently mercurated selectively at predetermined sites were prepared by post-synthetic electrophilic aromatic substitution with mercuric acetate. The reactive sites included natural (cytosine and uracil) as well as artificial (phenol and 6-phenyl-1*H*-carbazole) nucleobases. With the latter, dimercuration at the desired carbon atoms was achieved by appropriate placement of activating substituents on the aromatic rings. NMR affinity measurements revealed formation of high-affinity Hg(II)-mediated base pairs between 5-mercuricytosine and uracil, guanine and hypoxanthine, in other words bases that coordinate Hg(II) with concomitant deprotonation of the donor atom. A similar pattern was observed in oligonucleotide hybridization, with duplexes placing either a thymine or guanine opposite to the 5-mercuricytosine exhibiting the highest melting temperatures, comparable to respective values of duplexes comprising only canonical base pairs or a single Hg(II)-mediated TT mispair. With 1,8-dimercury-6-phenyl-1*H*-carbazole, incorporation of a second mercury atom did not lead to increased duplex stability but, with thymine as the partner, dinuclear Hg(II)-mediated base pairing was nonetheless supported by DFT calculations.

At the 3′-terminus of a homothymine triplex-forming oligonucleotide, 5-mercuricytosine promotes hybridization when placed opposite to a T•A or A•T base pair in the target duplex but the nature of the stabilizing interaction remained unclear. In most cases, the 5-mercuricytosine (or 5-mercuriuracil) modification inhibited triplex formation, in all likelihood through competing intrachain Hg(II)-mediated base pairing.

NMR studies with the 2,6-dimercuryphenol *C*-nucleoside suggested formation of stable dinuclear Hg(II)-mediated base triples with adenine, cytosine and (especially) uracil. This novel binding mode was successfully exploited in a model for the viral PAN RNA, consisting of homothymine*homoadenine•homothymine triple helix with a variable base triplet in the middle. Incorporation of a single 2,6-dimercuryphenol in the middle of the homothymine strand greatly increased both the Hoogsteen and the Watson—Crick melting temperatures of the triplex, compared not only to its unmercurated counterpart but also the canonical adenine base.

5 Experimental

5.1 General methods

All solvents involved in organic synthesis were of reagent grade and dried over 3Å or 4Å molecular sieves. All reactions were monitored by thin layer chromatography (TLC) performed on Merck 60 (silica gel F254) plates. TLC plates were visualized by exposure to ultraviolet light. Chromatographic purification of products was accomplished using flash column chromatography on silica gel (230-400 mesh). Freshly distilled triethylamine was for used for HPLC elution buffers. The products were characterized by micrOTOF-Q ESI-MS, and ^{1}H, ^{13}C, ^{31}P, and ^{199}Hg NMR by Bruker Daltonics QTOF and Bruker Biospin NMR spectrometers. The NMR spectra were recorded at 400, 500 and 600 MHz frequency and the chemical shifts are given in ppm and quoted relative to the residual solvent peak as an internal standard.

5.2 Oligonucleotide synthesis

The oligonucleotides were synthesized on an Applied Biosystems 3400 DNA/RNA synthesizer by conventional phosphoramidite strategy. In the case of **ON18z** and **ON23f**, coupling time of the modified nucleoside phosphoramidite was extended to 300s. Based on the trityl response, all couplings appeared to proceed with normal efficiency. The cleavage from solid support and deprotection of phosphate and base moieties were accomplished by treatment of 25% aqueous ammonia at 55 °C for overnight. Purification of oligonucleotides carried out by RP-HPLC using an analytical column (Hypersil ODS C18, 250 mm × 4.6 mm, 5 μm) and eluting with a linear gradient of MeCN (5 to 40% over 20 or 25 min) in 50 mM triethylammonium acetate buffer (TEAA).

Mercuration of oligonucleotides was carried out by treatment with $Hg(OAc)_2$. The detailed conditions are described in scheme 3 as well as in the original publications.[228–230,232] Chromatographic purification of the mercurated oligonucleotides was achieved by various different conditions. **ON18c-Hg**, **ON20c-Hg**, and **ON20u-Hg** were directly purified by RP-HPLC using an analytical column (Hypersil ODS C18, 250 mm × 4.6 mm, 5 μm) and eluting with a linear gradient of MeCN (5 to 35% over 25 min or 10 to 40% over 35 min) in 50 mM

triethylammonium acetate buffer (TEAA). Repeated purifications were carried out to remove excess free Hg(II). **ON18z-Hg2** was purified in two steps on the same analytical column (Hypersil ODS C18, 250 mm × 4.6 mm, 5 μm). The first purification was carried out by elution with a linear gradient of MeCN (10 to 40% over 20 min) in 50 mM triethylammonium acetate buffer (TEAA) containing 1 mM ethanethiol, after which fractions containing the desired material were purified by elution with a linear gradient of MeCN (15 to 45% over 25 min) in 50 mM triethylammonium acetate buffer (TEAA) without ethanethiol. **ON23f-Hg2** was also purified in two steps, first by IE-HPLC on a DNASwift^{TM} SAX-1S column (150 mm × 5 mm, monolithic) eluting with a linear gradient of $NaClO_4$ (16.5 to 165 mM over 20 min with 1.5 min^{-1} flow rate) in 20 mM TRIS•MsOH buffer, after which the fractions containing the desired product were purified by RP-HPLC on a Hypersil ODS C18 column (250 mm × 10 mm, 5 μm) eluting with a linear gradient of MeCN (10 to 40% over 20 min) 50 mM triethylammonium acetate buffer.

5.3 Enzymatic digestion

The site of dimercuration in oligonucleotides **ON18z-Hg2** and **ON23f-Hg2** was verified by P1 nuclease digestion. **ON18z-Hg2** and **ON23f-Hg2** were treated with P1 nuclease (approximately 2 μg) at 60 and 37 °C in a 25 mM triethylammonium acetate and 25 mM TRIS buffer, respectively. The **ON18z-Hg2** samples were directly withdrawn from the reaction mixture and analyzed by ESI-TOF-MS at appropriate time intervals. In the case of **ON23f-Hg2**, the samples were first desalted by RP-HPLC under the same conditions as used in the purification. Detailed procedures of enzymatic digestion can be found in the original publications.

5.4 UV melting temperature studies

The UV melting temperatures curves (absorbance versus temperature) were measured at 260 nm on a PerkinElmer Lambda 35 UV-vis spectrophotometer equipped with a Peltier temperature controller using quartz cuvettes with 10 mm optical path length. The temperature was changed at a rate of 0.5 °C min^{-1} from 10 to 90 °C. The measurements were carried out at pH 7.4 in 20 mM cacodylate buffer with ionic strength of 0.10 M, adjusted with $NaClO_4$. Thermal stabilities of 5-mercuricytosine duplexes (**ON18c-Hg**) were determined at 3.0 μM concentration, whereas a 1.0 μM oligonucleotide concentration was used in all other experiments. The Watson-Crick and Hoogsteen T_m values were determined as inflection points on the UV melting curves.

5.5 CD measurements

The CD spectra were recorded on an Applied Photophysics Chirascan Spctropolarimeter equipped with Peltier temperature control unit. The measurements were performed over a temperature range from 5 °C to 90 °C and a wavelength range from 200 to 400 nm, sampling at 5 or 10 °C intervals. An internal thermometer was used to confirm the accurate target temperatures. Identical samples were used for both UV and CD melting measurements.

5.6 Calculation of dissociation constants for the Hg(II)-mediated base triples

Equation (2), used to calculate the dissociation constants of the base triples formed by the 2,6-dimercuriphenol *C*-nucleoside **16** with AMP, CMP and UMP, was derived from the previously published[258] equation (3) on ternary complex formation.

$$\frac{[ABC]}{[A]_{tot}} = \frac{\left(\frac{[A]_{tot}+[B]_{tot}+K_{AB}-\sqrt{([A]_{tot}+[B]_{tot}+K_{AB})^2-[A]_{tot}[B]_{tot}}}{2}\right)}{[A]_{tot}} \times \frac{\left(\frac{[C]_{tot}+[B]_{tot}+K_{BC}-\sqrt{([C]_{tot}+[B]_{tot}+K_{BC})^2-[C]_{tot}[B]_{tot}}}{2}\right)}{[B]_{tot}} \quad (3)$$

where $[A]_{tot}$, $[B]_{tot}$ and $[C]_{tot}$ are the total concentrations of the three components and K_{AB} and K_{BC} the dissociation constants of the binary complexes A:B and B:C. Assuming equimolar concentrations for all components ($[A]_{tot} = [B]_{tot} = [C]_{tot} = c$) and identical dissociation constants for the two binary complexes ($K_{AB} = K_{BC} = K_d$), equation (3) simplifies to equation (4).

$$\delta_{obs} = \frac{\left(K_d + 2c - \sqrt{K_d^2+4K_dc}\right)^2}{4c^2} \quad (4)$$

Finally, normalization to the chemical shift scale gives equation (2).

Acknowledgements

This thesis is based on experimental work performed in the Laboratory of Organic Chemistry and Chemical Biology at the Department of Chemistry, University of Turku during the years of December 2015–May 2016 and May 2017–January 2020. The financial support from Erasmus Mundus EXPERTS SUSTAIN Consortium, Finnish National Agency for Education (CIMO), Turku University Foundation, and Finnish Cultural Foundation are gratefully acknowledged.

I would like to express my profound gratitude to my supervisor Assistant Professor Tuomas Lönnberg for giving me an opportunity to pursue my studies under your guidance in the fascinating world of nucleic acids. I am impressed with your outstanding knowledge in chemistry, and dedication to work. I thank you for your constant support, inspiration, and guidance. I appreciate your level of patience and thank you for being there in all good and bad times. Whenever I had troubles, I always have knocked on your door and wrote you emails irrespective with time without any doubt. That always has turned out into constructive criticism and endless discussions which improved my knowledge and understandings. This journey would have indeed difficult without you. You are THE BEST SUPERVISOR I ever had. I must say that I am fortunate to have had you as my PhD supervisor. I thank you for everything from bottom of my heart. You will be always first in my memories of Finland.

I am grateful to Professor Yoshiyuki Tanaka and Dr. Miguel Galindo for carefully evaluating my thesis. Your valuable comments helped to improve this thesis. I am thankful to Professor Jens Müller for accepting to be my opponent.

I wish to thank my collaborators Dr. Petri Tähtinen and Professor Vaishali Shinde for your valuable contributions in papers which are included in this thesis. I appreciate our insightful discussions and your words of enthusiasm.

My special thanks to Professor Pasi Virta, head of bioorganic group and the new head of chemistry department. Our discussions have always helped me. I appreciate your guidance and constant encouraging words for me.

I wish to thank all my colleagues who have been always supportive. My gratitude goes to all present and former co-workers in the bioorganic group for maintaining a work-leisure balancing environment. I wish to thank Ms. Madhuri Hande, Dr. Ville

Tähtinen, Mr. Asmo Aro-Heinilä, Mr. Lange Saleh Yakubu, Dr. Sajal Kumar Maity, Mr. Petja Rosenqvist, Mr. Aapo Aho, Dr. Emilia Kiuru, Dr. Satu Mikkola, Dr. Mikko Ora, Dr. Heidi Korhonen, Mr. Antti Äärelä, Mr. Vijay Gulumkar, Dr. Tuomas Karskela, Mr. Tommi Österlund, Mr. Afari Mark and Dr. Tharun Kumar Kotammagari. It was a pleasant time with all of you.

Thanks a million, to Kirsi Laaksonen, Mauri Nauma, Kari Loikas and Tinna Buss for providing extraordinary support. I am very sure that Mauri can repair anything in this world. I believe that you guys are lifeline of this department and no one can work without you. I also thank Dr. Jari Sinkkonen and Dr. Jani Rahkila for helping me at the instrument center.

I extend my gratitude to former supervisor Dr. H. V. Thulasiram for his constant support and motivation towards research. I thank my collaborators: Professor Santosh Haram and Professor Suresh Waghmode for their scientific inputs. I thank Dr. Abhishek Cukkemane for collaborating and appreciate his evergreen enthusiasm during work. I would also like to thank Emeritus Professor Dilip Dhavale Mr. Pradeep Kharade, Mrs. Shital Zakade who assisted me at the very beginning of my career and taught me great things about NMR. I am grateful to Mr. Vishnu Mujumdar for his kind words of appreciation.

I take this opportunity to thank my friends beyond chemistry universe for their love, affection, celebrations, outings and delicious food! I am very much thankful to Foodie Fintians: Princess Madhuri, Amit Tewari, Prashali Bajpai, Ekansh Saxena, Suvendu Rakshit and Neha Sharma. We shaped it together. Life became easy with our cheerful meets. Love you all!

My warmest thanks are devoted to my parents Uttam and Nilawati for their unconditional love, care, prayers and sacrifices for educating and preparing for my future. Special thanks to my younger brother Ganesh who always trust my capabilities and supports me. You are the best brother in the world. I could fly high just because my family was there to encourage me. My gratitude becomes speechless when I think of you. Thank you, thank you, and thank you…. Finally, I would like to thank the almighty God who made all things possible in my life. Thank you for your constant support and love throughout my life!

With all respect & gratitude, I wish to express my great thanks to all the people who stood by me directly or indirectly.

Dattatraya Uttam Ukale Turku, January 2021.

References

(1) Franklin, R. E.; Gosling, R. G. *Nature* **1953**, *172*, 156–157.
(2) Watson, J. D.; Crick, F. H. C. *Nature* **1953**, *171*, 737–738.
(3) Willins, M. H. F.; Stokes, A. R.; Wilson, H. R. *Nature* **1953**, *171*, 738–740.
(4) Wilkins, M. H. F. *Science* **1963**, *140*, 941–950.
(5) Ehrenhofer-Murray, A. *DNA Structure and Function*; Elsevier, **1994**.
(6) Bloomfield, V. A.; Bloomfield. D. M.; Crothers, I. T.; *Nucleic Acids : Structure , Properties , and Functions Bases*; Sausalito, Calif. : University Science Books. **2000**.
(7) Blackburn, G. M.; Gait, M. J.; Loakes, D. D. M. W. *Nucleic Acids in Chemistry and Biology*, III.; Blackburn, G. M., Gait, M. J., Loakes, D., Williams, D. M., Eds.; Royal Society of Chemistry: Cambridge, **2007**.
(8) Neidle, S. Principles of Nucleic Acid Structure; Elsevier, **2008**.
(9) Travers, A.; Muskhelishvili, G. *FEBS J.* **2015**, *282*, 2279–2295.
(10) Crick, F. *Nature* **1970**, *227*, 561–563.
(11) Eddy, S. R. *Nat. Rev. Genet.* **2001**, *2*, 919–929.
(12) Schubert, S.; Kurreck, J. *Curr. Drug Targets* **2004**, *5*, 667–681.
(13) Hannon, G. J.; Rossi, J. J. *Nature* **2004**, *431*, 371–378.
(14) Großhans, H.; Filipowicz, W. *Nature* **2008**, *451*, 414–416.
(15) Mattick, J. S. *PLoS Genet.* **2009**, *5*. e1000459.
(16) Broderick, J. A.; Zamore, P. D. *Gene Ther.* **2011**, *18*, 1104–1110.
(17) Deleavey, G. F.; Damha, M. J. *Chem. Biol.* **2012**, *19*, 937–954.
(18) Donohue, J.; Trueblood, K. N. *J. Mol. Biol.* **1960**, *2*, 363–371.
(19) Olson, W. K.; Bansal, M.; Burley, S. K.; Dickerson, R. E.; Gerstein, M.; Harvey, S. C.; Heinemann, U.; Lu, X.-J.; Neidle, S.; Shakked, Z.; Sklenar, H.; Suzuki, M.; Tung, C.-S.; Westhof, E.; Wolberger, C.; Berman, H. M. *J. Mol. Biol.* **2001**, *313*, 229–237.
(20) Marky, L. A.; Lee, H.-T.; Garcia, A. Watson-Crick Base Pairs and Nucleic Acids Stability. In *Encyclopedia of Life Sciences*; John Wiley & Sons, Ltd: Chichester, UK, 2010; pp 1–9.
(21) Steger, G.; Giegerich, R. RNA Struct. Fold. Biophys. Tech. Predict. Methods **2013**, 335–362.
(22) Hoogsteen, K. *Acta Crystallogr.* **1959**, *12*, 822–823.
(23) Cheng, Y. K.; Pettitt, B. M. *J. Am. Chem. Soc.* **1992**, *114*, 4465–4474.
(24) Nikolova, E. N.; Kim, E.; Wise, A. A.; O'Brien, P. J.; Andricioaei, I.; Al-Hashimi, H. M. *Nature* **2011**, *470*, 498–504.
(25) Duca, M.; Vekhoff, P.; Oussedik, K.; Halby, L.; Arimondo, P. B. *Nucleic Acids Res.* **2008**, *36*, 5123–5138.
(26) Jain, A.; Wang, G.; Vasquez, K. M. *Biochimie* **2008**, *90*, 1117–1130.
(27) Davis, J. T.; Spada, G. P. *Chem. Soc. Rev.* **2007**, *36*, 296–313.
(28) Doi, Y.; Chiba, J.; Morikawa, T.; Inouye, M. *J. Am. Chem. Soc.* **2008**, *130*, 8762–8768.
(29) Hirao, I.; Kimoto, M.; Yamashige, R. *Acc. Chem. Res.* **2012**, *45*, 2055–2065.
(30) Minuth, M.; Richert, C. *Angew. Chemie - Int. Ed.* **2013**, *52*, 10874–10877.
(31) Kamiya, Y.; Donoshita, Y.; Kamimoto, H.; Murayama, K.; Ariyoshi, J.; Asanuma, H. *ChemBioChem* **2017**, *18*, 1917–1922.

(32) Kawasaki, F.; Murat, P.; Li, Z.; Santner, T.; Balasubramanian, S. *Chem. Commun.* **2017**, *53*, 1389–1392.
(33) Benner, S. A. *Acc. Chem. Res.* **2004**, *37*, 784–797.
(34) Stambaský, J.; Hocek, M.; Kočovský, P. *Chem. Rev.* **2009**, *109*, 6729–6764.
(35) Liu, H. *Science.* **2003**, *302*, 868–871.
(36) Gao, J.; Liu, H.; Kool, E. T. *Angew. Chemie Int. Ed.* **2005**, *44*, 3118–3122.
(37) Liu, H.; Gao, J.; Kool, E. T. *J. Org. Chem.* **2005**, *70*, 639–647.
(38) Friedman, R. A.; Honig, B. *Biopolymers* **1992**, *32*, 145–159.
(39) Hunter, C. A.; Lu, X. *J. Mol. Biol.* **1997**, *265*, 603–619.
(40) Kool, E. T. Annu. Rev. Biophys. Biomol. Struct. **2001**, 30, 1–22.
(41) Yakovchuk, P.; Protozanova, E.; Frank-Kamenetskii, M. D. *Nucleic Acids Res.* **2006**, *34*, 564–574.
(42) Mak, C. H. *J. Phys. Chem. B* **2016**, *120*, 6010–6020.
(43) Martin, R. B. *Acc. Chem. Res.* **1985**, *18*, 32–38.
(44) Sigel, H. *Chem. Soc. Rev.* **1993**, *22*, 255.
(45) Kazakov, S. A.; Hecht, S. M. *Nucleic Acid-Metal Ion Interactions*; **2006**.
(46) Müller, J. *Metallomics* **2010**, *2*, 318–327.
(47) Ono, A.; Torigoe, H.; Tanaka, Y.; Okamoto, I. *Chem. Soc. Rev.* **2011**, *40*, 5855–5866.
(48) Morris, D. L. *Biomol. Concepts* **2014**, *5*, 397–407.
(49) Pages, B. J.; Ang, D. L.; Wright, E. P.; Aldrich-Wright, J. R. *Dalt. Trans.* **2015**, *44*, 3505–3526.
(50) Lippert, B.; Sanz Miguel, P. J. *Acc. Chem. Res.* **2016**, *49*, 1537–1545.
(51) Zhou, W.; Saran, R.; Liu, J. *Chem. Rev.* **2017**, *117*, 8272–8325.
(52) Lenkinski, R. E.; Reuben, J. *J. Am. Chem. Soc.* **1976**, *98*, 3089–3094.
(53) Ortiz, P.; Fernández-Bertrán, J.; Reguera, E. *Spectrochim. Acta - Part A Mol. Biomol. Spectrosc.* **2005**, *61*, 1977–1983.
(54) Hancock, R. D.; Martell, A. E. *Chem. Rev.* **1989**, *89*, 1875–1914.
(55) Chen, Z.; Morel-Desrosiers, N.; Morel, J.-P.; Detellier, C. *Can. J. Chem.* **1994**, *72*, 1753–1757.
(56) Araki, K.; Shiraishi, S. *Carbohydr. Res.* **1986**, *148*, 121–126.
(57) Alvarez, A. M.; Morel-Desrosiers, N.; Morel, J.-P. *Can. J. Chem.* **1987**, *65*, 2656–2660.
(58) Lippert, B. *Coord. Chem. Rev.* **2000**, *200–202*, 487–516.
(59) Taherpour, S.; Golubev, O.; Lönnberg, T. *Inorganica Chim. Acta* **2016**, *452*, 43–49.
(60) Bhattacharyya, D.; Arachchilage, G. M.; Basu, S. *Front. Chem.* **2016**, *4*, 1–14.
(61) Aoki, S.; Kimura, E. *Chem. Rev.* **2004**, *104*, 769–787.
(62) Taherpour, S.; Lönnberg, H.; Lönnberg, T. *Org. Biomol. Chem.* **2013**, *11*, 991–1000.
(63) Taherpour, S.; Golubev, O.; Lönnberg, T. *J. Org. Chem.* **2014**, *79*, 8990–8999.
(64) Ouameur, A. A.; Arakawa, H.; Ahmad, R.; Naoui, M.; Tajmir-Riahi, H. A. *DNA Cell Biol.* **2005**, *24*, 394–401.
(65) McCall, M. J.; Taylor, M. R. *Biochim. Biophys. Acta - Nucleic Acids Protein Synth.* **1975**, *390*, 137–139.
(66) Sigel, H.; Da Costa, C. P.; Martin, R. B. *Coord. Chem. Rev.* **2001**, *219–221*, 435–461.
(67) Mikulski, C. M.; Cocco, S.; De Franco, N.; Karayannis, N. M. *Inorganica Chim. Acta* **1982**, *67*, 61–66.
(68) He, Y.; Lopez, A.; Zhang, Z.; Chen, D.; Yang, R.; Liu, J. *Coord. Chem. Rev.* **2019**, *387*, 235–248.
(69) Clarke, M. J.; Johnson, A.; O'Connell, L. *Inorganica Chim. Acta* **1993**, *210*, 151–157.
(70) Romerosa, A.; Suarez-Varela, J.; Hidalgo, M. A.; Avila-Rosón, J. C.; Colacio, E. *Inorg. Chem.* **1997**, *36*, 3784–3786.
(71) Yamane, T.; Davidson, N. *Biochim. Biophys. Acta* **1962**, *55*, 609–621.
(72) Menzer, S.; Hillgeris, E. C.; Lippert, B. *Inorganica Chim. Acta* **1993**, *211*, 221–226.
(73) Golubev, O.; Lönnberg, T.; Lönnberg, H. *Molecules* **2014**, *19*, 16976–16986.
(74) Golubev, O.; Lönnberg, T.; Lönnberg, H. *J. Inorg. Biochem.* **2014**, *139*, 21–29.

(75) Dengale, R. A.; Thopate, S. R.; Lönnberg, T. *Chempluschem* **2016**, *81*, 978–984.
(76) Golubev, O.; Turc, G.; Lönnberg, T. *J. Inorg. Biochem.* **2016**, *155,* 36-43.
(77) Katz, S. *J. Am. Chem. Soc.* **1952**, *74*, 2238–2245.
(78) Shionoya, M.; Tanaka, K. *Curr. Opin. Chem. Biol.* **2004**, *8*, 592–597.
(79) Mandal, S.; Müller, J. *Curr. Opin. Chem. Biol.* **2017**, *37*, 71–79.
(80) Müller, J. *Coord. Chem. Rev.* **2019**, *393*, 37–47.
(81) Naskar, S.; Guha, R.; Müller, J. *Angew. Chemie - Int. Ed.* **2020**, *59*, 1397–1406.
(82) Tanaka, K.; Shionoya, M. *Coord. Chem. Rev.* **2007**, *251*, 2732–2742.
(83) Clever, G. H.; Kaul, C.; Carell, T. *Angew. Chemie Int. Ed.* **2007**, *46*, 6226–6236.
(84) Müller, J. *Eur. J. Inorg. Chem.* **2008**, 24, 3749–3763.
(85) Clever, G. H.; Shionoya, M. *Coord. Chem. Rev.* **2010**, *254*, 2391–2402.
(86) Stulz, E.; Clever, G.; Shionoya, M.; Mao, C. *Chem. Soc. Rev.* **2011**, *40*, 5633–5635.
(87) Takezawa, Y.; Shionoya, M. *Acc. Chem. Res.* **2012**, *45*, 2066–2076.
(88) Scharf, P.; Müller, J. *Chempluschem* **2013**, *78*, 20–34.
(89) Takezawa, Y.; Müller, J.; Shionoya, M. *Chem. Lett.* **2017**, *46*, 622–633.
(90) Thomas, C. A. *J. Am. Chem. Soc.* **1954**, *76*, 6032–6034.
(91) Gruenwedel, D. W. *Biophys. Chem.* **1994**, *52*, 115–123.
(92) Gruenwedel, D. *J. Inorg. Biochem.* **1993**, *52*, 251–261.
(93) Gruenwedel, D. W.; Davidson, N. *J. Mol. Biol.* **1966**, *21*, 129–144.
(94) Chrisman, R. W.; Mansy, S.; Peresie, H. J.; Ranade, A.; Berg, T. A.; Tobias, R. S. *Bioinorg. Chem.* **1977**, *7*, 245–266.
(95) Mansy, S.; Frick, J. P.; Tobias, R. S. *Biochim. Biophys. Acta - Nucleic Acids Protein Synth.* **1975**, *378*, 319–332.
(96) Savoie, R.; Jutier, J. J.; Prizant, L.; Beauchamp, A. L. *Spectrochim. Acta Part A Mol. Spectrosc.* **1982**, *38*, 561–568.
(97) Morzyk-Ociepa, B.; Michalska, D. *J. Mol. Struct.* **2001**, *598*, 133–144.
(98) Mansy, S.; Tobias, R. S. *J. Chem. Soc. Chem. Commun.* **1974**, No. 23, 957–958.
(99) Mansy, S.; Tobias, R. S. *Biochemistry* **1975**, *14*, 2952–2961.
(100) Mansy, S.; Tobias, R. S. *J. Am. Chem. Soc.* **1974**, *96*, 6874–6885.
(101) Mansy, S.; Tobias, R. S. *Inorg. Chem.* **1975**, *14*, 287–291.
(102) Mansy, S.; Wood, T. E.; Sprowles, J. C.; Tobias, R. S. *J. Am. Chem. Soc.* **1974**, *96*, 1762–1770.
(103) Nandi, U. S.; Wang, J. C.; Davidson, N. *Biochemistry* **1965**, *4*, 1687–1696.
(104) Katz, S. *Biochim. Biophys. Acta - Spec. Sect. Nucleic Acids Relat. Subj.* **1963**, *68*, 240–253.
(105) Katz, S. *Nature* **1962**, *194*, 569–569.
(106) Katz, S. *Nature* **1962**, *195*, 997–998.
(107) Yamane, T.; Davidson, N. *J. Am. Chem. Soc.* **1961**, *83*, 2599–2607.
(108) Eichhorn, G. L.; Clark, P. *J. Am. Chem. Soc.* **1963**, *85*, 4020–4024.
(109) Dove, W. F.; Yamane, T. *Biochem. Biophys. Res. Commun.* **1960**, *3*, 608–612.
(110) Davidson, N.; Widholm, J.; Nandi, U. S.; Jensen, R.; Olivera, B. M.; Wang, J. C. *Proc. Natl. Acad. Sci.* **1965**, *53*, 111–118.
(111) Young, P. R.; Nandi, U. S.; Kallenbach, N. R. *Biochemistry* **1982**, *21*, 62–66.
(112) Luck, G.; Zimmer, C. *Eur. J. Biochem.* **1971**, *18*, 140–145.
(113) Gruenwedel, D. W. *Eur. J. Biochem.* **1972**, *25*, 544–549.
(114) Williams, M. N.; Crothers, D. M. *Biochemistry* **1975**, *14*, 1944–1951.
(115) Clegg, M. S.; Gruenwedel, D. W. *Zeitschrift für Naturforsch. C* **1979**, *34*, 259–265.
(116) Gruenwedel, D. W. *Zeitschrift für Naturforsch. C* **1989**, *44*, 1015–1019.
(117) Gruenwedel, D. W.; Cruikshank, M. K. *Nucleic Acids Res.* **1989**, *17*, 9075–9086.
(118) Gruenwedel, D. W.; Cruikshank, M. K. *Biochemistry* **1990**, *29*, 2110–2116.
(119) Gruenwedel, D. W.; Cruikshank, M. K. *J. Inorg. Biochem.* **1991**, *43*, 29–36.
(120) Ok, S. R.; Gruenwedel, D. W. *Zeitschrift für Naturforsch. C* **1993**, *48*, 488–494.
(121) Sarker, M.; Chen, F.-M. *Biophys. Chem.* **1991**, *40*, 135–147.

(122) Walter, A.; Luck, G. *Nucleic Acids Res.* **1977**, *4*, 539–550.
(123) Adler, A. J.; Grossman, L.; Fasman, G. D. *Biochemistry* **1969**, *8*, 3846–3859.
(124) Simpson, R. B. *J. Am. Chem. Soc.* **1961**, *83*, 4711–4717.
(125) Simpson, R. B. *J. Am. Chem. Soc.* **1964**, *86*, 2059–2065.
(126) Hubert, J.; Beauchamp, A. L. *Acta Crystallogr. Sect. B Struct. Crystallogr. Cryst. Chem.* **1980**, *36*, 2613–2616.
(127) Prizant, L.; Olivier, M. J.; Rivest, R.; Beauchamp, A. L. *J. Am. Chem. Soc.* **1979**, *101*, 2765–2767.
(128) Charland, J.-P.; Britten, J. F.; Beauchamp, A. L. *Inorganica Chim. Acta* **1986**, *124*, 161–167.
(129) Charland, J. P.; Beauchamp, A. L. *Inorg. Chem.* **1986**, *25*, 4870–4876.
(130) Hubert, J.; Beauchamp, A. L. *Can. J. Chem.* **1980**, *58*, 1439–1443.
(131) Prizant, L.; Olivier, M. J.; Rivest, R.; Beauchamp, A. L. *Can. J. Chem.* **1981**, *59*, 1311–1317.
(132) Charland, J. P.; Simard, M.; Beauchamp, A. L. *Inorganica Chim. Acta* **1983**, *80*, 57–58.
(133) Grenier, L.; Charland, J.-P.; Beauchamp, A. L. *Can. J. Chem.* **1988**, *66*, 1663–1669.
(134) Zamora, F.; Sabat, M.; Lippert, B. *Inorganica Chim. Acta* **1998**, *267*, 87–91.
(135) Zamora, F.; Kunsman, M.; Sabat, M.; Lippert, B. *Inorg. Chem.* **1997**, *36*, 1583–1587.
(136) Mansy, S.; Frick, J. P.; Tobias, R. S. *Biochim. Biophys. Acta - Nucleic Acids Protein Synth.* **1975**, *378*, 319–332.
(137) Canty, A. J.; Tobias, R. S. *Inorg. Chem.* **1979**, *18*, 413–417.
(138) Buncel, E.; Norris, A. R.; Racz, W. J.; Taylor, S. E. *J. Chem. Soc., Chem. Commun.* **1979**, No. 13, 562–563.
(139) Krumm, M.; Zangrando, E.; Randaccio, L.; Menzer, S.; Danzmann, A.; Holthenrich, D.; Lippert, B. *Inorg. Chem.* **1993**, *32*, 2183–2189.
(140) Müller, J.; Zangrando, E.; Pahlke, N.; Freisinger, E.; Randaccio, L.; Lippert, B. *Chem. - A Eur. J.* **1998**, *4*, 397–405.
(141) Dale, R. M. K.; Martin, E.; Livingston, D. C.; Ward, D. C. *Biochemistry* **1975**, *14*, 2447–2457.
(142) Kosturko, L. D.; Folzer, C.; Stewart, R. F. *Biochemistry* **1974**, *13*, 3949–3952.
(143) Carrabine, J. A.; Sundaralingam, M. *Biochemistry* **1971**, *10*, 292–299.
(144) Dale, R. M. K.; Ward, D. C. *Biochemistry* **1975**, *14*, 2458–2469.
(145) Höpp, M.; Erxleben, A.; Rombeck, I.; Lippert, B. *Inorg. Chem.* **1996**, *35*, 397–403.
(146) Norris, A. R.; Kumar, R. *Inorganica Chim. Acta* **1984**, *93*, 33–35.
(147) Zamora, F.; Sabat, M.; Lippert, B. *Inorg. Chem.* **1996**, *35*, 4858–4864.
(148) Norris, A. R.; Kumar, R. *Inorganica Chim. Acta* **1984**, *93*, 84–86.
(149) Müller, J. *Beilstein J. Org. Chem.* **2017**, *13*, 2671–2681.
(150) Tanaka, K.; Clever, G. H.; Takezawa, Y.; Yamada, Y.; Kaul, C.; Shionoya, M.; Carell, T. *Nat. Nanotechnol.* **2006**, *1*, 190–194.
(151) Miyake, Y.; Togashi, H.; Tashiro, M.; Yamaguchi, H.; Oda, S.; Kudo, M.; Tanaka, Y.; Kondo, Y.; Sawa, R.; Fujimoto, T.; Machinami, T.; Ono, A. *J. Am. Chem. Soc.* **2006**, *128*, 2172–2173.
(152) Okamoto, I.; Ono, T.; Sameshima, R.; Ono, A. *Chem. Commun.* **2012**, *48*, 4347–4349.
(153) Tanaka, Y.; Kondo, J.; Sychrovský, V.; Šebera, J.; Dairaku, T.; Saneyoshi, H.; Urata, H.; Torigoe, H.; Ono, A. *Chem. Commun.* **2015**, *51*, 17343–17360.
(154) Mandal, S.; Hebenbrock, M.; Müller, J. *Angew. Chemie - Int. Ed.* **2016**, *55*, 15520–15523.
(155) Torigoe, H.; Ono, A.; Kozasa, T. *Chem. - A Eur. J.* **2010**, *16*, 13218–13225.
(156) Uchiyama, T.; Miura, T.; Takeuchi, H.; Dairaku, T.; Komuro, T.; Kawamura, T.; Kondo, Y.; Benda, L.; Sychrovský, V.; Bouř, P.; Okamoto, I.; Ono, A.; Tanaka, Y. *Nucleic Acids Res.* **2012**, *40*, 5766–5774.
(157) Yamaguchi, H.; Šebera, J.; Kondo, J.; Oda, S.; Komuro, T.; Kawamura, T.; Dairaku, T.; Kondo, Y.; Okamoto, I.; Ono, A.; Burda, J. V.; Kojima, C.; Sychrovský, V.; Tanaka, Y. *Nucleic Acids Res.* **2014**, *42*, 4094–4099.
(158) Torigoe, H.; Miyakawa, Y.; Ono, A.; Kozasa, T. *Thermochim. Acta* **2012**, *532*, 28–35.

(159) Šebera, J.; Burda, J.; Straka, M.; Ono, A.; Kojima, C.; Tanaka, Y.; Sychrovský, V. *Chem. - A Eur. J.* **2013**, *19*, 9884–9894.
(160) Marino, T. *J. Mol. Model.* **2014**, *20*, 20–23.
(161) Funai, T.; Tagawa, C.; Nakagawa, O.; Wada, S.; Ono, A.; Urata, H. *Chem. Commun.* **2020**, *56*, 12025-12028.
(162) Okamoto, I.; Iwamoto, K.; Watanabe, Y.; Miyake, Y.; Ono, A. *Angew. Chemie - Int. Ed.* **2009**, *48*, 1648–1651.
(163) Guo, X.; Ingale, S. A.; Yang, H.; He, Y.; Seela, F. *Org. Biomol. Chem.* **2017**, *15*, 870–883.
(164) Ono, A.; Cao, S.; Togashi, H.; Tashiro, M.; Fujimoto, T.; Machinami, T.; Oda, S.; Miyake, Y.; Okamoto, I.; Tanaka, Y. *Chem. Commun.* **2008**, *39*, 4825-4827.
(165) Ihara, T.; Ishii, T.; Araki, N.; Wilson, A. W.; Jyo, A. *J. Am. Chem. Soc.* **2009**, *131*, 3826–3827.
(166) Ono, T.; Yoshida, K.; Saotome, Y.; Sakabe, R.; Okamoto, I.; Ono, A. *Chem. Commun.* **2011**, *47*, 1542–1544.
(167) Megger, D. A.; Fonseca Guerra, C.; Bickelhaupt, F. M.; Müller, J. *J. Inorg. Biochem.* **2011**, *105*, 1398–1404.
(168) Jash, B.; Müller, J. *Chem. - A Eur. J.* **2018**, *24*, 10636–10640.
(169) Jash, B.; Müller, J. *J. Biol. Inorg. Chem.* **2020**, *25*, 647–654.
(170) Mandal, S.; Hebenbrock, M.; Müller, J. *Angew. Chemie Int. Ed.* **2016**, *55*, 15520–15523.
(171) Megger, D. A.; Müller, J. *Nucleosides, Nucleotides and Nucleic Acids* **2010**, *29*, 27–38.
(172) Mandal, S.; Hebenbrock, M.; Müller, J. *Chem. - A Eur. J.* **2017**, *23*, 5962–5965.
(173) Naskar, S.; Müller, J. *Chem. - A Eur. J.* **2019**, *25*, 16214–16218.
(174) FrØystein, N. A.; Sletten, E. *J. Am. Chem. Soc.* **1994**, *116*, 3240–3250.
(175) Dingley, A. J.; Grzesiek, S. *J. Am. Chem. Soc.* **1998**, *120*, 8293–8297.
(176) Tanaka, Y.; Oda, S.; Yamaguchi, H.; Kondo, Y.; Kojima, C.; Ono, A. *J. Am. Chem. Soc.* **2007**, *129*, 244–245.
(177) Tanaka, Y.; Ono, A. *Dalt. Trans.* **2008**, 37, 4965–4974.
(178) Tanaka, Y.; Yamaguchi, H.; Oda, S.; Kondo, Y.; Nomura, M.; Kojima, C.; Ono, A. *Nucleosides, Nucleotides and Nucleic Acids* **2006**, *25*, 613–624.
(179) Buchanan, G. W.; Stothers, J. B. *Can. J. Chem.* **1982**, *60*, 787–791.
(180) Pervushin, K.; Ono, A.; Fernández, C.; Szyperski, T.; Kainosho, M.; Wüthrich, K. *Proc. Natl. Acad. Sci. U. S. A.* **1998**, *95*, 14147–14151.
(181) Buchanan, G. W.; Bell, M.-J. *Magn. Reson. Chem.* **1986**, *24*, 493–497.
(182) Buchanan, G. W.; Bell, M. J. *Can. J. Chem.* **1983**, *61*, 2445–2448.
(183) Schmidt, O. P.; Jurt, S.; Johannsen, S.; Karimi, A.; Sigel, R. K. O.; Luedtke, N. W. *Nat. Commun.* **2019**, *10*, 1–11.
(184) Buncel, E.; Boone, C.; Joly, H.; Kumar, R.; Norris, A. R. *J. Inorg. Biochem.* **1985**, *25*, 61–73.
(185) Dairaku, T.; Furuita, K.; Sato, H.; Šebera, J.; Nakashima, K.; Ono, A.; Sychrovský, V.; Kojima, C.; Tanaka, Y. *Inorganica Chim. Acta* **2016**, *452*, 34–42.
(186) Dairaku, T.; Furuita, K.; Sato, H.; Šebera, J.; Yamanaka, D.; Otaki, H.; Kikkawa, S.; Kondo, Y.; Katahira, R.; Matthias Bickelhaupt, F.; Fonseca Guerra, C.; Ono, A.; Sychrovský, V.; Kojima, C.; Tanaka, Y. *Chem. Commun.* **2015**, *51*, 8488–8491.
(187) Manna, S.; Srivatsan, S. G. *Org. Lett.* **2019**, *21*, 4646–4650.
(188) Atwell, S.; Meggers, E.; Spraggon, G.; Schultz, P. G. *J. Am. Chem. Soc.* **2001**, *123*, 12364–12367.
(189) Ennifar, E.; Walter, P.; Dumas, P. *Nucleic Acids Res.* **2003**, *31*, 2671–2682.
(190) Schlegel, M. K.; Essen, L. O.; Meggers, E. *J. Am. Chem. Soc.* **2008**, *130*, 8158–8159.
(191) Kaul, C.; Müller, M.; Wagner, M.; Schneider, S.; Carell, T. *Nat. Chem.* **2011**, *3*, 794–800.
(192) Kondo, J.; Yamada, T.; Hirose, C.; Okamoto, I.; Tanaka, Y.; Ono, A. *Angew. Chemie - Int. Ed.* **2014**, *53*, 2385–2388.
(193) Kondo, J.; Tada, Y.; Dairaku, T.; Saneyoshi, H.; Okamoto, I.; Tanaka, Y.; Ono, A. *Angew. Chemie - Int. Ed.* **2015**, *54*, 13323–13326.

(194) Kondo, J.; Sugawara, T.; Saneyoshi, H.; Ono, A. *Chem. Commun.* **2017**, *53*, 11747–11750.
(195) Liu, H.; Shen, F.; Haruehanroengra, P.; Yao, Q.; Cheng, Y.; Chen, Y.; Yang, C.; Zhang, J.; Wu, B.; Luo, Q.; Cui, R.; Li, J.; Ma, J.; Sheng, J.; Gan, J. *Angew. Chemie Int. Ed.* **2017**, *56*, 9430–9434.
(196) Miyachi, H.; Matsui, T.; Shigeta, Y.; Hirao, K. *Phys. Chem. Chem. Phys.* **2010**, *12*, 909–917.
(197) Benda, L.; Straka, M.; Sychrovský, V.; Bouř, P.; Tanaka, Y. *J. Phys. Chem. A* **2012**, *116*, 8313–8320.
(198) Ono, A.; Kanazawa, H.; Ito, H.; Goto, M.; Nakamura, K.; Saneyoshi, H.; Kondo, J. *Angew. Chemie Int. Ed.* **2019**, *58*, 16835–16838.
(199) Bagno, A.; Saielli, G. *J. Am. Chem. Soc.* **2007**, *129*, 11360–11361.
(200) Seeman, N. C. *Mater. Today* **2003**, *6*, 24–29.
(201) Teller, C.; Willner, I. *Curr. Opin. Biotechnol.* **2010**, *21*, 376–391.
(202) Yang, H.; Metera, K. L.; Sleiman, H. F. *Coord. Chem. Rev.* **2010**, *254*, 2403–2415.
(203) Wilner, O. I.; Willner, I. *Chem. Rev.* **2012**, *112*, 2528–2556.
(204) Seeman, N. C.; Sleiman, H. F. *Nat. Rev. Mater.* **2017**, *3*, 1-23.
(205) Madsen, M.; Gothelf, K. V. *Chem. Rev.* **2019**, *119*, 6384-6458.
(206) Graham, M. K.; Brown, T. R.; Miller, P. S. *Biochemistry* **2015**, *54*, 2270–2282.
(207) Smith, N. M.; Amrane, S.; Rosu, F.; Gabelic, V.; Mergny, J. L. *Chem. Commun.* **2012**, *48*, 11464–11466.
(208) Kuklenyik, Z.; Marzilli, L. G. *Inorg. Chem.* **1996**, *35*, 5654–5662.
(209) Kamal, A.; She, Z.; Sharma, R.; Kraatz, H. B. *Electrochim. Acta* **2017**, *243*, 44–52.
(210) Ding, W.; Xu, M.; Zhu, H.; Liang, H. *Eur. Phys. J. E* **2013**, *36*.
(211) Megger, D. A.; Fonseca Guerra, C.; Hoffmann, J.; Brutschy, B.; Bickelhaupt, F. M.; Müller, J. *Chem. - A Eur. J.* **2011**, *17*, 6533–6544.
(212) Kondo, J.; Tada, Y.; Dairaku, T.; Hattori, Y.; Saneyoshi, H.; Ono, A.; Tanaka, Y. *Nat. Chem.* **2017**, *9*, 956–960.
(213) Tanaka, K.; Tengeiji, A.; Kato, T.; Toyama, N.; Shionoya, M. *Science* **2003**, *299*, 1212–1213.
(214) Johannsen, S.; Megger, N.; Böhme, D.; Sigel, R. K. O.; Müller, J. *Nat. Chem.* **2010**, *2*, 229–234.
(215) Tanaka, K.; Clever, G. H.; Takezawa, Y.; Yamada, Y.; Kaul, C.; Shionoya, M.; Carell, T. *Nat. Nanotechnol.* **2006**, *1*, 190–194.
(216) Müller, J. *Eur. J. Inorg. Chem.* **2008**, *2008*, 3749–3763.
(217) Takezawa, Y.; Hu, L.; Nakama, T.; Shionoya, M. *Angew. Chemie - Int. Ed.* **2020**, *59*, 21488-21492.
(218) Dale, R. M. K.; Livingston, D. C.; Ward, D. C. *Proc. Natl. Acad. Sci. U. S. A.* **1973**, *70*, 2238–2242.
(219) Johannsen, S.; Paulus, S.; Düpre, N.; Müller, J.; Sigel, R. K. O. *J. Inorg. Biochem.* **2008**, *102*, 1141–1151.
(220) Urata, H.; Yamaguchi, E.; Funai, T.; Matsumura, Y.; Wada, S. I. *Angew. Chemie - Int. Ed.* **2010**, *49*, 6516–6519.
(221) Funai, T.; Miyazaki, Y.; Aotani, M.; Yamaguchi, E.; Nakagawa, O.; Wada, S. I.; Torigoe, H.; Ono, A.; Urata, H. *Angew. Chemie - Int. Ed.* **2012**, *51*, 6464–6466.
(222) Funai, T.; Nakamura, J.; Miyazaki, Y.; Kiriu, R.; Nakagawa, O.; Wada, S. I.; Ono, A.; Urata, H. *Angew. Chemie - Int. Ed.* **2014**, *53*, 6624–6627.
(223) Takezawa, Y.; Nakama, T.; Shionoya, M. *J. Am. Chem. Soc.* **2019**, *141*, 19342–19350.
(224) Funai, T.; Aotani, M.; Kiriu, R.; Nakamura, J.; Miyazaki, Y.; Nakagawa, O.; Wada, S. ichi; Torigoe, H.; Ono, A.; Urata, H. *ChemBioChem* **2020**, *21*, 517–522.
(225) Nakama, T.; Takezawa, Y.; Sasaki, D.; Shionoya, M. *J. Am. Chem. Soc.* **2020**, *142*, 10153–10162.
(226) Aro-Heinilä, A.; Lönnberg, T.; Virta, P. *Bioconjug. Chem.* **2019**, *30*, 2183–2190.
(227) Aro-Heinilä, A.; Lönnberg, T.; Virta, P. *ChemBioChem* **2021,** *22*, 354-358.
(228) Ukale, D.; Shinde, V. S.; Lönnberg, T. *Chem. - A Eur. J.* **2016**, *22*, 7917–7923.

(229) Ukale, D. U.; Lönnberg, T. *ChemBioChem* **2018**, *19*, 1096–1101.
(230) Ukale, D. U.; Lönnberg, T. *Angew. Chemie - Int. Ed.* **2018**, *57*, 16171–16175.
(231) Ukale, D.; Maity, S.; Hande, M.; Lönnberg, T. *Synlett* **2019**, *30*, 1733–1737.
(232) Ukale, D. U.; Tähtinen, P.; Lönnberg, T. *Chem. - A Eur. J.* **2020**, *26*, 2164–2168.
(233) Ukale, D.; Lönnberg, T. *ChemBioChem* **2021**, 10.1002/cbic.202000821.
(234) Hande, M.; Maity, S.; Lönnberg, T. *Int. J. Mol. Sci.* **2018**, *19*, 1588.
(235) Maity, S. K.; Lönnberg, T. *Chem. - A Eur. J.* **2018**, *24*, 1274–1277.
(236) Hande, M.; Saher, O.; Lundin, K. E.; Edvard Smith, C. I.; Zain, R.; Lönnberg, T. *Molecules* **2019**, *24,* 1180-1193.
(237) Maity, S.; Hande, M.; Lönnberg, T. *ChemBioChem* **2020**, *21*, 2321–2328.
(238) Räisälä, H.; Lönnberg, T. *Chem. – A Eur. J.* **2019**, *25*, 4751–4756.
(239) Maity, S. K.; Lönnberg, T. A. *ACS Omega* **2019**, *.4*, 18803-18808.
(240) Bonesi, S. M.; Erra-Balsells, R. *J. Heterocycl. Chem.* **2001**, *38*, 77–87.
(241) Martin, R. B. *Acc. Chem. Res.* **1985**, *18*, 32–38.
(242) Newmark, R. A.; Cantor, C. R. *J. Am. Chem. Soc.* **1968**, *90*, 5010–5017.
(243) Petersen, S. B.; Led, J. J. *J. Am. Chem. Soc.* **1981**, *103*, 5308–5313.
(244) Yamaguchi, H.; Šebera, J.; Kondo, J.; Oda, S.; Komuro, T.; Kawamura, T.; Dairaku, T.; Kondo, Y.; Okamoto, I.; Ono, A.; Burda, J. V.; Kojima, C.; Sychrovský, V.; Tanaka, Y. *Nucleic Acids Res.* **2014**, *42*, 4094–4099.
(245) Baaske, P.; Duhr, S.; Braun, D. *Appl. Phys. Lett.* **2007**, *91*, 133901.
(246) Gaussian 16, Revision C.01, M. J. Frisch, G. W. Trucks, H. B. Schlegel, G. E. Scuseria, M. A. Robb, J. R.; Cheeseman, G. Scalmani, V. Barone, G. A. Petersson, H. Nakatsuji, X. Li, M. Caricato, A. V. M.; Nakajima, Y. Honda, O. Kitao, H. Nakai, T. Vreven, K.; Throssell, J. A. Montgomery, Jr., J. E. Peralta, F. Ogliaro, M. J. Bearpark, J. J. Heyd, E. N. Brothers, K.; N. Kudin, V. N. Staroverov, T. A. Keith, R. Kobayashi, J. Normand, K. Raghavachari, A. P. Rendell, J. C.; Burant, S. S. Iyengar, J. Tomasi, M. Cossi, J. M. Millam, M. Klene, C. Adamo, R. Cammi, J. W. O.; R. L. Martin, K. Morokuma, O. Farkas, J. B. Foresman, and D. J. F. Gaussian, Inc. Wallingford CT **2016**.
(247) Toulouse, J.; Sharkas, K.; Brémond, E.; Adamo, C. *J. Chem. Phys.* **2011**, *135*, 101102.
(248) Weigend, F.; Ahlrichs, R. *Phys. Chem. Chem. Phys.* **2005**, *7*, 3297–3305.
(249) Frisch, M. J.; Pople, J. A.; Binkley, J. S. *J. Chem. Phys.* **1984**, *80*, 3265–3269.
(250) Hehre, W. J.; Ditchfield, K.; Pople, J. A. *J. Chem. Phys.* **1972**, *56*, 2257–2261.
(251) Hariharan, P. C.; Pople, J. A. *Theor. Chim. Acta* **1973**, *28*, 213–222.
(252) Svinarchuk, F.; Paoletti, J.; Malvy, C. *J. Biol. Chem.* **1995**, *270*, 14068–14071.
(253) Rusling, D. A.; Rachwal, P. A.; Brown, T.; Fox, K. R. *Biophys. Chem.* **2009**, *145*, 105–110.
(254) Mitton-Fry, R. M.; DeGregorio, S. J.; Wang, J.; Steitz, T. A.; Steitz, J. A. *Science.* **2010**, *330*, 1244–1247.
(255) Liu, H.; Cai, C.; Haruehanroengra, P.; Yao, Q.; Chen, Y.; Yang, C.; Luo, Q.; Wu, B.; Li, J.; Ma, J.; Sheng, J.; Gan, J. *Nucleic Acids Res.* **2017**, *45*, 2910–2918.
(256) Gondeau, C.; Maurizot, J. C.; Durand, M. *Nucleic Acids Res.* **1998**, *26*, 4996–5003.
(257) Miyahara, T.; Nakatsuji, H.; Sugiyama, H. *J. Phys. Chem. A* **2013**, *117*, 42–55.
(258) Douglass, E. F.; Miller, C. J.; Sparer, G.; Shapiro, H.; Spiegel, D. A. *J. Am. Chem. Soc.* **2013**, *135*, 6092–6099.

UNIVERSITY OF TURKU

Painosalama Oy, Turku, Finland 2021

ISBN 978-951-29-8365-0 (PRINT)
ISBN 978-951-29-8366-7 (PDF)
ISSN 0082-7002 (Print)
ISSN 2343-3175 (Online)